

This Page Is Inserted by IFW Operations
and is not a part of the Official Record

BEST AVAILABLE IMAGES

Defective images within this document are accurate representations of the original documents submitted by the applicant.

Defects in the images may include (but are not limited to):

- BLACK BORDERS
- TEXT CUT OFF AT TOP, BOTTOM OR SIDES
- FADED TEXT
- ILLEGIBLE TEXT
- SKEWED/SLANTED IMAGES
- COLORED PHOTOS
- BLACK OR VERY BLACK AND WHITE DARK PHOTOS
- GRAY SCALE DOCUMENTS

IMAGES ARE BEST AVAILABLE COPY.

**As rescanning documents *will not* correct images,
please do not report the images to the
Image Problem Mailbox.**



results of BLAST

BLASTN 2.2.8 [Jan-05-2004]

Reference:

Altschul, Stephen F., Thomas L. Madden, Alejandro A. Schäffer, Jinghui Zhang, Zheng Zhang, Webb Miller, and David J. Lipman (1997), "Gapped BLAST and PSI-BLAST: a new generation of protein database search programs", Nucleic Acids Res. 25:3389-3402.

RID: 1079021225-7405-40579272083.BLASTQ3

Query=

(321 letters)

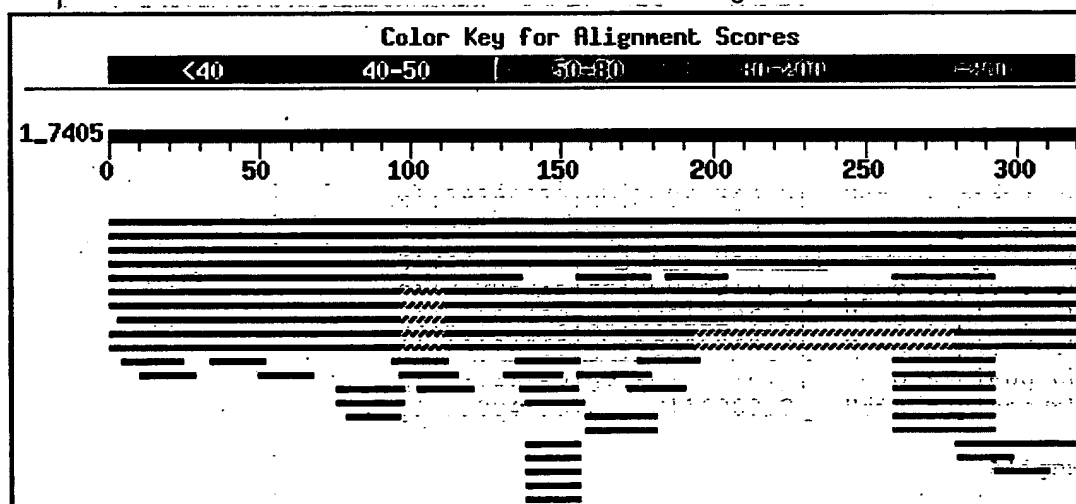
Database: All GenBank+EMBL+DDBJ+PDB sequences (but no EST, STS, GSS, or phase 0, 1 or 2 HTGS sequences)
2,102,977 sequences; 10,130,642,339 total letters

If you have any problems or questions with the results of this search please refer to the [BLAST FAQs](#)

[Taxonomy reports](#)

Distribution of 54 Blast Hits on the Query Sequence

Mouse-over to show define and scores. Click to show alignments



Sequences producing significant alignments:

Query ID	Subject ID	Description	Score (bits)	E Value	Significance
gi 18483167 gb AF453828.1	Homo sapiens G protein-coupled r...	595	e-167	LU	
gi 18702459 gb AF403384.2	Homo sapiens LGR8 mRNA, complete...	595	e-167	LU	

gi 20070357 ref NM_130806.2	Homo sapiens leucine-rich repe...	595	e-167	LUG
gi 11137618 emb AL138708.17	Human DNA sequence from clone ...	436	e-119	
gi 28628570 gb AY196483.1	Equus caballus INSL3/relaxin rec...	157	2e-35	
gi 15811372 gb AF346501.1 AF346501	Mus musculus G protein c...	137	1e-29	LU
gi 17978287 ref NM_080468.1	Mus musculus leucine-rich repe...	137	1e-29	LUG
gi 34870240 ref XM_344073.1	Rattus norvegicus similar to G...	113	2e-22	LU
gi 13549251 gb AC077689.9	Mus Musculus Strain C57BL6/J Chr...	109	3e-21	
gi 13027370 gb AC068627.16	Mus Musculus Chromosome 5 RP23-...	109	3e-21	
gi 34527833 dbj AK122647.1	Homo sapiens cDNA FLJ16077 fis,...	52	7e-04	LU
gi 19526153 gb AC107219.5	Homo sapiens BAC clone RP11-575B...	52	7e-04	
gi 34367144 emb BX647985.1 HSM808131	Homo sapiens mRNA; cDN...	52	7e-04	LU
gi 34367139 emb BX647980.1 HSM808126	Homo sapiens mRNA; cDN...	52	7e-04	LU
gi 34367134 emb BX647975.1 HSM808121	Homo sapiens mRNA; cDN...	52	7e-04	LU
gi 10441729 gb AF190500.1 AF190500	Homo sapiens leucine-ric...	52	7e-04	LU
gi 11056007 ref NM_021634.1	Homo sapiens leucine-rich repe...	52	7e-04	LUG
gi 26086935 dbj AK039086.1	Mus musculus adult male hypotha...	44	0.16	LU
gi 13276126 emb AL163612.5 CNS01RII	Human chromosome 14 DNA...	44	0.16	
gi 28604186 gb AC127237.3	Mus musculus BAC clone RP24-363G...	42	0.63	
gi 5649182 gb AC006516.10	Homo sapiens X BAC GSHB-557D6 (G...	42	0.63	
gi 37805621 emb BX247946.5	Zebrafish DNA sequence from clo...	42	0.63	
gi 26984446 emb AL590151.7	Zebrafish DNA sequence from clo...	42	0.63	L
gi 41237250 gb AC124987.9	Mus musculus chromosome 3, clone...	42	0.63	
gi 21844669 gb AC117218.3	Mus musculus BAC clone RP23-344B...	40	2.5	
gi 11465143 gb AC021015.4	Homo sapiens BAC clone RP11-320C...	40	2.5	
gi 27228870 gb AC104838.3	Homo sapiens chromosome 1 clone ...	40	2.5	
gi 15638922 gb AC096588.1	Homo sapiens BAC clone RP11-725D...	40	2.5	
gi 17105311 gb AC103552.1	Homo sapiens chromosome 1 clone ...	40	2.5	
gi 27374559 emb AL772387.13	Mouse DNA sequence from clone ...	40	2.5	
gi 13751970 emb AL390741.12	Human DNA sequence from clone ...	40	2.5	
gi 38490679 gb AC146269.3	Pan troglodytes BAC clone RP43-2...	38	9.8	
gi 29373192 gb AC122212.2	Mus musculus BAC clone RP23-99K1...	38	9.8	
gi 29469637 gb AC127598.3	Mus musculus BAC clone RP23-84E1...	38	9.8	
gi 22507257 gb AC131941.1	Mus musculus BAC clone RP23-109A...	38	9.8	
gi 37693685 gb AC107369.9	Mus musculus chromosome 15, clon...	38	9.8	
gi 37991976 gb AC113544.9	Mus musculus chromosome 10, clon...	38	9.8	
gi 37951418 gb AC110029.8	Mus musculus chromosome 1, clone...	38	9.8	
gi 29294030 gb AC092340.5	Homo sapiens chromosome 16 clone...	38	9.8	
gi 22474940 gb AC120036.5	Homo sapiens chromosome 8, clone...	38	9.8	
gi 32188047 dbj AP000842.6	Homo sapiens genomic DNA, chrom...	38	9.8	
gi 21206235 gb AC020910.7	Homo sapiens chromosome 19 clone...	38	9.8	
gi 29150339 gb AC012186.8	Homo sapiens chromosome 16 clone...	38	9.8	
gi 29124065 gb AC092368.3	Homo sapiens chromosome 16 clone...	38	9.8	
gi 29029240 gb AC106814.3	Homo sapiens chromosome 16 clone...	38	9.8	
gi 22004395 gb AC116903.3	Homo sapiens chromosome 15, clon...	38	9.8	

Alignments

Get selected sequences

Select all

Deselect all

☒ >gi|18483167|gb|AF453828.1| **LU** Homo sapiens G protein-coupled receptor affectir
 (GREAT) mRNA, complete cds
 Length = 2436

Score = 595 bits (300), Expect = e-167
 Identities = 314/321 (97%)
 Strand = Plus / Plus

Query: 1 ggtgtgaacttgctggcttttctcatcattgtgttttccctatattactatgttctgttcc 60
 |||
 Sbjct: 1856 ggtgtgaacttgctggcttttctcatcattgtgttttccctatattactatgttctgttcc 1915

Query: 61 attcaaaaaaccgccttgagaccacagaagtaaggaattgttttgaagagaggtggct 120
 |||
 Sbjct: 1916 attcaaaaaaccgccttgagaccacagaagtaaggaattgttttgaagagaggtggct 1975

Query: 121 gttgcaaactggtttcttttttatagtgttctctgatgccatctgctggattcctgtattt 180
 |||
 Sbjct: 1976 gttgcaaactggtttcttttttatagtgttctctgatgccatctgctggattcctgtattt 2035

Query: 181 gtagttaaaatcctttccctcttccgggtgaaataccagacacaaatgacttcctggata 240
 |||
 Sbjct: 2036 gtagttaaaatcctttccctcttccgggtgaaataccagacacaaatgacttcctggata 2095

Query: 241 gtgannnnnncccttcagttaacagtgtttgaatccaatcctctataactctcacaacc 300
 |||
 Sbjct: 2096 gtgatttttttcccttcagttaacagtgtttgaatccaatcctctataactctcacaacc 2155

Query: 301 aacttttttaaggacaagttg 321
 |||
 Sbjct: 2156 aacttttttaaggacaagttg 2176

>gi|18702459|gb|AF403384.2| **LU** Homo sapiens LGR8 mRNA, complete cds
 Length = 2838

Score = 595 bits (300), Expect = e-167
 Identities = 314/321 (97%)
 Strand = Plus / Plus

Query: 1 ggtgtgaacttgctggcttttctcatcattgtgttttccctatattactatgttctgttcc 60
 |||
 Sbjct: 1892 ggtgtgaacttgctggcttttctcatcattgtgttttccctatattactatgttctgttcc 1951

Query: 61 attcaaaaaaccgccttgagaccacagaagtaaggaattgttttgaagagaggtggct 120
 |||
 Sbjct: 1952 attcaaaaaaccgccttgagaccacagaagtaaggaattgttttgaagagaggtggct 2011

Query: 121 gttgcaaactggtttcttttttatagtgttctctgatgccatctgctggattcctgtattt 180
 |||
 Sbjct: 2012 gttgcaaactggtttcttttttatagtgttctctgatgccatctgctggattcctgtattt 2071

Query: 181 gtagttaaaatcctttccctcttccgggtgaaataccagacacaaatgacttcctggata 240

|||||
 Sbjct: 2072 gtagttaaatacctttccctcttccgggtggaaataccagacacaatgacttcctggata 2131

Query: 241 gtgannnnnncccttccagttaacagtgccttgaatccaatcctctataactctcacaacc 300

|||||
 Sbjct: 2132 gtgatttttttcccttccagttaacagtgccttgaatccaatcctctataactctcacaacc 2191

Query: 301 aacttttttaaggacaagttg 321

|||||
 Sbjct: 2192 aacttttttaaggacaagttg 2212

┌>gi|20070357|ref|NM_130806.2| **LUG** Homo sapiens leucine-rich repeat-containing
 receptor 8 (LGR8), mRNA
 Length = 2838

Score = 595 bits (300), Expect = e-167

Identities = 314/321 (97%)

Strand = Plus / Plus

Query: 1 ggtgtgaacttgctggcctttctcatcattgtgttttccctatattactatgttctgttcc 60

|||||
 Sbjct: 1892 ggtgtgaacttgctggcctttctcatcattgtgttttccctatattactatgttctgttcc 1951

Query: 61 attcaaaaaaccgccttgagaccacagaagtaaggaattgttttgaagagaggtggct 120

|||||
 Sbjct: 1952 attcaaaaaaccgccttgagaccacagaagtaaggaattgttttgaagagaggtggct 2011

Query: 121 gttgcaaatacgtttcttttttatagtgttctctgatgccatctgctggattcctgtattt 180

|||||
 Sbjct: 2012 gttgcaaatacgtttcttttttatagtgttctctgatgccatctgctggattcctgtattt 2071

Query: 181 gtagttaaatacctttccctcttccgggtggaaataccagacacaatgacttcctggata 240

|||||
 Sbjct: 2072 gtagttaaatacctttccctcttccgggtggaaataccagacacaatgacttcctggata 2131

Query: 241 gtgannnnnncccttccagttaacagtgccttgaatccaatcctctataactctcacaacc 300

|||||
 Sbjct: 2132 gtgatttttttcccttccagttaacagtgccttgaatccaatcctctataactctcacaacc 2191

Query: 301 aacttttttaaggacaagttg 321

|||||
 Sbjct: 2192 aacttttttaaggacaagttg 2212

┌>gi|11137618|emb|AL138708.17| **D** Human DNA sequence from clone RP11-432E15 on chi
 STSs, GSSs and a CpG island, complete sequence
 Length = 170522

Score = 436 bits (220), Expect = e-119
 Identities = 220/220 (100%)
 Strand = Plus / Plus

Query: 1 ggtgtgaacttgctggcttttctcatcattgtgttttcctatattactatgttctgttcc 60
 |||
 Sbjct: 42034 ggtgtgaacttgctggcttttctcatcattgtgttttcctatattactatgttctgttcc 42093

Query: 61 attcaaaaaaccgccttgagaccacagaagtaaggaattgttttggaagagaggtggct 120
 |||
 Sbjct: 42094 attcaaaaaaccgccttgagaccacagaagtaaggaattgttttggaagagaggtggct 42153

Query: 121 gttgcaaatcggtttcttttttatagtgttctctgatgccatctgctggattcctgtattt 180
 |||
 Sbjct: 42154 gttgcaaatcggtttcttttttatagtgttctctgatgccatctgctggattcctgtattt 42213

Query: 181 gtagttaaaatcctttccctcttccgggtggaaataccag 220
 |||
 Sbjct: 42214 gtagttaaaatcctttccctcttccgggtggaaataccag 42253

Score = 167 bits (84), Expect = 2e-38
 Identities = 98/105 (93%)
 Strand = Plus / Plus

Query: 217 ccagacacaatgacttcctggatagtgannnnnnnccttcagttaacagtgttttgaat 276
 |||
 Sbjct: 46976 ccagacacaatgacttcctggatagtgattttttccttcagttaacagtgttttgaat 47035

Query: 277 ccaatcctctatactctcacaaccaactttttaaggacaagttg 321
 |||
 Sbjct: 47036 ccaatcctctatactctcacaaccaactttttaaggacaagttg 47080

☐ >gi|28628570|gb|AY196483.1|
 Length = 653

Equus caballus: INSL3/relaxin receptor LGR8 mRNA, partial

Score = 157 bits (79), Expect = 2e-35
 Identities = 126/139 (90%), Gaps = 2/139 (1%)
 Strand = Plus / Plus

Query: 1 ggtgtgaacttgctggcttttctcatcattgtg-ttttcctatattactatgttctgttc 59
 |||
 Sbjct: 516 ggtgtgaacttgctggcttttctcatcattgtgttttcctata-tattatgttctgttc 574

Query: 60 cattcaaaaaaccgccttgagaccacagaagtaaggaattgttttggaagagaggtggc 119
 |||
 Sbjct: 575 cattcaaaaaactgccttgagacttcagaagttaggaacccatttgaagaaaagtggc 634

Query: 120 tgttgcaaactggttcttt 138
 |||||
 Sbjct: 635 tgttgcaaactggttcttt 653

┌>gi|15811372|gb|AF346501.1|AF346501 **LU** Mus musculus G protein coupled receptor
 (Great) mRNA, complete cds
 Length = 2539

Score = 137 bits (69), Expect = 1e-29
 Identities = 173/210 (82%)
 Strand = Plus / Plus

Query: 112 gaggtggctgttgcaaactggttcttttttatagtgttctctgatgccatctgctggatt 171
 |||||
 Sbjct: 2039 gaggtggctgttgcaaaccggttcttttttatcgtgttctctgatgccatctgctggatc 2098

Query: 172 cctgtatttgtagttaaaatcctttccctcttcgggtggaaataccagacacaatgact 231
 |||||
 Sbjct: 2099 cctgtgtttgtcgtaagatcctgtctctccttcaagtggagataccaggcacaatcact 2158

Query: 232 tcctggatagtgannnnnnnccttcagttaacagtgctttgaatccaatcctctatact 291
 |||||
 Sbjct: 2159 tcctggatcgtggttttttcccttcgggtgaacagcgccttaaaccctcctctacact 2218

Query: 292 ctcacaaccaactttttaaggacaagttg 321
 |||||
 Sbjct: 2219 ctgacgacctcctttttaaggacaagttg 2248

Score = 73.8 bits (37), Expect = 2e-10
 Identities = 82/97 (84%)
 Strand = Plus / Plus

Query: 1 ggtgtgaacttgctggcttttctcatcattgtgttttctatattactatgttctgttcc 60
 |||||
 Sbjct: 1928 ggtgtgaacttgctggcttttctcgatcgtgatttctatgttaccatgttctgttcc 1987

Query: 61 attcaaaaaaccgccttgacagaccacagaagtaagga 97
 |||||
 Sbjct: 1988 attcataaaacagcccttcagactgcagaagtgagga 2024

┌>gi|17978287|ref|NM_080468.1| **LUG** Mus musculus leucine-rich repeat-containing
 receptor 8 (Lgr8), mRNA
 Length = 2539

Score = 137 bits (69), Expect = 1e-29
 Identities = 173/210 (82%)
 Strand = Plus / Plus

03/11/2004

Sbjct: 1984 tcttgatcgtggttttttcttccggtaaacagcgccttaaaccccatcctctacact 2043

Query: 292 ctcacaaccaactttttaaggacaagttg 321

||||| ||| | |||||

Sbjct: 2044 ctcaccacctccctttttaaggacaagttg 2073

Score = 52.0 bits (26), Expect = 7e-04

Identities = 77/94 (81%)

Strand = Plus / Plus

Query: 4 gtgaacttgctggcttttctcatcattgtgttttctatattactatgttctgttccatt 63

||||| ||||| ||| ||||| ||| ||||| ||| ||||| |||||

Sbjct: 1756 gtgaacttgctggcttttctcgtcatcacgttctcctatgtcaccatgttctgttccatt 1815

Query: 64 caaaaaaccgccttgagaccacagaagtaagga 97

|| ||||| ||| | ||||| ||||| |||||

Sbjct: 1816 cagaaaacagccctccagactgcagaagtgagga 1849

>gi|13549251|gb|AC077689.9|

sequence

Length = 213462

D Mus Musculus Strain C57BL6/J Chromosome 5 RP23-30:

Score = 109 bits (55), Expect = 3e-21

Identities = 76/83 (91%)

Strand = Plus / Minus

Query: 112 gaggtggctggttgcaaactcgtttctttttatagtggttctctgatgccatctgctggatt 171

||||| ||||| ||||| ||||| ||||| ||||| ||||| ||||| |||||

Sbjct: 50779 gaggtggctggttgcaaaccggttctttttatcggttctctgatgccatctgctggattc 50720

Query: 172 cctgtatttgtagttaaaatcct 194

||||| ||||| ||||| |||||

Sbjct: 50719 cctgtgtttgtcgttaagatcct 50697

Score = 73.8 bits (37), Expect = 2e-10

Identities = 82/97 (84%)

Strand = Plus / Minus

Query: 1 ggtgtgaacttgctggcttttctcatcattgtgttttctatattactatgttctgttcc 60

||||| ||||| ||||| ||||| ||||| ||||| ||||| ||||| |||||

Sbjct: 50890 ggtgtgaacttgctggcttttctcgtcatcgtgatttctatgtcaccatgttctgttcc 50831



Query: 61 attcaaaaaaccgccttgagaccacagaagtaagga 97

||||| ||||| ||| | ||||| ||||| |||||

Sbjct: 50830 attcataaaacagcccttcagactgcagaagtgagga 50794

Score = 44.1 bits (22), Expect = 0.16
Identities = 37/42 (88%)
Strand = Plus / Minus

Query: 280 atcctctataactctcacaaccaacttttttaaggacaagttg 321
||||||| ||||| || ||| |||||||||||||||||
Sbjct: 40065 atcctctacactctgacgacctccttttttaaggacaagttg 40024

 >gi|13027370|gb|AC068627.16|  Mus Musculus Chromosome 5 RP23-389F6, complete se
Length = 180673

Score = 109 bits (55), Expect = 3e-21
Identities = 76/83 (91%)
Strand = Plus / Minus

Query: 112 gaggtggctgttgcaaatacgtttcttttttatagtgttctctgatgccatctgctggatt 171
||||||||||||||| || ||||||||||| |||||||||||||||||
Sbjct: 172567 gaggtggctgttgcaaaccgggttcttttttatcgtgttctctgatgccatctgctggatc 172508

Query: 172 cctgtatttgtagttaaaatcct 194
||||| ||||| ||||| |||||
Sbjct: 172507 cctgtgtttgtcgtaagatcct 172485

Score = 73.8 bits (37), Expect = 2e-10
Identities = 82/97 (84%)
Strand = Plus / Minus

Query: 1 ggtgtgaacttgctggcttttctcatcattgtgttttctatattactatgttctgttcc 60
||||||||||||||| ||| |||| ||| ||||||||| || || ||||||||| |||
Sbjct: 172678 ggtgtgaacttgctggcttttctcgtcgtgatttctatgtcaccatgttctgttcc 172619

Query: 61 attcaaaaaaccgccttgacagaccacagaagtaagga 97
||||| ||||| ||||| ||||| ||||||| |||||
Sbjct: 172618 attcataaaacagcccttcagactgcagaagtgagga 172582

Score = 44.1 bits (22), Expect = 0.16
Identities = 37/42 (88%)
Strand = Plus / Minus

Query: 280 atcctctataactctcacaaccaacttttttaaggacaagttg 321
||||||| ||||| || ||| |||||||||||||||||
Sbjct: 161853 atcctctacactctgacgacctccttttttaaggacaagttg 161812

Lambda	K	H
1.37	0.711	1.31

Gapped

Lambda	K	H
1.37	0.711	1.31

Gap Penalties: Existence: 5, Extension: 2

Number of Hits to DB: 8,323,323

Number of Sequences: 2102977

Number of extensions: 13347

Number of successful extensions: 148

Number of sequences better than 10.0: 0

Number of HSP's better than 10.0 without gapping: 0

Number of HSP's successfully gapped in prelim test: 55

length of query: 321

length of database: 10,130,642,339

A: 0

X1: 11 (20.0 bits)

X2: 15 (30.0 bits)

X3: 25 (50.0 bits)

S1: 12 (25.0 bits)



Entrez

PubMed

Nucleotide

Protein

Genome

Structure

PMC

Taxonomy

Books



Entrez
Nucleotide

Search Nucleotide

for

Limits

Preview/Index

History

Clipboard

Details

Display

GenBank

Show: 20

Send to

File

Get Subsequence

Features

☐ 1: AF453828. Homo sapiens G pr...[gi:18483167]

Links

LOCUS AF453828 2436 bp mRNA linear PRI 09-SEP-2002
 DEFINITION Homo sapiens G protein-coupled receptor affecting testicular
 descent (GREAT) mRNA, complete cds.

ACCESSION AF453828

VERSION AF453828.1 GI:18483167

KEYWORDS .

SOURCE Homo sapiens (human)

ORGANISM Homo sapiens

Eukaryota; Metazoa; Chordata; Craniata; Vertebrata; Euteleostomi;
 Mammalia; Eutheria; Primates; Catarrhini; Hominidae; Homo.

REFERENCE 1 (bases 1 to 2436)

AUTHORS Gorlov, I.P., Kamat, A., Bogatcheva, N.V., Jones, E., Lamb, D.J.,

Truong, A., Bishop, C.E., McElreavey, K. and AgoulNIK, A.I.

TITLE Mutations of the GREAT gene cause cryptorchidism

JOURNAL Hum. Mol. Genet. 11 (19), 2309-2318 (2002)

PUBMED 12217959

REFERENCE 2 (bases 1 to 2436)

AUTHORS AgoulNIK, A.I.

TITLE Direct Submission

JOURNAL Submitted (30-NOV-2001) Ob/Gyn, Baylor College of Medicine, 6550
 Fannin St., Su. 861, Houston, TX 77030, USA

FEATURES

source

Location/Qualifiers

1..2436

/organism="Homo sapiens"

/mol_type="mRNA"

/db_xref="taxon:9606"

/chromosome="13"

/map="13q12-q13"

gene

1..2436

/gene="GREAT"

CDS

71..2335

/gene="GREAT"

/codon_start=1

/product="G protein-coupled receptor affecting testicular
descent"

/protein_id="AAL73946.1"

/db_xref="GI:18483168"

/translation="MIVFLVFKHLFSLRLITMFFLLHFIVLINVKDFALTQGSMTFS

CQKGYFPCGNLTCKLPRAFHCDGKDDCGNGADEENC GDTSGWATIFGTVHGNANSVAL

TQECFLKQYPQCCDCKETELECVDLKSVPMSNNVTLLSLKKNKIHSPLDKVFIKY

TKLKKIFLQHN CIRHISRKAFFGLCNLQILYNHNCITTLRPGIFKDLHLQTLWLILDD

NPITRISQRLFTGLNSLFFLSMVNNYLEALPKQMCAMPQLNWDLEGNRIKYL TNST

FLSCDSLTVLFLPRNQIGFVPEKTFSSLKNLGELDLSSNTITELSPHLFKDLKLLQKL

NLSSNPLMYLHKNQFESLKLQSLDLERIEIPNINTRMFQPMKNLSHIYFKNFRYCSY

APHVRICMPLTDGISSFEDLLANNILRIFVWVIAFITCFGNLFVIGMRSFIKAENTTH

AMSIKILCCADCLMGVYLFFVGIFDIKYRGQYQKYALLWMESVQCRLMGFLAMLSTEV

SVLLLTYLTLKFLVIVFPFSNIRPGKRQTSVILICIWMAGFLIIVFVWVNFYFGNF

YKNGVCFPLYDQTEDIGSKGYSLGIFLGVNLLAFLIIVFSYITMFCSIQKTALQTT

EVRNCFGREVAVANRFFIFVSDAICWIPVFVVKILSLFRVEIPDTMTSWIVIFFLPV

NSALNPILYTLTNTNFFKDKLKQLLHKHQKRSIFKIKKKSLSTSIVWIEDSSSLKLGVL
NKITLGDSIMKPVS"

ORIGIN

```
1 gaacttacta catcagaact cctgctgagg tataagagga tacgtctaata aactcaattg
61 ctgtaaacct atgattggtt ttctggtttt taaacatctc ttcagcctca gattgattac
121 aatgttcttt ctacttcatt tcatcggtct gatcaatgtc aaagattttg cactgactca
181 aggtagcatg atcactcctt catgccaaaa aggatatatt ccctgtggga atcttaccaa
241 gtgcttacct cgagcttttc actgtgatgg caaggatgac tgtgggaacg gggcggacga
301 agagaactgt ggtgacacta gtggatgggc gaccatattt ggcacagtgc atggaaatgc
361 taacagcgtg gccttaacac aggagtgtt tctaaaaacag tatccacaat gctgtgactg
421 caaagaaact gaattggaat gtgtaaatgg tgacttaaaag tctgtgccga tgatttctaa
481 caatgtgaca ttactgtctc ttaagaaaaa caaaatccac agtcttcag ataaagtttt
541 catcaaatac acaaaactta aaaagatat tcttcagcat aattgcatta gacacatatc
601 caggaaagca ttttttgat tatgtaatct gcaaattatt tatctcaacc acaactgcat
661 cacaaccctc agacctgga tattcaaaga cttacatcag ctaacttggc taattctaga
721 tgacaatcca ataaccagaa ttccacagcg cttgtttacg ggattaaatt ccttgttttt
781 cctgtctatg gtttaataact acttagaagc tcttcccaag cagatgtgtg cccaaatgcc
841 tcaactcaac tgggtggatt tgggaaggca tagaataaag tatctcacia attctacgtt
901 tctgtcgtgc gattcgtctc cagtgtgtt tctgcctaga aatcaaattg gttttgttcc
961 agagaagaca ttttcttcat taaaaattt aggagaactg gatctgtcta gcaatacgat
1021 aacggaacta tcacctcacc tttttaaaga cttgaagctt ctacaaaagc tgaacctgtc
1081 atccaatcct cttatgtatc ttcacaagaa ccagtttgaa agtcttaaac aacttcagtc
1141 tctagacctg gaaaggatag agattccaaa tataaacaca cgaatgttcc aacctatgaa
1201 gaatctttct cacatttatt tcaaaaactt tcgatactgc tctatgtctc cccatgtccg
1261 aatatgtatg cccttgacgg acggcatttc ttcatttgag gacctcttgg ctaacaatat
1321 cctcagaata tttgtctggg ttatagcttt cattacctgc tttggaaatc tttttgtcat
1381 tggcatgaga tctttcatta aagctgaaaa tacaactcac gctatgtcca tcaaaatcct
1441 ttgttgtgct gattgcctga tgggtgttta cttgttcttt gttggcattt tcatataaaa
1501 ataccgaggg cagtatcaga agtatgcctt gctgtggatg gagagcgtgc agtgccgctt
1561 catgggggtc ctggccatgc tgtccacoga agtctctgtt ctgctactga cctacttgac
1621 tttggagaag ttcttggtca ttgtcttccc cttcagtaac attcgacctg gaaaacggca
1681 gacctcagtc atctcattt gcatctggat ggcgggattt ttaatagctg taattccatt
1741 ttggaataag gattattttg gaaactttta tgggaaaaat ggagtatgtt tcccacttta
1801 ttatgaccaa acagaagata ttggaagcaa aggtatttct cttggaattt tccataggtg
1861 gaacttgctg gcttttctca tcattgtgtt ttctatatt actatgttct gttccattca
1921 aaaaaccgcc ttgcagacca cagaagtaag gaattgtttt ggaagagagg tggctgttgc
1981 aaatcgtttc ttttttatag tgttctctga tgccatctgc tggattcctg tatttgtagt
2041 taaaatcctt tccctcttcc gggtggaat accagacaca atgacttctt ggatagtgat
2101 ttttttctt ccagttaaca gtgctttgaa tccaatctc tatactctca caaccaactt
2161 ttttaaggac aagttgaaac agctgctgca caaacatcag aggaaatcaa ttttcaaaat
2221 taaaaaaaaa agtttatcta catccattgt gtggatagag gactcctctt ccctgaaact
2281 tgggggtttt aacaaaataa cacttggaag cagtataatg aaaccagttt cctagcaatc
2341 attttggatc actggacttt cagtggacta cctaaaacag gggacagctt ttggaagatg
2401 acatctgcaa tgcttttcat ctttaccaac ggcaag
```

Disclaimer | Write to the Help Desk
NCBI | NLM | NIH

Mar 15 2004 07:22:16

APHVRCMPLTDGISSFEDLLANNILRIFVWVIAFITCFGNLFVIGMRSFIKAENTTH
 AMSIKILCCADCLMGVYLFFVGFIDIKYRGQYQKYALLWMESVQCRLMGFLAMLSTEV
 SVLLLTYLTLKFLVIVFPFSNIRPGKRQTSVILICIWMAGFLIAVIFWNKDYFGNF
 YGKNGVCFPLYDQTEDIGSKGYSLGIFLGVNLLAFLIIVFSYITMFCSIQKTALQTT
 EVRNCFGREVAVANRFFFIVFSDAICWIPVFVVKILSLFRVEIPDTMTSWIVIFFLPV
 NSALNPILYTLTTNFFKDKLKQLLHKHQKRSIFKIKKKSLSLTSIVWIEDSSSLKLGLV
 NKITLGDSIMKPSV"

ORIGIN

```

1  actcactata gggctcgagc ggccgcccgg gcaggtgaac ttactacatc agaactcctg
61  ctgaggtata agaggatacg tctaataact caattgctgt aaacctatga ttgtttttct
121 ggttttttaa catctcttca gcctcagatt gattacaatg ttctttctac ttcatttcat
181 cgttctgatc aatgtcaaag attttgact gactcaaggt agcatgatca ctcttctatg
241 ccaaaaagga tattttcctt gtgggaatct taccaagtgc ttaccccgag cttttcactg
301 tggatggcaag gatgactgtg ggaacggggc ggacgaagag aactgtggtg acactagtgg
361 atgggcgacc atatttggca cagtgcattg aaatgctaac agcgtggcct taacacagga
421 gtgctttcta aaacagtatc cacaatgctg tgactgcaa gaaactgaat tggaatgtgt
481 aaatggtgac ttaaagtctg tgccgatgat ttctaacaat gtgacattac tgtctcttaa
541 gaaaaacaaa atccacagtc ttccagataa agttttcatc aaatacacia aacttaaaaa
601 gatatttctt cagcataatt gcattagaca catatccagg aaagcatttt ttggattatg
661 taatctgcaa atattatata tcaaccacia ctgcatcaca accctcagac ctggaatatt
721 caaagactta catcagctaa cttggctaata tctagatgac aatccaataa ccagaatttc
781 acagcgttgg ttacgggat taaattcctt gtttttcctg tctatgggta ataactactt
841 agaagctctt cccaagcaga tgtgtgcccc aatgcctcaa ctcaactggg tggatttggg
901 aggcaataga ataaagtatc tcacaaattc tacgtttctg tcgtgcgatt cgctcacagt
961 gctgtttctg cctagaaatc aaattggttt tgttccagag aagacatttt cttcattaaa
1021 aaatttagga gaactggatc tgtctagcaa tacgataacg gagctatcac ctcacctttt
1081 taaagacttg aagcttctac aaaagctgaa cctgtcatcc aatcctctta tgtatcttca
1141 caagaaccag tttgaaagtc ttaaacaact tcagtctcta gacctggaaa ggatagagat
1201 tccaaatata aacacacgaa tgtttcaacc catgaagaat ctttctcaca tttatttcaa
1261 aaactttcga tactgtcctt atgtcctcca tgtccgaata tgtatgcctt tgacggacgg
1321 cattttctta tttgaggacc tcttggtctaa caatacctc agaataattg tctgggttat
1381 agctttctat accctgtttg gaaatctttt tgtcattggc atgagatctt tcattaaagc
1441 tgaaaatata actcacgcta tgtccatcaa aatcctttgt tgtgctgatt gcctgatggg
1501 tgtttacttg ttctttgttg gcattttcga tataaaatac cgagggcagt atcagaagta
1561 tgccttgctg tggatggaga gcgtgcagt cgcctcatg gggttcctgg ccatgctgtc
1621 caccgaagtc tctgttctgc tactgacctt cttgactttg gagaagttcc tggctattgt
1681 cttcccttcc agtaacattc gacctggaaa acggcagacc tcagtcatcc tcatttgcac
1741 ctggatggcg ggatttttaa tagctgtaat tccattttgg aataaggatt attttggaaa
1801 cttttatggg aaaaatggag tatgtttccc actttattat gaccaaacag aagatattgg
1861 aagcaaaggg tattctcttg gaattttcct aggtgtgaac ttgctggctt ttctcatcat
1921 tgtgttttcc tatattacta tgttctgttc cattcaaaaa accgccttgc agaccacaga
1981 agtaaggaat tgttttggaa gagaggtggc tgttgcaaat cgtttctttt ttatagtgtt
2041 ctctgatgcc atctgctgga ttctgtatt tgtagttaa atcctttccc tcttccgggt
2101 ggaaatacca gacacaatga ctctcagat agtgattttt ttcttccag ttaacagtgc
2161 tttgaatcca atcctctata ctctcacaac caactttttt aaggacaagt tgaaacagct
2221 gctgcacaaa catcagagga aatcaatttt caaaattaaa aaaaaagtt tatctacatc
2281 cattgtgtgg atagaggact cctcttccct gaaacttggg gttttgaaca aaataacact
2341 tggagacagt ataatagaac cagtttctta gcaatcattt tggatcactg gacttccagt
2401 ggactaccta aaacagggga cagcttttgg aagatgacat ctgcaatgct ttctatcttt
2461 accaacggca agcctttctg cacagagagc acagcagaat ggctcctgtc actgcattcc
2521 aatggcagct gtactatcta ccaaccatgc tgaggacagc accaaagggt cctctcctca
2581 ccccatatgc ctgaaaagca catgtgaatt cgtgtatagt gggctgaggt gcagctgac
2641 tctagctaat caacacaacc caccaacaaa tgaccacagg ttggcactgt gtggtctttc
2701 acatcgggtt gcaactgtcca tgaaatagaa aactcacia catctgattc cagtgtggcc
2761 ataataacag aaatctaaca actctttcct tgccttttca atatcaaata aaaccatcag
2821 catcctgctg gattgata

```

//

[Disclaimer](#) | [Write to the Help Desk](#)

[NCBI](#) | [NLM](#) | [NIH](#)

Mar 15 2004 07:22:16

Mutations of the *GREAT* gene cause cryptorchidism

Ivan P. Gorlov¹, Aparna Kamat¹, Natalia V. Bogatcheva¹, Eric Jones², Dolores J. Lamb^{2,3}, Anne Truong¹, Colin E. Bishop^{1,4}, Ken McElreavey⁵ and Alexander I. AgoulNIK^{1,*}

¹Department of Obstetrics and Gynecology, ²Scott Department of Urology, ³Department of Molecular and Cellular Biology and ⁴Human and Molecular Genetics Department, Baylor College of Medicine, Houston, TX 77030, USA and

⁵Reproduction, Fertility and Populations, Institut Pasteur, 75724, Paris Cedex 15, France

Received May 20, 2002; Revised and Accepted July 17, 2002

DDBJ/EMBL/GenBank accession no. AF453828

In humans, failure of testicular descent (cryptorchidism) is one of the most frequent congenital malformations, affecting 1–3% of newborn boys. The clinical consequences of this abnormality are infertility in adulthood and a significantly increased risk of testicular malignancy. Recently, we described a mouse transgene insertional mutation, *crsp*, causing high intraabdominal cryptorchidism in homozygous males. A candidate gene *Great* (G-protein-coupled receptor affecting testis descent), was identified within the transgene integration site. *Great* encodes a seven-transmembrane receptor with a close similarity to the glycoprotein hormone receptors. The *Great* gene is highly expressed in the gubernaculum, the ligament that controls testicular movement during development, and therefore may be responsible for mediating hormonal signals that affect testicular descent. Here we show that genetic targeting of the *Great* gene in mice causes infertile bilateral intraabdominal cryptorchidism. The mutant gubernaculae fail to differentiate, indicating that the *Great* gene controls their development. Mutation screening of the human *GREAT* gene was performed using DHPLC analysis of the genomic DNA from 60 cryptorchid patients. Nucleotide variations in *GREAT* cDNA were found in both the patient and the control populations. A unique missense mutation (T222P) in the ectodomain of the *GREAT* receptor was identified in one of the patients. This mutant receptor fails to respond to ligand stimulation, implicating the *GREAT* gene in the etiology in some cases of cryptorchidism in humans.

INTRODUCTION

A distinctive manifestation of male dimorphism in many animals is a scrotal position of the gonads. During development the testes descend through a complex, multistage process whereby the embryonic gonads migrate from their initial abdominal position to the scrotum. Failure of this process causes undescended testes or cryptorchidism, which in humans represents one of the most common birth defects (1,2). The clinical consequences of this abnormality are infertility in adulthood and a significantly increased risk of testicular malignancy (3,4).

Testicular descent in mammals consists of two major stages: transabdominal and inguinoscrotal descent (1). During both stages, a crucial role has been attributed to the genital mesentery connecting the gonads and genital ducts to the abdominal wall (1,2,5). Specifically, two ligaments direct movements of the testis. The caudal genital ligament, or gubernaculum, undergoes intensive differentiation in males, whereas the cranial suspensory ligament (CSL) gradually regresses (1,5). During the first transabdominal stage [between 10 and 15 weeks of gestation in human embryos and between

15.5 and 17.5 d.p.c (days post coitum) in mice], the testes remain close to the future inguinal region during enlargement of the abdominal cavity. In contrast, in the female, the ovary moves relatively more cranially. During the inguinoscrotal phase of migration, which ends at birth in humans, the testes move from the inguinal region to the scrotum. This occurs in parallel with a shortening of the gubernacular cord, outgrowth of the gubernacular bulb and eversion of the cremaster muscle. In mice, the inguinoscrotal phase occurs within 2–3 weeks after birth (1).

A critical role in testicular descent has been attributed to hormones (6,7). Fetal testicular testosterone appears to play a key role in the prevention of the outgrowth of the cranial gonadal ligaments. Mice lacking androgen receptors (*Tfm*) have testicular feminization, with intraabdominal testes situated at the level of the bladder neck and no eversion of the scrotal sac (8,9). *Tfm* male mice, as well as male rats treated prenatally with antiandrogens, retain the cranial suspensory ligament (8,10). The connection between cryptorchidism and hormones is also manifested in congenital disorders that cause hypogonadism or androgen resistance, such as functional prepubertal castrate syndrome, Noonan syndrome, Klinefelter

*To whom correspondence should be addressed at: Department of Obstetrics and Gynecology, Baylor College of Medicine, 6550 Fannin Street, Suite 861, Houston, TX 77030, USA. Tel: +1 7137986087; Fax: +1 7137985074; Email: agoulNIK@bcm.tmc.edu

syndrome, Reifenstein syndrome and hypogonadotropic eunuchoidism (11).

Mutation of the testicular hormone *Ins13* (insulin-like factor 3, also called Rlf, relaxin-like factor) in the mouse results in bilateral intraabdominal cryptorchidism, due to impaired development of the gubernaculum (12,13). *Ins13* is expressed in pre- and postnatal Leydig cells in the testis and at reduced levels in postnatal thecal cells of the ovary (14,15). It has been suggested that *Ins13* may act as an inducer of the growth and differentiation of the gubernaculum, thereby mediating trans-abdominal testicular descent (13). The receptor for *Ins13* remains unknown.

Recently, we described a mouse transgene insertional mutation, *crsp*, causing high intraabdominal cryptorchidism in homozygous males (16). The integration was accompanied by a 550 kb deletion in the proximal part of chromosome 5, affecting several genes in the region. Direct sequencing of the affected region led to the identification of a new gene, named *Great* (16). The gene encodes a novel G-protein-coupled receptor (GPCR) and belongs to the same family of GPCRs as three glycoprotein hormone receptors (FSHR, LHR and TSHR). Expression of *Great* is restricted to the testis, brain and skeletal muscles, with the highest level of expression in the gubernaculum, making this gene an excellent candidate for the mutant phenotype.

In the present work, we show that genetic targeting of the *Great* gene in mice causes infertility secondary to bilateral intraabdominal cryptorchidism. The gubernaculae of the mutant males fail to differentiate, indicating that the *Great* gene controls their development. Furthermore, we have cloned the human *GREAT* gene and screened genomic DNAs from 60 cryptorchid patients for mutations within the gene. Several nucleotide substitutions were found in *GREAT* cDNA, in both the patient and the control populations. A unique missense mutation (T222P) in the ectodomain of the *GREAT* receptor has been identified in one of the patients. We established that relaxin, recently identified as a ligand for the *GREAT* receptor (17), fails to stimulate cAMP production in cells transfected with the mutant receptor.

RESULTS

Genetic targeting of the *Great* gene in mice results in high intraabdominal cryptorchidism

To assess the role of the *Great* gene in the cryptorchid phenotype of the *crsp* mutation, we have produced animals with a mutant allele of the gene. We have targeted *Great* in ES cells using insertional-type constructs (18). Targeting of the gene resulted in the duplication of exons 12–16 and insertion of the 10 kb vector DNA into the 16th intron (Fig. 1). Heterozygous *Great*^{ko/+} males and females showed a normal phenotype. Crosses of the heterozygous carriers with the original *crsp* mice produced *crsp/Great*^{ko} double heterozygotes. Intercrossing between heterozygous *Great*^{ko/+} animals resulted in the production of *Great*^{ko/Great}^{ko} homozygotes. Analysis of the testicular phenotype in 14 *Great*^{ko/Great}^{ko} males and >50 *crsp/Great*^{ko} males reveals that these animals exhibit the same high intraabdominal cryptorchidism observed

in the original *crsp* mutation (Fig. 2A). All tested heterozygous males had a fertile wild-type phenotype with a normal scrotal position of the testes. The size of the adult mutant testes is significantly decreased. At 60 days, the average testis weight of the wild-type and heterozygous *Great*^{ko/+} animals was 84.5 ± 5.3 mg (*n* = 8) and the *crsp/Great*^{ko} testis weight was 31.0 ± 1.1 mg (*n* = 6) (a 63% reduction). Furthermore, histological examination reveals progressive degeneration of the spermatocytes, with absence of spermatids and mature sperm (Fig. 2B). As in original *crsp* mutants, gubernacular development in *Great* knockout males is distinctively altered. The mutant mice have an extended thread-like gubernaculum, and the inguinal canal fails to form. Other urogenital structures in the mutant males are normal, including the seminal vesicles, prostate and external genitalia. Mutant males exhibit normal mounting and copulatory behavior. Vaginal plugs are present in females after copulation with mutant males, indicating that the males produce an ejaculate.

Analysis of *Great* gene expression at the RNA level by RT-PCR revealed the presence of a specific RNA transcript in the *crsp/Great*^{ko} mutant animals. We detected *Great* mRNA using a primer pair derived from exons 9 and 16 (before vector insertion) and primers from exons 17–18 (after vector insertion) (Fig. 2C) (16). RT-PCR with primers from exons 2 and 18 failed to amplify the expected 2 kb cDNA fragment from *crsp/Great*^{ko} brain RNA (Fig. 2C), however, indicating inclusion of the backbone of the targeting vector DNA into the cDNA transcript (18) and the absence of properly processed *Great* cDNA.

The first stage of testicular descent (the transabdominal stage) occurs in mice between 15.5 and 17.5 d.p.c. (1). We analyzed expression of the *Great* gene by northern blot hybridization in mouse embryos at 7–18 d.p.c. Expression of the *Great* gene was detected as early as in 7 d.p.c. embryos, with stable expression on 11 d.p.c. and thereafter (Fig. 3). Four different bands have been detected on the northern blot, apparently representing several alternatively spliced transcripts (Fig. 3). In RNA isolated from mouse or human brain, the main transcript is ~4.4 kb; in testis, it is ~1.6 kb (data not shown).

Cloning of the human *GREAT* gene

The human *GREAT* cDNA was predicted through comparisons of the mouse cDNA with corresponding human genomic sequence from chromosome 13q12–13 upstream of the *BRCA2* region. Subsequently, full-length cDNA has been isolated by RT-PCR from a human gubernaculum RNA sample (GenBank accession no. AF453828). Comparison of the human and mouse cDNA sequences revealed that the human open reading frame starts 51 bp 5' to the first mouse ATG codon. This leads to the additional 17 amino acids at the N-terminal end of the human *GREAT* product. Overall identity of the mouse and human *GREAT* genes is 82% at nucleotide and amino acid level. The human gene has the same exon-intron structure as its mouse counterpart. Phylogenetic analysis of the mouse and human *GREAT* receptors shows that they belong to the LGR group of receptors, with the highest homology to the LGR7 receptor (19). Hsu *et al.* (17) named the human *GREAT* gene *LGR8* to indicate its close homology to the other members of the LGR group. *GREAT* is a third

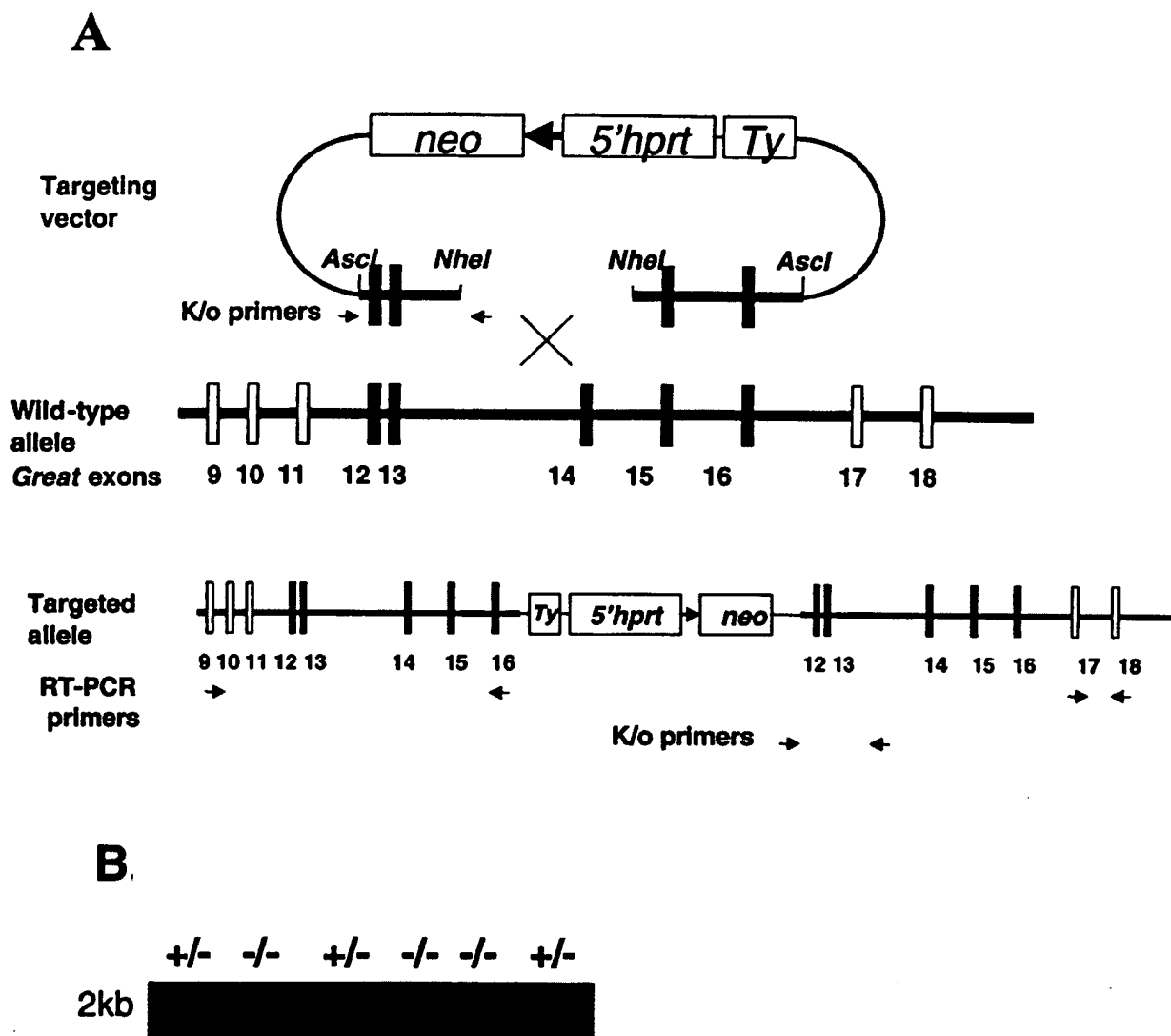


Figure 1. Generation of mice with a mutant allele of the *Great* gene. (A) An insertional targeting construct (top) was prepared through isolation of the phage containing *Great* exons 12–16 from the *5'hpri* genomic library (18), converting phage into a plasmid and creating a gap with *NheI* restrictase. *Neo*, neomycin resistance cassette; *5'hpri*, 5' half of the *hpri*; *Ty*, tyrosinase minigene; the *loxP* site is shown as a thick arrow, the *Great* genomic fragment is in bold, and black and white boxes represent *Great* exons. The wild-type chromosome is in the middle. After homologous integration (bottom) of the targeting construct, the *NheI* gap is repaired, the backbone of the targeting vector is inserted into the chromosome, and the genomic fragment included into targeting vector is duplicated (exons in black). To verify homologous integration, we have used PCR analysis of the embryonic stem (ES) cell DNA with one primer designed from the vector backbone and the other designed from the genomic sequence deleted from the targeting construct (K/o primers). Also indicated are the positions of the primers used to assess presence of *Great* transcripts in the RNA isolated from *Great*^{+/crsp} males (RT-PCR primers). (B) Identification of the ES recombinant clones with a mutation of the *Great* gene. The mutant allele (+/–) contains both K/o primers, providing successful amplification of the 2 kb DNA fragment.

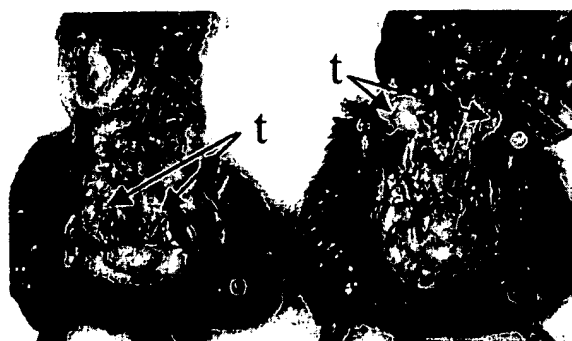
member of the leucine-rich repeat (LRR) subgroup, with a hallmark LDL-receptor domain at the N-terminal region of the protein (19).

Mutation analysis of the *GREAT* gene in cryptorchid patients

Cryptorchidism is a common human congenital abnormality with a multifactorial etiology that likely reflects the involvement of endocrine, environmental and hereditary factors. Eighteen

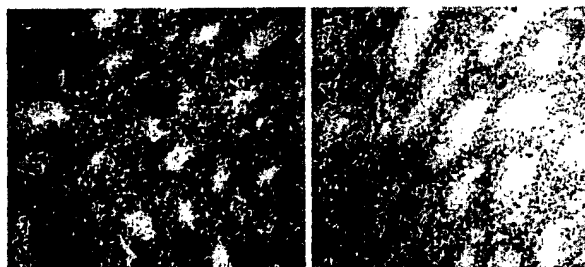
exons of the *GREAT* gene have been identified and subjected to mutation analysis using a recently developed high-throughput denaturing high-performance liquid chromatography (DHPLC) approach (20) and direct sequencing. We performed a mutation screen of the human *GREAT* gene in 61 cases of idiopathic unilateral or bilateral cryptorchidism. The results of the mutation analysis are shown in Figure 4. Two silent mutations were observed in exon 12, in both cryptorchid (40 out of 61) and normal men. These are the A/G transversions at nucleotide positions 957 and 993 (position 1 is taken as the first A of the

A.



B.

+/crsp

Great^{ko}/crsp

C.

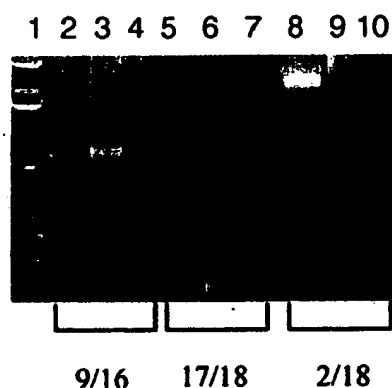


Figure 2. Phenotype of *Great*^{ko}/*crsp* males. (A) Undescended testes in *Great*^{ko}/*crsp* male mice. In the mutant mouse (right), the testes (t) are located in a high intraabdominal position near the kidneys and are much smaller than the wild-type *+/crsp* heterozygous testes (left). (B) Testes histology of *Great*^{ko}/*crsp* mice. Hematoxylin-eosin-stained sections of 4-week-old wild-type testis (left, $\times 10$) and mutant cryptorchid testis (right, $\times 10$) are shown. Note the absence of spermatogenesis, vacuolization of the Sertoli cells and lesions of the seminiferous epithelium in the mutant. (C) RT-PCR analysis of *Great* gene expression in *Great*^{ko}/*crsp* males. RNA was isolated from brains of the *+/crsp* (lanes 2, 5 and 8) and *Great*^{ko}/*crsp* (lanes 3, 6 and 9) mice. Primer pairs located before (exons 9 and 16, lanes 2-4) and after (exons 17 and 18, lanes 5-7) integration of the vector backbone (see Fig. 1) produced RT-PCR fragments indicating the presence of *Great* transcripts in the mutant animals. Use of the primers corresponding to the second and last exons of the *Great* gene (exons 2 and 18, lanes 8-10) failed to amplify an expected 2 kb fragment from *Great*^{ko}/*crsp* RNA, indicating the absence of properly spliced transcripts in the mutant. Lane 1, 1 kb Plus Ladder (Life Technologies, Rockville, MD); lanes 4, 7 and 10, mouse genomic DNA as a negative control.

a polymorphic allele not associated with a cryptorchid phenotype.

In one of the patients of European origin, we identified a unique mutation in exon 8 (Fig. 4B). The patient had bilateral cryptorchidism, with the gonads located in the inguinal canal at the external ring. The mutation resulted in an A-to-C nucleotide change at position 664, and was in heterozygous condition. This nucleotide change causes a missense substitution T222P. Analysis of the 192 control samples (162 from the same geographical area as the mutant carrier) did not reveal a sequence variation in this position. Importantly, no other variations in 18 exons of the *GREAT* gene of this patient have been detected. Direct sequencing of the 350 bp fragment upstream of the ATG codon also did not reveal any variations.

Signal transduction by wild-type, I604, and T222P variants of *GREAT*

It was shown recently that relaxin, a hormone important for the growth and remodeling of reproductive and other tissues during pregnancy is capable of activating the *GREAT* receptor through an adenosine 3', 5'-monophosphate (cAMP)-dependent pathway (17). To investigate the significance of the amino acid substitution in the mutant receptor, we have analyzed relaxin-induced signal transduction in cells transfected with a wild-type and a mutant cDNA. The cAMP concentration was determined in the transfected cells treated with increasing amounts of relaxin. As shown in Figure 5, treatment of cells transfected with a wild-type or mutant I604V *GREAT* cDNA with relaxin resulted in dose-dependent increases in cAMP production. In contrast, cAMP levels in cells transfected with a mutant T222P *GREAT* showed little response in cAMP production.

In the next experiment, we have co-transfected wild-type receptor cDNA with either T222P mutant or an empty vector DNA to study possible interactions between wild-type and mutant polypeptides. As shown in Figure 6, relaxin stimulation causes the same increase in cAMP production in both cases, indicating that the non-functional mutant receptor does not affect the signaling properties of the wild-type protein coexpressed in cells.

initiation codon). Three different haplotypes were detected: A957 and A993, A957 and G993, and G957 and G993.

In four cryptorchid men, an A/G transversion was observed at nucleotide position 1810 in the fifth transmembrane domain. This nucleic acid substitution is predicted to result in a conservative amino acid change of an isoleucine to a valine residue (I604V). The same sequence variant was detected in 2 out of 30 controls. Thus this sequence variant is most likely

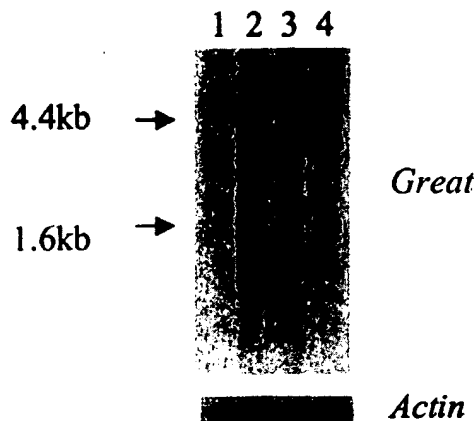


Figure 3. Northern blot analysis of the *Great* gene in developing mouse embryos. Four *Great* transcripts can be seen, with their size shown on the left. To control the amount of RNA in different lanes, hybridization of the same blot with β -actin is shown at the bottom of the figure. Expression of the *Great* gene can be detected in the 7 d.p.c. embryo, with stable expression after day 11. Lane 1, 7-day embryo; lane 2, 11-day embryo; lane 3, 15-day embryo; lane 4, 17-day embryo.

DISCUSSION

Recently we have described a new mouse transgene insertional mutation, *crsp*, causing intraabdominal cryptorchidism in homozygous males. Transgene insertion caused a 550 kb deletion in the distal part of chromosome 5. Positional cloning lead to the identification of a new G-protein-coupled receptor gene, *Great*, deleted in the *crsp* mice. Based on the high level of *Great* expression in the gubernaculum, the mesentery ligament playing a critical role in testicular descent during development, we proposed that *Great* is indeed responsible for the cryptorchid phenotype in *crsp* mice. Using a gene targeting approach, we showed here that the mutation of the gene caused the same testicular abnormality both in homozygous *Great*^{ko}/*Great*^{ko} males and in *Great*^{ko}/*crsp* compound heterozygotes. Notably, all mutant males exhibit the same testicular abnormality, regardless of genetic background. The *Great*^{ko}/+ heterozygous males had a normal wild-type phenotype. The high abdominal position of the testes in the *Great*^{ko}/*Great*^{ko} males suggests that the first, androgen-independent, phase of testicular descent is affected by this mutation. Significantly, analysis of *Great* expression during mouse development showed a marked increase during this period. The gubernaculum fails to differentiate in the mutant male, apparently not responding to extracellular developmental signals.

Based on the remarkable similarity between the testicular phenotype of the *Great* mutant mice and *Ins13* knockout mutants (12,13) we have suggested previously (16) that *Ins13* could in fact be an endogenous ligand for the GREAT receptor. Confirming this prediction, relaxin (a hormone closely related to *Ins13*) was shown to be able to activate GREAT receptor signaling through a cAMP-dependent pathway (17). Significantly, mutation of relaxin does not cause testicular abnormalities (21), indicating that *Ins13* may be the true cognate ligand of *Great* during development of the male gonads. It is interesting to note that *Great*^{ko}/*Great*^{ko} females

have normal fertility and litter size, and a normal development of mammary glands (N. Bogatcheva and A.I. AgoulNIK, unpublished data), in contrast to the relaxin or *Ins13* mutants (13,21,22). It is possible that LGR7, which is closely related to the GREAT GPCR receptor (17,19), may be responsible for the signaling of relaxin and/or *Ins13* in females.

We have cloned the human *GREAT* gene and performed a mutation analysis in 61 cryptorchid patients. Several polymorphic sites have been identified within the *GREAT* gene, and are present in both the control and the patient population. We detected one functionally deleterious mutant allele of the *GREAT* gene among 61 patients with the diagnosis of clinical cryptorchidism. Notably, only half of the patients (26 out of 49) had bilateral cryptorchidism, including mutant carriers. A more expanded analysis is obviously needed to estimate the significance of *GREAT* mutations in the occurrence of human disease. The primary analysis using the DHPLC approach may result in some underestimation of the frequency of mutations. The reported sensitivity of the DHPLC screening of unknown mutations varies, and depends strongly on the presence of a high-melting-point DNA domain embedded in a low-melting-point sequence (20). Neither the DHPLC approach nor direct sequencing of the PCR fragments can detect partial deletions (if the breakpoint of the deletion lies outside of the amplicons) or complete deletions of one of the alleles.

Two polymorphic sites have been found in the 12th exon of the *GREAT* gene. Both substitutions are synonymous—they do not alter the amino acid sequence. In some patients, as well as in control samples, we found a nucleotide substitution in the predicted fifth transmembrane domain (1604V). Interestingly, the corresponding mouse sequence also contains a valine. These results imply that the predicted amino acid substitution is evolutionarily more conserved, present in the general population and probably not associated with the abnormal phenotype. Direct measurements of the relaxin-mediated stimulation of this variant did not reveal differences in comparison with the wild-type protein.

A unique T222P mutation found in one of the patients with bilateral cryptorchidism is located in the fourth LRR of the receptor ectodomain. LRRs, which are among the most common module found in the extracellular regions of proteins, consist of alternatively spaced α helices and β strands that are positioned parallel to each other. In ectodomains of glycoprotein hormone receptors, numerous LRRs form a horseshoe-shaped structure (23). It is generally believed that this structure is essential for glycoprotein hormone binding (24,25). Although neither relaxin nor *INS13* belong to the family of glycoprotein hormones, we suggested that a mutation in one of the LRRs could impair the binding of the receptor with a ligand and/or downstream transmission of the signal. Indeed, we have shown that the mutant receptor is not able to mediate relaxin-induced cAMP production.

The analysis of the secondary structure of the protein region surrounding the mutation site in the receptor predicted destabilization of the α helices. PHD (profile network prediction Heidelberg, <http://www.ebi.ac.uk/~rost/predictprotein/>) analysis showed that the mutant receptor has higher structural flexibility in the region surrounding proline 222 in the fourth LRR compared with the same region in the wild-type protein (threonine 222). The T222P substitution can therefore cause a

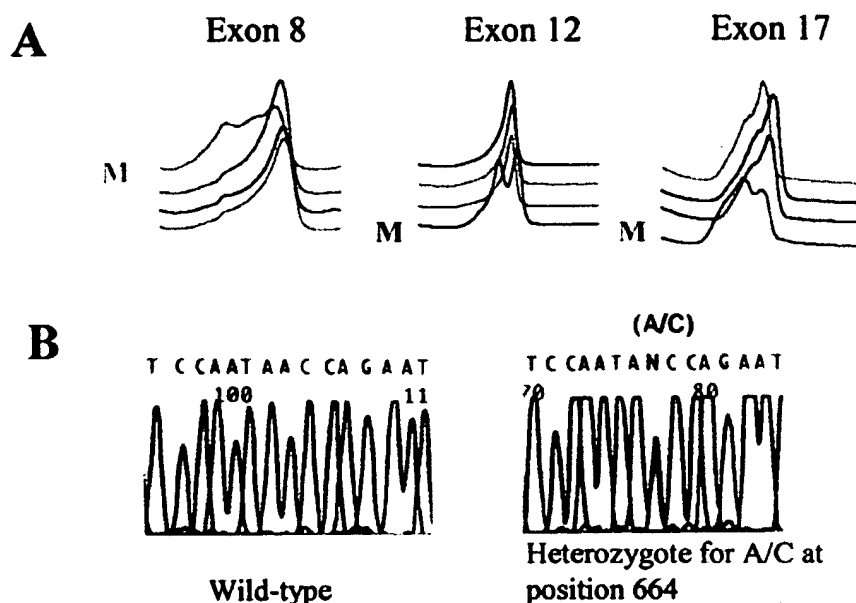


Figure 4. Mutation analysis of the *GREAT* gene in cryptorchid patients. (A) DHPLC profiles showing sequence variations in exons 8, 12 and 17. In each case, three homozygous wild-type and one heterozygous mutant (M) profiles are shown. The presence of the DNA heteroduplex can be seen as a double-peak profile. (B) Sequence variation detected by direct sequencing of the PCR fragment corresponding to exon 8 from patient 1F (right) and wild-type control (left). An A-to-C nucleotide substitution at position 664 is in heterozygous condition.

deterioration in relaxin-GREAT signal transduction, either through impairing ligand binding or through modification of the relaxin-induced conformational changes essential for G-protein activation. Thus, mutations in the GREAT receptor can be responsible for the cryptorchid phenotype by directly affecting the proposed INSL3 signaling during development.

The other possibility is that the mutant receptor is not properly expressed or localized in the cells. As, in the experiments described in this study, we did not monitor cell membrane expression of the transfected receptor, we cannot formally exclude such a scenario. Nevertheless, the facts that mutation occurred in the middle of the extracellular part of the receptor, and similar mutants of other glycoprotein hormone receptors are expressed correctly, indicate that there is a functional defect of the mutant receptor. Regardless of the specific mechanisms, T222P mutation is functionally inactive.

The question arises as to why the human patient heterozygous for T222P mutation has bilateral cryptorchidism whereas *crsp*^{+/+} or *Great*^{ko/+} heterozygous mice show no testicular descent abnormalities. Several possible explanations can be put forward. Obviously, there is a clear difference between deletion mutations in the mouse and the missense mutation in the human. In the latter case, both alleles are apparently expressed in heterozygotes, producing mutant and wild-type receptor. It is interesting to note that the abnormality in patient is less severe than in the mouse mutants, indicating that there is some degree of receptor signaling. One explanation is that the mutant receptor might bind the ligand, competing with the wild-type receptor and thus compromising the response to hormone stimulation. The mutant receptor may also irreversibly sequester G proteins and stoichiometrically inhibit G signalling in a dominant-negative manner, as shown

previously for α_{1B} -adrenergic GPCR (26). However, the co-transfection experiments with wild-type and mutant receptors did not support this scenario. At least *in vitro*, under the conditions used in our experiments, there was no interaction or suppression of wild-type receptor signaling. The other reason could be a relatively higher concentration of the cognate ligand in mice than in humans during the prenatal period, or a higher affinity of the mouse receptor for the hormone sufficient to mediate testicular descent even in the presence of only half the amount of receptor. Lastly, we cannot exclude the possibility that the patient with this mutation was in fact compound heterozygous for an additional mutation, located in another exon of the gene. Further analysis of the properties of the mutant and wild-type receptors are now underway to clarify the mechanism of ligand-receptor interaction.

MATERIALS AND METHODS

Gene targeting and production of mice with *Great* mutation

We isolated a genomic λ phage clone containing exons 12–16 of the *Great* gene from a 5' HPRT library (18) kindly provided by A. Bradley. An insertional targeting vector was constructed by conversion of the λ phage into a plasmid, gapping the genomic insert with *NheI*, followed by linearization of the vector with the same restriction enzyme. We electroporated the targeting construct DNA into AB2.1 ES cells and selected recombinant clones with G418 as described previously (18). Analysis of the DNA from ES clones was performed by PCR, with K/o primers derived from the vector backbone and from the *NheI*-deleted

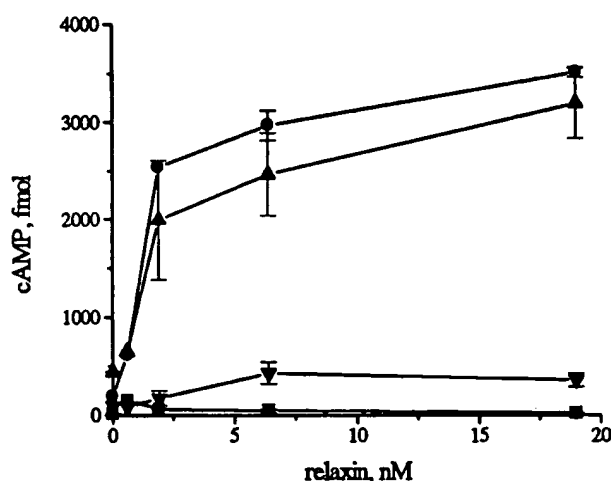


Figure 5. Functional analysis of mutant GREAT receptors. Porcine relaxin stimulates dose-dependent cAMP production in transfected HEK 293T cells expressing wild-type (circle) and mutant I604V (upward-pointing triangles) GREAT. In contrast, relaxin stimulation of cells expressing mutant T222P (downward-pointing triangles) GREAT has little effect on cAMP production. Relaxin does not affect cAMP production in cells transfected with an empty pCR3.1 vector (squares). cAMP Production was normalized based on the efficiency of transfection estimated by the activity of secreted alkaline phosphatase produced by the co-transfected reported pAP-tag5 plasmid. Intracellular cAMP was measured in duplicate by a specific enzyme immunoassay.

fragment: (vector53527) 5'-AGAAGAGCAGAATAGCAGT-3' and (insert-reverse) 5'-ACCGCTCAGGGTCGAACT-3'. During homologous integration, the gap in the targeting vector is repaired and the PCR produces a 2 kb fragment. We injected three selected independent clones into C57BL/6J blastocysts and reimplanted these into pseudopregnant female mice using standard procedures. Chimeric males were bred to C57BL/6J females to produce mice heterozygous for the targeted allele. *Great*^{ko/+} heterozygous males were bred to *crsp/crsp* homozygous females to produce *Great*^{ko/crsp} di-heterozygotes. The presence of the *Great*^{ko} mutant allele was detected by PCR of the tail DNA. Intercrossing of the *Great*^{ko/+} heterozygotes produced homozygous animals, which have been identified by long-range PCR (Roche/Biochemical) with primers outside the genomic fragment used in the targeting vector: (forward) 5'-CATGGTGGGTAACCGGCT-3' and (reverse) 5'-GCAATCCAAAGCCTCTAGC-3'. PCR conditions were denaturation at 94°C for 2 min, 10 cycles of 92°C for 10 s, 55°C for 30 s and 72°C for 15 min, followed by 25 cycles of 92°C for 10 s, 55°C for 30 s and 72°C for 15 min + 20 s per cycle, with a final extension at 72°C for 5 min. Presence of the 16 kb fragment indicates the presence of the wild-type allele.

The animal studies were approved by the Baylor College of Medicine Institutional Committee on animal care.

RT-PCR analysis of gene expression

Total RNA from mouse and human tissues was extracted with the TRIzol reagent (Life Technologies, Rockville, MD). First-strand cDNA was synthesized using the oligo(dT) primer and RETROscript kit (Ambion, Austin, TX). The following primers were used for analysis of *Great* expression: (Receptor2F)

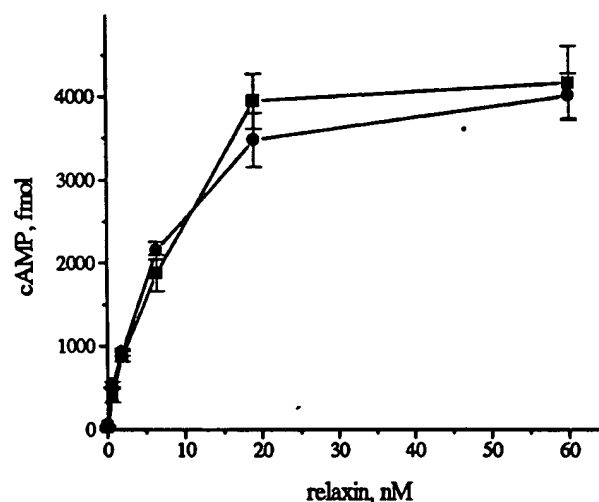


Figure 6. Co-transfection of the mutant T222P and wild-type receptors does not affect relaxin-stimulated cAMP production. Porcine relaxin stimulates a dose-dependent increase in cAMP production in HEK 293T cells transfected with the wild-type receptor and vector DNA (squares) or with mutant and wild-type receptors (circles).

5'-AGCAGTATGGTGGCTCCTCTG-3', (Receptor9F)
5'-ATGGTGGGTAACCGGCTCGAG-3' (Receptor17F)
5'-AAAACAGCCCTTCAGACTGC-3', (Receptor16R)
5'-TCCCATAAAAGTTGCCGAAA-3' and (Receptor 18R)
5'-CCACGATCCAGGAAGTGATT-3'. Cycling conditions were denaturation at 94°C for 1 min, followed by 35 cycles of 94°C for 30 s, 55°C for 30 s and 72°C for 90 s, with a final extension at 72°C for 5 min.

Northern blot analysis

Northern blots with 2 µg of poly(A)⁺ RNA isolated from embryos of different age were used (Clontech Labs, Palo Alto, CA). 1.3 kb 3'-end cDNA of the *GREAT* gene was labeled by random priming (Stratagene, La Jolla, CA) and hybridized overnight in PerfectHyb Plus hybridization buffer (Sigma, USA) at 65°C. Blots were washed under highly stringent conditions at 68°C three times for 30 min with 0.1 × SSC: 0.1% SDS and exposed to Kodak X-Omat film with one intensifying screen at -80°C.

Histopathological analysis

Dissected testes were fixed in Bouin's solution (Sigma), embedded in paraffin, sectioned, and stained with hematoxylin-eosin according to standard protocols. Photomicrographs were taken with an Axiolab microscope equipped with an automatic camera (Karl Zeiss, Germany).

Cloning of the human *GREAT* gene

Eighteen exons of the human *GREAT* gene were identified through BLAST analysis of the human genomic DNA with the mouse cDNA sequence. Primers flanking both sides of the predicted open reading frame (ORF) were designed: [5'-untranslational

Table 1. Primer sequences, PCR annealing temperature and DHPLC melting temperature for 18 exons of the human *GREAT* gene

Exon no.	Primer sequence	PCR annealing temperature (°C)	DHPLC melting temperature (°C)
1	F: CATCAGAACTCCTGCTGAGGT R: TTTTGGGAATTGCACTCATT	52	58
2	F: GAAAATTAAATGGGACAACACG R: CATAAAGTGAGGCACACATGG	55	61
3	F: CAAATTGTTAAATTTTGTGAGATGG R: TCTGTGCATCACAATCATGT	50	56
4	F: GGCTGAATGAGTTTCATTAAACA R: GCACAAGCAACACTATTGGG	55	55, 57
5	F: CAAGCATGTGGCTTCTAGGG R: AAAACATCTTACACCACCACGA	50	56
6	F: CCAACATGAGAATAGGACTTCG R: TCGAGCCTTGAAAAAGTACCA	55	55, 57
7	F: CATAATCATCATCAGTGGCTCA R: TCAAATAGTGAAAACATACATTAGCA	50	56
8	F: GGGGAGGCAGGTTTATTTC R: AAGCTAGTGCTAGATGTCATTGC	55	56, 58
9	F: CTCCTAATCTTTGCCATACA R: TGGCTAGTTTCTTAAATCAGG	55	55, 60
10	F: GGAGGAAAGATAGTAACAACCTGGAA R: CAGTGTCAGACCAAGGCTGT	58	57
11	F: ACTACAGCAGACGCAAAACCC R: CTAGTGGCAAAGCAGTCTCAC	55	58
12	F: TGGCTGACTCATAACGC R: GATTGGATGACAGGTTTCCTT	55	56.5
13	F: GGAACATACCTCACCTT R: GACTTCATACATGTGCAATG	50	55, 57
14	F: AAAACGTTTCATCTCAACACCA R: TTGTTGCATAGAAACACATTGC	50	57.5
15	F: CCCGATAGGACTGCAACTGT R: GTGCCCAGGATGTATAATTCA	55	57
16	F: GACATTGGAAACTGATGACAT R: CACAGTCTTGACTATGTTATCT	55	54, 60
17	F: GGGTAAGGGATACTCAACCT R: GTGTCCTAGACTCTGGCCTT	52	58
18	F: GCATTGACTGCAAAGTGTTATT R: CAAAAGCTGTCCCTGTTTT	55	56.5

region (UTR)] 5'-TCAATTGCTGTAAACCTATGATTG-3' and (3-UTR) 5'-CTTGCCGTTGGTAAAGATGAA-3'. These primers were used to amplify a cDNA with 2265 bp *GREAT* ORF. Both strands of the fragment were sequenced to confirm the predicted splice sites/exons of the gene.

Patient and control DNA samples

A total of 61 cases of idiopathic bilateral or unilateral cryptorchidism were used for the study. Twenty cases of European origin were obtained from French clinics and 41 samples of mixed origin from the Urology Department of Baylor College of Medicine. A total of 193 men of known fertility and absence of a clinical history of cryptorchidism were used as a control. Among them, 62 samples were from France, 100 from Germany and 31 from the USA. The population studies were approved by the authors' Institutional Review Boards.

DHPLC mutation analysis and sequencing

Mutation analysis was performed on an automated WAVE Nucleic Acid Fragment Analysis System according to conditions recommended by the manufacturer (Transgenomic,

Omaha, NE). Using available genomic sequence information, we have designed 18 pairs of primers for amplification of each exon and flanking intron sequence of the human *GREAT* gene (Table 1). PCR was performed in 25 µl volume using *ampliTaq* (Perkin Elmer, Branchburg, NJ), and a 5-µl aliquot was analyzed on agarose gel. Prior to DHPLC analysis, 15 µl (containing 100–300 ng of DNA) of the experimental sample was mixed with 5 µl of the control amplicon. PCR products were then denatured at 95°C for 5 min and gradually cooled down to room temperature at 1°C/min decrements. Gradient parameters were determined based on size and G/C content of the amplicons. DHPLC conditions for successful resolution of heteroduplex formation have been established using the DNA melt software of the WAVEMaker software (Transgenomic). The column temperature was calculated using software supplied with the WAVE system. The predicted melting profiles for 6 exons of the gene required runs at two temperatures, the remaining 12 exons were analyzed at one temperature (Table 1). Chromatograms of the elution profiles obtained from the experimental samples were compared with those of the controls. All samples showing deviation from the wild-type profile were subject to direct sequencing. PCR fragments were separated on an agarose gel and purified

using Ultrafree-DA spin columns (Millipore, Bedford, MA). Both strands of the DNA fragment were sequenced by the dye terminator method on an automated 373 DNA sequencing machine using the same primers as for PCR.

Expression of *GREAT* in mammalian cells

Full-length wild-type *GREAT* cDNA was amplified by RT-PCR from human gubernaculum RNA with 5'-UTR and 3'-UTR primers. The resulting 2.3 kb cDNA was subcloned into the eukaryotic cell expression vector PCR3.1 (Invitrogen, San Diego, CA). Efficient targeting of the receptor to the cell surface was provided by an internal *GREAT* signal peptide encoded by the first 36 amino acids of the cDNA sequence (16). The plasmids were purified using the Concert Midi-prep plasmid preparation kit (Life Technologies, Rockville, MD). The sequence of the construct was verified by sequencing of both strands using gene-specific and vector-derived primers.

To produce targeted mutations in the *GREAT* cDNA, we used the QuikChange Site-Directed Mutagenesis kit from Stratagene (La Jolla, CA). The resulting cDNA sequence was verified by sequencing of both DNA strands. A 1 kb cDNA *EcoRI/HindIII* fragment from the wild-type plasmid was substituted with the same fragment from the mutagenized plasmid; junction sites were verified by sequencing. This final plasmid, containing mutant *GREAT* cDNA, was used for further experiments.

293T cells derived from human embryonic kidney (HEK) fibroblasts were maintained in DMEM supplemented with 10% FBS, 1 mM glutamine, and an antibiotic/antimycotic mixture (all from Life Technologies, Rockville, MD). For the cAMP determination experiment, cells were seeded in 24-well plates one to two days prior to transfection. The cells were transfected at 80% of confluency with 500 ng/well of plasmid of interest and 25 ng/well of reporter plasmid (pAP—tag5, GeneHunter Corporation, Nashville, TN) in OptiMEM without antibiotic using the FuGENE 6 transfection reagent (Roche, Indianapolis, IN). In co-transfection experiments, cells were transfected with 250 ng/well of each plasmid (wild-type plus vector, or wild-type plus mutant). After 24 h, the efficiency of transfection was estimated by the activity of secreted alkaline phosphatase in the media using pNPP as a substrate (Sigma). Cells were stimulated with 0–60 nM porcine relaxin (27) in the presence of 0.25 mM IBMX (Sigma) for 30 min, then harvested by aspiration and centrifuged. The pellet was washed briefly with PBS and extracted with cAMP extraction buffer (Amersham Pharmacia Biotech) for 40 min. Aliquots of supernatant were used in an enzyme immunoassay (Amersham Pharmacia Biotech) for the cAMP determination. The cAMP concentrations in each well were measured in duplicate. All experiments were repeated three times using cells from independent transfections.

ACKNOWLEDGEMENTS

We thank E. Wright, M. Ty and, J. Chronister for excellent technical support, Dr A. Bradley for the lambda phage library, Dr O. D. Sherwood for a generous gift of porcine relaxin, and Dr I. AgoulNIK for helpful comments. We thank Dr D. Kieback

for providing control DNA samples. This research was supported by NIH Grants R01 HD37067 (to A.I.A.) and P01 HD36289 (to A.I.A., D.J.L., and C.E.B.).

Note added in proof

After submission of the manuscript it was reported that chemically synthesized INSL3 peptide could activate *GREAT/LGR8* receptor (Kumagai *et al.*, *J. Biol. Chem.*, in press. Published online July 11, 2002 as Manuscript C200398200).

REFERENCES

- Hutson, J.M., Hasthorpe, S. and Heyns, C.F. (1997) Anatomical and functional aspects of testicular descent and cryptorchidism. *Endocr. Rev.*, **18**, 259–280.
- Husmann, D.A. and Levy, J.B. (1995) Current concepts in the pathophysiology of testicular undescend. *Urology*, **46**, 267–276.
- Kogan, S.J. (1987) Fertility in cryptorchidism. *Eur. J. Pediatric.*, **146**(Suppl. 2), S21–S24.
- Benson, R.C., Beard, C.M., Kelalis, P.P. and Kurland, L.T. (1991) Malignant potential of the cryptorchid testis. *Mayo Clin. Proc.*, **66**, 372–378.
- Barteczko, K.J. and Jacob, M.I. (2000) The testicular descent in human. *Adv. Anat. Embryol. Cell Biol.*, **156**, 1–98.
- Hutson, J.M. and Donahoe, P.K. (1986) The hormonal control of testicular descent. *Endocr. Rev.*, **7**, 270–283.
- Nef, S. and Parada, L.F. (2000) Hormones in male sexual development. *Genes Dev.*, **14**, 3075–3086.
- Lyon, M.F., Glenister, P.H. (1980) Reduced reproductive performance in androgen-resistant *Tfm/Tfm* female mice. *Proc. R. Soc. Lond. B Biol. Sci.*, **208**, 1–12.
- He, W.W., Kumar, M.V. and Tindall, A.J. (1991) A frame-shift mutation in the androgen receptor gene causes complete androgen insensitivity in the testicular-feminized mouse. *Nucleic Acids Res.*, **19**, 2373–2378.
- van der Schoot, P. and Elger, W. (1992) Androgen-induced prevention of the outgrowth of cranial gonadal suspensory ligaments in fetal rats. *J. Androl.*, **13**, 534–542.
- Buyse, M. and Feingold, M. (1979) Syndromes associated with abnormal external genitalia. In Vallet, H.L. and Porter, I.H. (eds), *Genetic Mechanisms of Sexual Development*. New York, Academic Press, pp. 425–435.
- Zimmermann, S., Steding, G., Emmen, J.M., Brinkmann, A.O., Nayem, K., Holstein, A.F., Engel, W. and Adham, I.M. (1999) Targeted disruption of the *Insl3* gene causes bilateral cryptorchidism. *Mol. Endocrinol.*, **13**, 681–691.
- Nef, S. and Parada, L.F. (1999) Cryptorchidism in mice mutant for *Insl3*. *Nat. Genet.*, **22**, 295–299.
- Roche, P.J., Butkus, A., Wintour, E.M. and Tregear, G. (1996) Structure and expression of Leydig insulin-like peptide mRNA in the sheep. *Mol. Cell. Endocrinol.*, **121**, 171–177.
- Zimmermann, S., Schotter, P., Engel, W. and Adham, I.M. (1997) Mouse Leydig insulin-like (*Ley I-L*) gene: structure and expression during testis and ovary development. *Mol. Reprod. Dev.*, **47**, 30–38.
- Overbeek, P.A., Gorlov, I.P., Sutherland, R.W., Houston, J.B., Harrison, W.R., Boettger-Tong, H.L., Bishop, C.E. and AgoulNIK, A.I. (2001) A transgenic insertion causing cryptorchidism in mice. *Genesis*, **30**, 26–35.
- Hsu, S.Y., Nakabayashi, K., Nishi, S., Kumagai, J., Kudo, M., Sherwood, O.D. and Hsueh, A.J.W. (2002) Activation of orphan receptors by the hormone relaxin. *Science*, **295**, 671–674.
- Zheng, B., Mills, A.A. and Bradley, A. (1999) A system for rapid generation of coat color-tagged knockouts and defined chromosomal rearrangements in mice. *Nucleic Acids Res.*, **27**, 2354–2360.
- Hsu, S.Y., Kudo, M., Chen, T., Nakabayashi, K., Bhalla, A., van der Spek, P.J., van Duin, M. and Hsueh, A.J. (2000) The three subfamilies of leucine-rich repeat-containing G protein-coupled receptors

- (LGR): identification of LGR6 and LGR7 and the signaling mechanism for LGR7. *Mol. Endocrinol.*, 14, 1257–1271.
20. Xiao, W. and Oefner, P.J. (2001) Denaturing high-performance liquid chromatography: a review. *Hum. Mutat.*, 17, 439–474.
 21. Zhao, L., Roche, P.J., Gunnersen, J.M., Hammond, V.E., Tregear, G.W., Wintour, E.M. and Beck, F. (1999) Mice without a functional relaxin gene are unable to deliver milk to their pups. *Endocrinology*, 140, 445–453.
 22. Spaniel-Borowski, K., Schafer, I., Zimmermann, S., Engel, W. and Adham, I.M. (2001) Increase in final stages of follicular atresia and premature decay of corpora lutea in *Insl3*-deficient mice. *Mol. Reprod. Dev.*, 58, 281–286.
 23. Hearn, M.T.W. and Gomme, P.T. (2000) Molecular architecture and biorecognition processes of the cystine knot protein superfamily: part I. The glycoprotein hormones. *J. Mol. Recogn.*, 13, 223–278.
 24. Jiang, X., Dreano, M., Buckler, D.R., Cheng, S., Ythier, A., Wu, H., Hendrickson, W.A. and el Tayar, N. (1995) Structural predictions for the ligand-binding region of glycoprotein hormone receptors and the nature of hormone-receptor interactions. *Structure*, 3, 1341–1353.
 25. Song, Y.S., Ji, I., Beauchamp, J., Isaacs, N.W. and Ji, T.H. (2001) Hormone interactions to Leu-rich repeats in the gonadotropin receptors. I. Analysis of Leu-rich repeats of human luteinizing hormone/chorionic gonadotropin receptor and follicle-stimulating hormone receptor. *J. Biol. Chem.*, 27, 3426–3435.
 26. Chen, S., Lin, F., Xu, M., Hwa, J. and Graham, R.M. (2000) Dominant-negative activity of an α_{1B} -adrenergic receptor signal-inactivating point mutation. *EMBO J.*, 19, 4265–4271.
 27. Sherwood, O.D. and O'Byrne, E.M. (1974) Purification and characterization of porcine relaxin. *Arch. Biochem. Biophys.*, 160, 185–196.

The Three Subfamilies of Leucine-Rich Repeat-Containing G Protein-Coupled Receptors (LGR): Identification of LGR6 and LGR7 and the Signaling Mechanism for LGR7

Sheau Yu Hsu, Masataka Kudo, Thomas Chen*,
Koji Nakabayashi, Alka Bhalla, Peter J. van der Spek,
Marcel van Duin, and Aaron J. W. Hsueh

Division of Reproductive Biology (S.Y.H., M.K., T.C. K.N., A.B.,
A.J.W.H.)

Department of Gynecology and Obstetrics
Stanford University School of Medicine
Stanford, California 94305-5317

Scientific Development Group (P.J. v.d.S., M.v.D.)
N.V. Organon
Oss, The Netherlands 5340

Glycoprotein hormone receptors, including LH receptor, FSH receptor, and TSH receptor, belong to the large G protein-coupled receptor (GPCR) superfamily but are unique in having a large ectodomain important for ligand binding. In addition to two recently isolated mammalian LGRs (leucine-rich repeat-containing, G protein-coupled receptors), LGR4 and LGR5, we further identified two new paralogs, LGR6 and LGR7, for glycoprotein hormone receptors. Phylogenetic analysis showed that there are three LGR subgroups: the known glycoprotein hormone receptors; LGR4 to 6; and a third subgroup represented by LGR7. LGR6 has a subgroup-specific hinge region after leucine-rich repeats whereas LGR7, like snail LGR, contains a low density lipoprotein (LDL) receptor cysteine-rich motif at the N terminus. Similar to LGR4 and LGR5, LGR6 and LGR7 mRNAs are expressed in multiple tissues. Although the putative ligands for LGR6 and LGR7 are unknown, studies on single amino acid mutants of LGR7, with a design based on known LH and TSH receptor gain-of-function mutations, indicated that the action of LGR7 is likely mediated by the protein kinase A but not the phospholipase C pathway. Thus, mutagenesis of conserved residues to allow constitutive receptor activation is a novel approach for the characterization of signaling pathways of selective orphan GPCRs. The

present study also defines the existence of three subclasses of leucine-rich repeat-containing, G protein-coupled receptors in the human genome and allows future studies on the physiological importance of this expanding subgroup of GPCR. (Molecular Endocrinology 14: 1257-1271, 2000)

INTRODUCTION

In vertebrates, gonadotropins and TSH are essential for the differentiation and growth of gonads and thyroid gland, respectively (1-4). Among these glycoprotein hormones with common α - and specific β -subunits, LH, FSH, and TSH are secreted by the anterior pituitary whereas the human chorionic gonadotropin (hCG) is secreted by placenta cells. These heterodimers bind specific plasma membrane receptors on target cells and signal mainly through the cAMP-dependent pathway. The receptors for these glycoprotein hormones belong to the large G protein-coupled, seven-transmembrane protein superfamily but are unique in having a large N-terminal extracellular (ecto-) domain important for interaction with the large glycoprotein hormone ligands (5, 6). Hallmarks of this subgroup of G protein-coupled receptors (GPCRs) are the leucine-rich repeats in the ectodomain that have been postulated to form a horseshoe-shaped interaction motif for ligand binding (7-9). Recently, putative receptors homologous to the mammalian glycoprotein hormone receptors were found in sea anemone (10, 11), nematode (12), pond snail *Lymnaea stagnalis* (13), and *Drosophila* (14), suggesting that

this subgroup of GPCR evolved early during evolution and that these invertebrate receptors represent ancient homologs of mammalian glycoprotein hormone receptors.

Based on the conserved sequences of mammalian glycoprotein hormone receptors and invertebrate homologs, we and others have recently isolated two novel mammalian leucine-rich repeat-containing, G protein-coupled receptors (LGRs) based on a homologous sequence search of the expressed sequence tags (ESTs) database (15–17). Because phylogenetic analysis showed that sea anemone LGR shares a closer relatedness to mammalian glycoprotein hormone receptors than to an LGR isolated from pond snail *Lymnaea stagnalis* (13, 15), one can predict that there are additional LGRs in mammalian genomes. Indeed, a recent search of the EST and genomic databases and subsequent characterization revealed that there are at least two additional mammalian LGRs. These two genes were named as LGR6 and LGR7 based on the chronological order of discovery. Analysis of primary sequences and domain arrangement in these LGRs showed that LGR6 is closely related to LGR4 and LGR5; whereas LGR7 and snail LGR are likely derived from a common ancestor. Together with the three known glycoprotein hormone receptors, these studies define the existence of three subgroups of LGRs in mammals. Based on the conserved mechanisms identified in constitutively activated LH and TSH receptors (18–20), studies of putative gain-of-function point mutants of LGR7 showed that this orphan receptor could mediate signaling through the protein kinase A-dependent pathway. Thus, site-directed mutagenesis of key residues in the functional domains of seven-transmembrane receptors provided a novel approach to reveal the signal transduction pathway of selective orphan GPCRs and to facilitate future identification of their cognate ligands.

RESULTS

cDNA Cloning of Two Novel Leucine-Rich Repeat-Containing GPCR, LGR6 and LGR7

Using the known invertebrate and mammalian LGRs as queries to search for homologous EST sequences, two candidate sets of sequences with homology to known LGRs were selected. cDNAs corresponding to these two novel genes, designated as LGR6 and LGR7, were obtained by reverse transcription-PCR using gene-specific primers and mRNA from human ovary and testis as templates. Using 5'- and 3'-rapid amplification of cDNA ends (RACE), a full-length LGR6 cDNA encoding an open reading frame (ORF) of 846 amino acids with a calculated molecular mass of 91.6 kDa was obtained (Fig. 1). Analysis of multiple cDNA clones showed that the deduced methionine translation start site is preceded with an in-frame stop codon

at position –177. Using a similar approach, two splicing variants of LGR7 were obtained which differ in the N terminus of the coding region. The long form of LGR7, LGR7(1), is 3759 nucleotides long and encodes an ORF of 757 amino acids with a calculated molecular mass of 87 kDa; whereas the short form of LGR7, LGR7(2), encodes an ORF of 723 amino acids with a corresponding mass of 82.9 kDa (Fig. 2). The LGR7(2) variant is 34 amino acids shorter than the LGR7(1), and these two variants could be derived from alternative splicing events at the N terminus of the coding region.

Comparison with known sequences in the GenBank showed that LGR6 and LGR7 are novel LGRs with closest relatedness to the newly isolated LGR4 and LGR5, and snail LGR, respectively. A motif search indicated that LGR6 and LGR7 contain an N terminus ectodomain composed of variable leucine-rich repeats and a seven-transmembrane region followed by unique C-terminal intracellular tail. The similarity between these LGRs and other known LGRs extends from the ectodomain to the seven-transmembrane region, and LGR6 shares approximately 45–47% identity with LGR4 and LGR5, as compared with 33% identity with the glycoprotein hormone receptors. However, LGR6 is distinct from LGR4 and LGR5 in having only 13 leucine-rich repeats instead of the 17 repeats found in LGR4 and LGR5 (Fig. 1A). Among the 13 leucine-rich repeats of LGR6, the first seven repeats align perfectly with leucine-rich repeats 1–3 and leucine-rich repeats 8–11 of LGR4 and LGR5, but the remaining leucine-rich repeats showed disparity in these receptors. In addition, distinctive sequence motifs, including a PYAYQCC motif and a GXFKPCE motif in the hinge region of the ectodomain, and the highly conserved cysteine residues for disulfide bond formation in extracellular loops 1 and 2, were completely conserved in LGR4, LGR5, and LGR6 (Fig. 1, A and B). A motif search using the ScanProsite program showed that both LGR6 and LGR7 contain N-glycosylation sites at the ectodomain and that LGR7 carries a protein kinase C phosphorylation site at the intracellular C-terminal sequences [STR, residues 750–752 of LGR7(1)]. Unlike LGR4 and LGR5 (15), both LGR6 and LGR7 lack protein kinase A phosphorylation sites in their C termini.

Among all known LGRs, LGR7 shares the highest identity with snail LGR (33%) (13) and less with the three mammalian glycoprotein hormone receptors (24%). As shown in Fig. 2, LGR7 and snail (Ls) LGR shared similar primary sequences and common domain arrangement as shown by the presence of the N-terminal low density lipoprotein (LDL) receptor cysteine-rich motif followed by leucine-rich repeats and the seven transmembrane region. However, the predicted tertiary structure of the LGR7 ectodomain differed from that of snail LGR; the ectodomain of snail LGR is bulkier and contains approximately 760 amino acids instead of the 410 amino acids found in LGR7(1) (Fig. 2A). In addition to the 10 leucine-rich repeats at the C terminus of the ectodomain, snail LGR contains

A.

rLGR4	MPGFLGLLCPLALQLLGSAGPSGAAPLCAAPCSGDRRVDSCGKGLTAVPEGLSAFTQA			
hLGR5	MDTSLRGLVLSLPLVLLQLATGGSSPRSGVLLRGCPHCHCEPDGRMLLRVDCSDGLSELPSNLSVFTSY			
hLGR6	MRLGEGRSARAGQNLRSAGSARRGAP			
	↑ LRR1	↑ LRR2	↑ LRR3	
rLGR4	LDISMNITQLPEDAFKSPFLEELQAGNDLSLHPKALSGLKELKVLTLQNNQLRTVPSEAIH	126		
hLGR5	LDLSMNISQLLPNPLPSLRFLLEELRAGNLTYPKGAFGLYSLKVLMLQNNQLRHVPTEALQ	135		
hLGR6	RDLSMNLTQLQPLFHLRLFLLEELRLSGNHLHGPQAFSGLYSLKILMLQNNQLGGIPABALW	92		
	↑ LRR4	↑ LRR5	↑ LRR6	
rLGR4	GLSALQSLRLDANHITSVPEDSFEGVLQRLHLWLDNLSLTFVVRPLSNLPTLQALTLALNHSS	191		
hLGR5	NLRSLQSLRLDANHISYVPPSCFQLHSLRLWLDNLTETPVQAFRLSALQAMTLALNKHIIH	200		
hLGR6	ELPSLQSL	100		
	↑ LRR7	↑ LRR8	↑ LRR9	
rLGR4	IPDFAFTMLSSLVVHLHNNKIKSLSQHCFDGLONLETDLNLYNLYLDEFFQAIKALPSLKELGPH	256		
hLGR5	IPDYAFGLSSLVVHLHNNRIHSLGKCFDGLHSLTDLNLYNLYLDEFFTAIRTLNKLKELGPH	265		
hLGR6	-----DLNLYNLYLDEFFTAIRTLNKLKELGPH	126		
	↑ LRR10	↑ LRR11		
rLGR4	SNSISVIPDGAFFGNNFLRTIHLVDFSVGNSAPHLSDLHCLVIRGASLVQMFPELTGTVHL	321		
hLGR5	SNNIRSIPEKAPVGNPSLTIHFYDNFIQVGRSAFQHLPELTLTLNGASQITEFFDLTGANL	330		
hLGR6	NNTIKAIPEKAPVGNPSLTIHFYDNFIQVGRSAFQHLPELTLTLNGASQITEFFDLTGANL	191		
	↑ LRR12	↑ LRR13	↑ LRR14	
rLGR4	ESLTLTGKISSIPDDLQONQKMLRTLDLYNNIRDLPSFNGCRALSEISLQRNQLISIKENTFO	386		
hLGR5	ESLTLTGKISSIPDLQONQKMLRTLDLYNNIRDLPSFNGCRALSEISLQRNQLISIKENTFO	395		
hLGR6	HNQIEELPSLHRCQKLEELGLQHNRIWEIGADTFSQLSSQLQALDSWNAIRSHPEAFSTLSLV	256		
	↑ LRR15	↑ LRR16	↑ LRR17	
rLGR4	GLTSLRILDLRNLIRESHGAFKLGTTITNLDVSPNELTSFPTGGLNGLNQLKLVGNPKLKDAL	451		
hLGR5	QLLSRLSLHAWNKIAIHPNAPSTLPSLIKLDSNLLSFFITGLRGLTHKLGTGNHALQSLI	460		
hLGR6	KLDLTONQLTTLPLAGLGLHHLKLEILTITRAGIRLLPSGMCCQLPRIRVLELSKGNLALSQAF	321		
	↑ C-flanking cysteine-rich region			
rLGR4	AARDPANLRLSVPTAYQCCAFPGVCSLCKLNTEDNSPQHSVTKKGGATDAANVTSTAENEHS	516		
hLGR5	SSENFPELKVIEPTAYQCCAFPGVCSLCKLNTEDNSPQHSVTKKGGATDAANVTSTAENEHS	525		
hLGR6	SKDSPKLRILEVPTAYQCCAFPGVCSLCKLNTEDNSPQHSVTKKGGATDAANVTSTAENEHS	386		
	↑ LRR18	↑ LRR19	↑ LRR20	
rLGR4	-----QIIHCTPSTGAPEPCYLLGSWMI	541		
hLGR5	-----LLDPEEDLKALHSVQCSFPGPFKPCHELDGWL	560		
hLGR6	DLDLQLEMDSKPHSPVQCSFPGPFKPCHELDGWL	425		

B.

	↑ TM1	↑ IL1	↑ TM2	↑ EL1	
LGR4	RLTYNFIPLVALLFNLLVITVFAS-CSSLPASKLFIGLISVSNLLAGIYITLTPLDAVSWGRF				605
LGR5	RIGWTIAVLAITCNALVTSTVFRS-PLYTSPKLLIGVIAAVNMLTGVSASVAGVDAFTPGSP				624
LGR6	RLAVNATVLLSVLCNGLVLLTVFAGGPVLPVPKPVVGAAGANTLTGICGLLASVDALTFQGP				490
	● ↑ TM3	↑ IL2	↑ TM4		
LGR4	AEFGIHWETGSGCKVAGSLAVFSSBSAVFLLTLAAVERSVFAKDMKHGKSSHLRQPVQVALLAL				670
LGR5	ARHGAMWENOVGCHVIGPLSIPASSSVFLLTLAALRGFSVKYSKAFETKAPFSSKLVIIILCA				689
LGR6	SEYQARWETGLGCRATGFLAVLGSBSVLLTLAAVQCSVSVSVCRVAYGKSPSLGSRVAGVLGCL				555
	↑ EL2	↑ TM5	↑ IL3		
LGR4	LGAAVAGCFPLPHQGYBASPLCLPFFPTGE--TPSLGPTVTLVLLNSLAPLMAIITYKLYCNLE				733
LGR5	LIALTHAAVPLLAGSKYASPLCLPFFGE--PSTMTKVALILLSELCLPMTIATYKLYCNLD				752
LGR6	ALAGLAAALPLASVGYGASPLCLPFFPTGE--TPSLGPTVTLVLLNSLAPLMAIITYKLYCNLE				620
	↑ TM6	↑ EL3	↑ TM7		
LGR4	KEDLSSESQSVLHVNALLPTNCLFPCVAFVTFAPLITALSISPEIMESVTLIPFLPACLEP				798
LGR5	KEDLESINDCSNVEHIALLLPTNCLFPCVAFVTFAPLITALSISPEIMESVTLIPFLPACLEP				817
LGR6	KEDFPAVDCMVEHVNALLPTNCLFPCVAFVTFAPLITALSISPEIMESVTLIPFLPACLEP				685
	↑ C-terminal tail region				
LGR4	VLYVFFPEKPKEDMKLLKRVTRKGSVSVISGQGGGQEDFYDQMYERHLOGLTVDCDCEG				863
LGR5	LYVLPKPKEDLVLEKQTVVTRSKHBSLMSINSDDVKQSCDSTQALVTVVSSITVTLDP				882
LGR6	LYVLPKPKEDLVLEKQTVVTRSKHBSLMSINSDDVKQSCDSTQALVTVVSSITVTLDP				750
	↑ LRR21				
LGR4	VLLTFPVSCHLIKSHSCVPLTAASQRPAYWSDQTSARSDYADESDSPVSDSSQVQACGR				928
LGR5	SSVPSFATPVTSCHLSVAVFVPL*				927
LGR6	GLETYGPPSVTLISCCQGPAPLEGSCHVEPEGRHFGHPQSPMDGELLRAEGSTPAGGLSGGG				815
	↑ LRR24				
LGR4	ACFYQSRGPPPLVRYAYNLQRVDR*				951
LGR5					
LGR6	GPQPSGLALLHTYPCRYFAQNRPLSRGPV*				846

Fig. 1. Comparison of Deduced Amino Acid Sequences for LGR6, LGR4, and LGR5

Sequence alignment for different regions of LGR6 with that of two closely related LGRs, LGR4 and LGR5. A, The ectodomain includes the multiple leucine-rich repeats (LRR) and a C-flanking cysteine-rich hinge region. Individual leucine-rich repeats are indicated by arrowheads. Putative N-glycosylation sites in the ectodomain are in **bold letters** and underlined. Conserved PYAYQCC and GXFKPCE motifs preceding transmembrane I are in **bold italics**. B, The seven-transmembrane region and the C-terminal tail. The transmembrane (TM) domain, intracellular loop (IL), and extracellular loop (EL) are indicated by arrowheads. Potential protein kinase C phosphorylation sites in the intracellular C-terminal region are in **bold letters** and underlined. The two conserved cysteines found in extracellular loops 1 and 2, and believed to form a disulfide bond, are marked by **solid circles**. Residue numbers are shown on the right and asterisks indicate the position of the stop codon. Shaded residues are identical in the three receptor proteins aligned, and gaps indicated by dashes are included for optimal protein alignment.

A.

LGR7 (1)	MTSGSVFFYILIFGKYFSHGGGQDV	25
LGR7 (2)	-----	25
LsLGR	MATMSGTTIVCLLYLTMLGNSQGVNLKIESPSPPTLCVSEGTFFHCDGMLQCVLMGSKC DGVSDCRNGMDESVEVTCGLQSEFQCHHTTCIDKILRCDRNDCCSNGLDRECD:YICPL GTHVKWNNHPCVPRDKQCDLDDCGNDSDEKICSRRECVATEFKCNSQCVAFGNLCDDL VDCVDSDEQVACDSKYFQCAEGLIKKBFVCDGVVDCKLTFADLNCKLCEDDFRFC SDTRCIQKSNVCDGYCDCKTCDDEVCANITYGCPMDTKYMCRSIYGEPRCIDKDNVNCM INDCRDGNVGTDEYYCSNDSECKNFQAMGFFYCPCEERCLAKHLYCDLHPDCINGEDEQS CLAPP	365
LsLGR	KCSQDFQCHH-GKCIPIBKRCDSVHDCVDWSEMMNC-ENHQAAMKSCLSGHCTIEHK	423
LGR7 (1)	KCSLGYPPCGNITKCLPQLLHCNGVDDCGNQADRDNGGDNNGWSMQDKYFASYRMTSQ	85
LGR7 (2)	-----	62
LRR1		
LsLGR	WCNFRHRECPD---GSDEKDCDPRVCEANQFRCKNGQCIDPLQVCVKGDYDGCADQSHL	460
LGR7 (1)	Y-PFEAETPECLVGSVPVQC---LCQGLELDCDETNLRAVPSV---SSNVTAMSLQWNL	137
LGR7 (2)	*****V-----	103
LRR2		
LsLGR	IMCSQRIHLEGGFRCKSFCTIEQTKVCDGTVDCLQGMWDENNCRVWCPHQAIQCCEGVT	540
LGR7 (1)	IRKLPPDCPKMYHDLQKLYLQNN-KITSISIVAFRL--NSLTLYLSHNRITPLKPGVP	194
LGR7 (2)	-----	160
LRR3		
LsLGR	MDCTGQKLKEMPVQMEEDLSKLMIGDNLMLTSTTFSATYY--DKVTYLDLSRNHLTEI	598
LGR7 (1)	EDL-----HRLWLIIEDNHLRSISPP--TFYGLNSLILLVMMNVLTSL	237
LGR7 (2)	-----	203
LRR4		
LsLGR	PIYSP-QNMWKLTHALADNMTSLKNCGLLGLSNLQHLHNGKIETIEEDTFSMIHL	657
LGR7 (1)	PDKPLCQHPRLHMLDLEGNHINLRLKLTITSCNLTVLVVRKINKINHLNENTFAPLQRL	297
LGR7 (2)	-----	263
LRR5		
LsLGR	TVLDLSNQRLTHVYKMPKGLKQITVLEISRNQINSIDNGAFNNLANVRLIDLSGNVKD	717
LGR7 (1)	DELDLGSNKIENLPLIFKDLKELSQLSLSYNPIQKIQAOFDYLVKLSLSEIGIBISN	357
LGR7 (2)	-----	323
LRR6		
LsLGR	YQKVFMLPRLVELKTDSTYRCPCLAPGKVKSPKQDFSSCEDLMSNHVL	768
LGR7 (1)	IQQRMFRLMFLSHIYFKKFOYCYAPHVRSCKPMTDGISSLNLLASIIQ	408
LGR7 (2)	-----	374

B.

TM1		
LsLGR	RVSINVLGVIALVGNFVVLFWVRDFRGGKVHSPFITNLAIGDFLNGVYLLIATADTY	828
LGR7 (1)	RVFVWVSVAVTCFNGIFVYCMRPYIRSENKLYAMSIISLCCADCLMOIYLFVIGGFDLKF	469
LGR7 (2)	-----	434
IL1		
LsLGR	RGVYISHDENWKSGLCQFAGFVSTFSELSVLTSTITLDRLLICILFLRRLTLGLRQA	888
LGR7 (1)	RGEYNKHAQLAMESTHCOQLVGSAILSTEVSLLLTPLTLERKVICIVYFRCVRPGKCR	528
LGR7 (2)	-----	494
IL2		
LsLGR	LIIVNSCIWVFLAVLFLAGFSTFSTFSTFSTFSTFSTFSTFSTFSTFSTFSTFSTFSTF	945
LGR7 (1)	ITVLILWITGFIAPFPLGKKEFFKTYGTNGVCPPLASEDSTESIGAQITYSVAIFLGIE	588
LGR7 (2)	-----	554
IL3		
LsLGR	LISPVLIASSTLADGFSVAKTRESAVRTAESCH---DQAMAPMTLIVMDFCCNVPIIV	1003
LGR7 (1)	LAAPFIIIVPSTGSMPTSVH--QGAITATETIRNQVKKMLAKRPPFIVITDALCNIPFV	646
LGR7 (2)	-----	612
IL4		
LsLGR	LQFVSLAGARADDQVYAMIAVFLPLNGATHPVITLSTAPFLGVRKRAHPRKSPTHS	1063
LGR7 (1)	VKFLSLQVRIPTGTTISNVVIFILPIMBALPILYTLTTPFKENTHFRFWYNYRQKSMO	706
LGR7 (2)	-----	672
IL5		
LsLGR	PTGDTKHSYVDDGTHSYCEKSPYRQLKRLRLSLNSSPPMYNTLHSDS*	1115
LGR7 (1)	SKQKTYAPSPFIWVENPLQENPFELMKPDLPTPCMSLISQSTR-LNSYS*	757
LGR7 (2)	-----	723

Fig. 2. Comparison of Deduced Amino Acid Sequences between Two Human LGR7 Variants and Snail LGR

Sequence alignment for different regions of two splicing variants (1 and 2) of LGR7 and snail LGR (LsLGR) was performed. A, Ectodomain with LDL receptor cysteine-rich motifs and leucine-rich repeats (LRR). Residues that are identical in LGR7(1) and LGR7(2) are shown as *double lines*, and residues that are missing in LGR7(2) are indicated by *bold asterisks*. The consensus LDL receptor cysteine-rich motif in LGR7 and the corresponding region of snail LGR are indicated by *bold italics*. C-terminal cysteine-rich hinge regions in the two receptors are *overlined*. Putative N-linked glycosylation sites are in *bold (N)*. B, The seven-transmembrane region and the C-terminal tail. Different structural motifs including transmembrane (TM) region, intracellular loop (IL), and extracellular loop (EL), are indicated by *arrowheads*; asterisks indicate the stop codon. Potential phosphorylation sites for protein kinase C are in *bold letters and underlined*. Shaded residues are identical in the LGR7 and snail LGR sequences. Residue numbers are shown on the *right* and gaps are included for optimal protein alignment.

12 LDL-receptor cysteine-rich motifs at the N terminus. In contrast, both LGR7 variants have only one such motif [residue 40–62 of LGR7(1), CLPQLLHC-NGVDDCGNQADEDC] preceding the conserved leucine-rich repeat domain. In addition, these two receptors are distinct in their hinge region of the ectodomain. In LGR7 and snail LGR, the hinge regions are approximately 30 amino acids long as compared with 72–123 amino acids found in other LGRs. The unique PYAYQCC and GXFKPCE motifs found in this region of other LGRs are absent in these two receptors. Thus, the overall structural features of LGR7 are similar to that of snail LGR.

Mammalian LGRs Have Diverged into Three Distinct Subtypes

Phylogenetic analysis using the neighbor-joining and parsimony methods showed that the 11 known LGRs from vertebrates and invertebrates can be divided into three distinct subgroups (Fig. 3A). The first subgroup contains the mammalian gonadotropin and TSH receptors, and LGRs from sea anemone, *Caenorhabditis elegans*, and *Drosophila*. The second branch contains only vertebrate receptors including LGR4, LGR5, and LGR6, whereas snail LGR and LGR7 belong to the third subgroup. To gain insight into the evolution of LGRs, phylogenetic analysis was performed together with diverse GPCRs with a polypeptide or neurotransmitter ligand using full-length receptor sequences. As shown in Fig. 3B, LGRs share a branch with diverse GPCRs known to have a peptide ligand, including a subgroup of angiotensin receptor-like GPCRs [angiotensin receptor, platelet-activating factor (PAF) receptor, and formyl-methionyl-leucyl-phenylalanine (FMLP) receptor] and another subgroup of bombesin receptor-like GPCRs (bombesin, gastrin, thrombin, and neuropeptide Y receptors). In contrast, the relatedness to other family 1 GPCRs (21), such as receptors for various kinins, amine derivatives, and somatostatin (SST), is more remote.

Tissue Expression Pattern of LGR6 and LGR7

To investigate the tissue expression pattern of LGR6 and LGR7, Northern blot analyses of different tissues were performed using multiple tissue blots containing rat poly (A)⁺ RNA and specific radiolabeled probes for LGR6 or LGR7. Specific LGR6 transcripts of 4.0 kb were detected in multiple tissues including testis, ovary, oviduct, uterus, thymus, small intestine, colon, spleen, kidney, adrenal, brain, and heart (Fig. 4A). In addition, a minor LGR6 transcript of >5.5 kb was also detected in the oviduct and heart, whereas a smaller transcript was found in the spleen. Likewise, LGR7 transcripts were also found in multiple tissues. As shown in Fig. 4B, a major LGR7 transcript of 5.5 kb was detected in all tissues tested with the exception of spleen. Furthermore, multiple smaller transcripts (2 or

3 kb) were detected in oviduct, uterus, colon, and brain.

Isolation of Human LGR6 and LGR7 Genes and their Chromosomal Localization

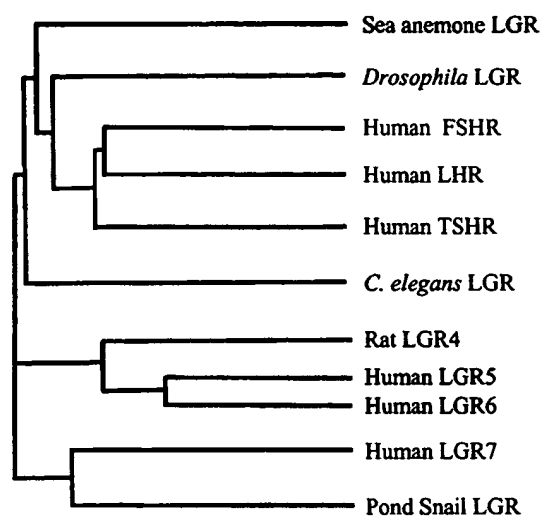
Using an LGR6 cDNA fragment corresponding to the transmembrane region as a probe, genomic clones for LGR6 were isolated from a bacterial artificial chromosome-based human genomic DNA library. For LGR7, a genomic DNA clone (AQ053279) from the genomic survey sequence database was found to contain the C terminus of the LGR7 gene and was obtained from Genome Systems (St. Louis, MO). To identify the chromosomal localization of LGR6 and LGR7 genes in the human genome, genomic fragments (>50 Kb) derived from these BAC clones were used as probes in fluorescence *in situ* hybridization (FISH) analysis. As shown in Fig. 5, A and B, LGR6 and LGR7 genes were localized to banded DNA in chromosome 1q32 and 4q32, respectively.

Signal Transduction by Mutant LGR7 as well as by Chimeric Receptors with the Ectodomain from the LH Receptor and the Transmembrane Region from LGR6 or LGR7

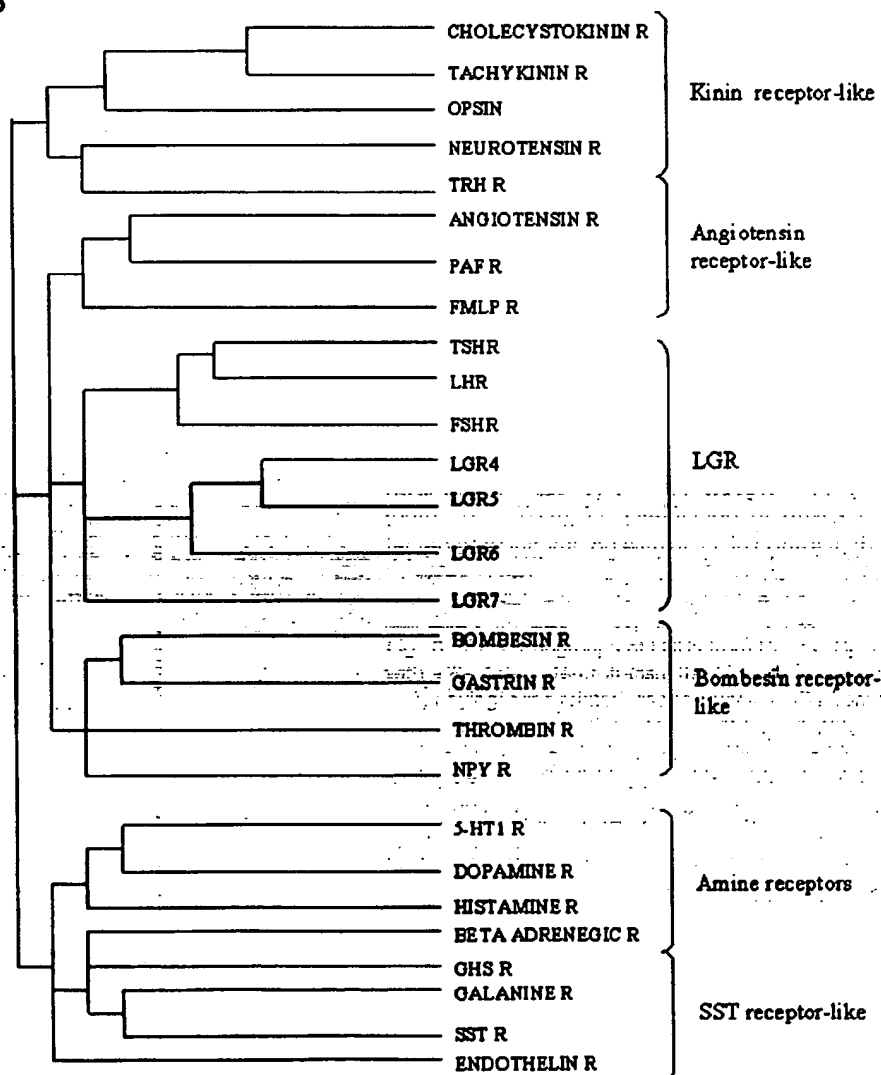
To investigate the signal transduction pathway of LGR6 and LGR7, wild-type and mutated receptors were constructed to analyze receptor binding and signal transduction. Earlier studies using mutant LH and TSH receptors found in patients with male-limited precocious puberty and nonimmune hyperthyroidism, respectively, indicated that these diseases are associated with constitutive receptor activation as a result of point mutations of key residues in the transmembrane VI region of these receptors (18–20, 22–25). To investigate the possibility that the orphan LGRs could be rendered constitutively active in the absence of their unknown ligands, detailed comparisons of this region were conducted between gain-of-function LH and TSH receptors and the two new receptors. It was found that a tripeptide motif (FTD, residue 576–578 in the LH receptor) is completely conserved in the three glycoprotein hormone receptors and LGR7, but not in LGR6. Previous studies have shown that mutations of D578 in the LH receptor and the corresponding D633 in the TSH receptor cause constitutive increases of basal cAMP production in cells expressing these mutant receptors (20, 22, 26). Accordingly, we constructed mutants for the two LGR7 variants, LGR7(1) and LGR7(2), by generating a point mutation at the corresponding residue in transmembrane VI. These mutants were named as LGR7(1) D637Y and LGR7(2) D603Y.

As shown in Fig. 6, transfection of 293T cells with increasing concentrations of the expression plasmid encoding the mutant LGR7 receptors [LGR7(1) D637Y or LGR7(2) D603Y], similar to those transfected with the plasmid encoding the D578Y gain-of-function mu-

A



B



tant LH receptor, resulted in dose-dependent increases of basal cAMP production by transfected cells. In contrast, cAMP levels in cells transfected with different amounts of wild-type LH receptor or LGR7 did not show an increase in basal cAMP production. To allow quantitative comparison of basal cAMP production by different receptors, cAMP levels in transfected cells were normalized based on the level of cell surface expression of an N-terminally tagged FLAG epitope in different LGRs (Fig. 6, shown as percentage changes vs. wild-type LH receptor). Although the D637Y mutation caused significant increases of basal cAMP levels in both LGR7(1) and LGR7(2) constructs, cells expressing mutant LGR7(1) consistently showed greater levels of cAMP increase as compared with those expressing the mutant LGR7(2) construct. To evaluate the specificity of the activating LGR7 mutation for the Gs protein, the effect of this mutation on a different signal transduction pathway, phosphatidylinositol (PI) turnover, was measured. As shown in Table 1, the Gs-activating mutants, LGR7(1) D637Y and LGR7(2) D603Y, did not stimulate inositol phosphate (IP) turnover by transfected 293T cells whereas hCG treatment significantly increased the IP content in cells expressing either wild-type or constitutively active mutant LH receptors.

Because chimeric receptors among the known glycoprotein hormone receptors have been successfully used to study signal transduction by these proteins (27), we further generated chimeric LH/LGR6 and LH/LGR7 receptors by fusing the ectodomain of the human LH receptor with the transmembrane region and C-terminal tail of either LGR6 [LH(EC)/LGR6(TM)] or LGR7(1) [LH(EC)/LGR7(TM)] to further investigate the putative signal transduction pathway of these orphan receptors. Although the chimeric LH(EC)/LGR6(TM) receptor is expressed on the cell surface as reflected by FLAG epitope expression, and is binding to 125 I-hCG as detected by the LH receptor binding assay (data not shown), no stimulation of cAMP was detected after incubation with hCG. In contrast, the same

hCG treatment increased cAMP production by cells expressing the wild-type LH receptor. Because activation of the LH receptor by hCG elicits increased PI turnover (28, 29), hydrolysis of PI in cells transfected with the chimeric receptor was also performed. Measurement of PI turnover showed a negligible increase of IP accumulation in cells expressing the chimeric LH(EC)/LGR6(TM) receptor after stimulation with hCG, whereas wild-type LH receptor-expressing cells showed an approximately 1.4-fold increase in PI hydrolysis after hCG treatment. In contrast to the chimeric receptor LH(EC)/LGR6(TM), the LH receptor ectodomain and LGR7 transmembrane region appeared to be incompatible because the chimeric LH(EC)/LGR7(TM) receptor was not found on the cell surface based on the assay of FLAG epitope expression.

DISCUSSION

Based on database analysis, we have isolated two novel GPCR genes belonging to the mammalian leucine-rich repeat-containing GPCRs. In addition to the subgroup of classical glycoprotein hormone receptors, LGR6 is evolutionarily related to two other mammalian LGRs (LGR4 and LGR5) whereas LGR7 shares a similar ancestry with snail LGR, thus indicating the presence of three subgroups of LGRs in the mammalian genome. The LGR7 was found to signal through the cAMP-dependent pathway, as reflected by increases in basal cAMP production in cells transfected with mutant LGR7 constructs carrying a point mutation in transmembrane VI. These orphan receptors are expressed in diverse tissues, and the identification of the signaling mechanism for LGR7 could facilitate the identification of its cognate ligand(s).

Recent expansion of the nucleic acid sequence database for diverse organisms have provided opportunities to identify novel mammalian gene paralogs

Fig. 3. Three Subgroups of LGRs from Diverse Species and the Evolutionary Relatedness between LGRs and Family 1 GPCRs with a Peptide or Neurotransmitter Ligand

A. Phylogenetic relatedness of diverse LGRs from mammals and invertebrates. Full-length amino acid sequences of 11 LGRs from mammals (LH, FSH, and TSH receptors plus LGR4 to LGR7), sea anemone, nematode, pond snail, and *Drosophila* were analyzed using the Blocks program. Sequence blocks predicted from this alignment were then used to construct the neighboring tree for establishing possible subfamily relationships. Comparable results were obtained using the parsimony method in the Phylogeny Inference Package. In the three major branches of LGR evolution, the three classical glycoprotein hormone receptors as well as LGRs from sea anemone, nematode, and *Drosophila* belong to the first subgroup whereas LGR6 is most closely related to the second subgroup containing LGR4 and LGR5. In contrast, LGR7 belongs to a third subgroup together with snail LGR. **B.** Diagrammatic representation of phylogenetic relatedness between mammalian LGRs and diverse family 1 GPCRs (21). Different subgroups of family 1 GPCRs with known ligands were first grouped based on sequence similarity, and full-length consensus sequences for each subgroup of family 1 GPCRs were generated using the Blocks program. Subsequently, the individual full-length amino acid sequences of different LGRs, and the consensus sequences of different subtypes of family 1 GPCRs with a peptide or neurotransmitter ligand, were analyzed together. The GPCRs included in the phylogenetic tree are adenosine receptors, cholecystokinin receptors, tachykinin receptors, opsins, neurotensin receptors, TSH-releasing hormone receptor, angiotensin receptors, PAF receptor, FMLP receptor, bombesin receptors, gastrin receptors, thrombin receptors, neuropeptide Y receptors, 5-HT type 1 serotonin receptors, dopamine receptors, β -adrenergic receptors, GH secretagogue receptor (GHS receptor), galanin receptors, somatostatin (SST) receptors, and endothelin receptors. R, Receptor.

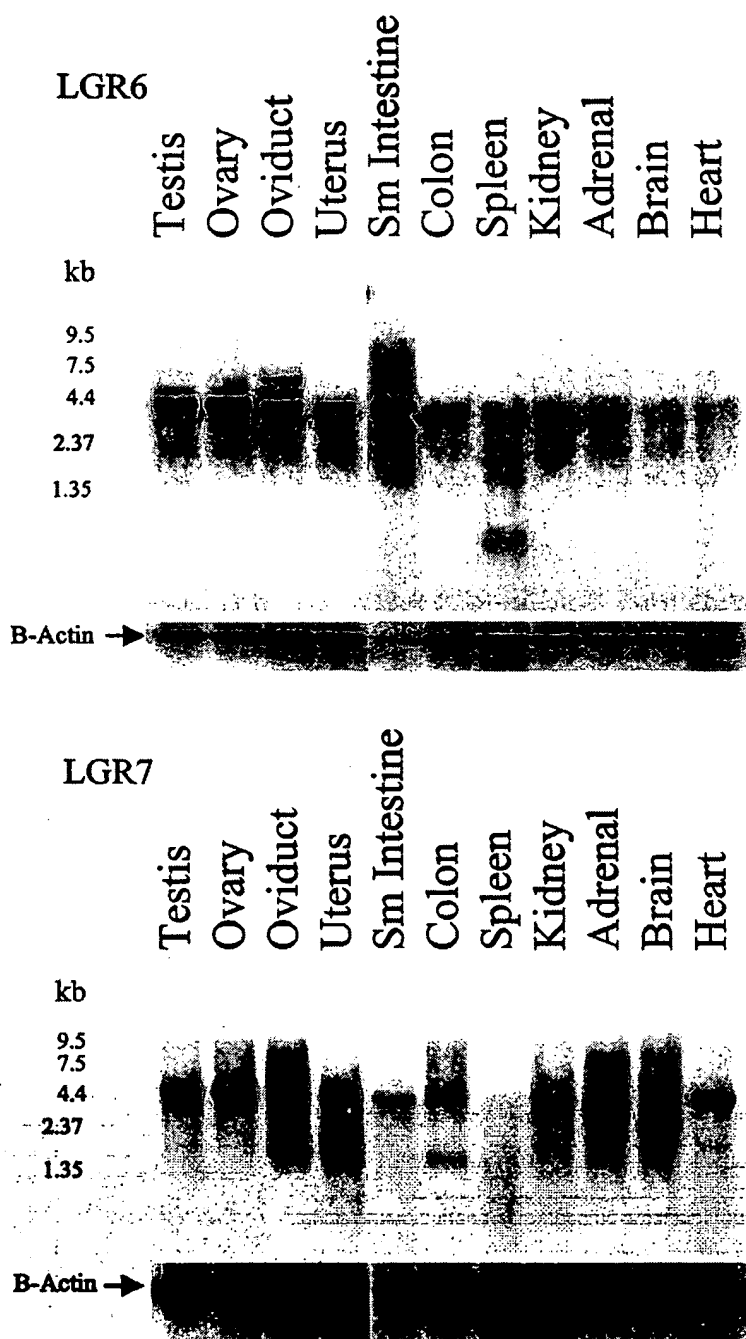


Fig. 4. Tissue Expression Pattern of LGR6 and LGR7

For Northern blot analysis, 2 μ g of poly (A)⁺-selected RNA from different tissues of immature rats were probed with a ³²P-labeled LGR6 or LGR7 cRNA probe. After washing under highly stringent conditions (0.1 × SSC, 1% SDS at 75 C), the blots were exposed to x-ray films with intensifying screens at -80 C. Subsequent hybridization with a β -actin cDNA probe was performed to estimate nucleic acid loading. A, LGR6 Northern blot. A major message of 4.0 kb was found in testis, ovary, oviduct, uterus, small intestine, colon, spleen, kidney, adrenal, brain, and heart. A transcript of higher mol wt (>5.5 kb) was also detected in the oviduct and heart. B, LGR7 Northern blot. A major message of 5.5 kb was found in multiple tissues while multiple transcripts of lower sizes were detected in oviduct, uterus, colon, and brain. Lower panels show the expression of β -actin in the same blots. The sizes of mol wt markers are shown on the left.

through pairwise sequence comparison (30). Although the physiological roles of most new genes are not known, alignment of their primary or secondary struc-

tures have allowed their preliminary grouping. Studies on the entire nematode genome indicated that the GPCR protein superfamily represents one of the most

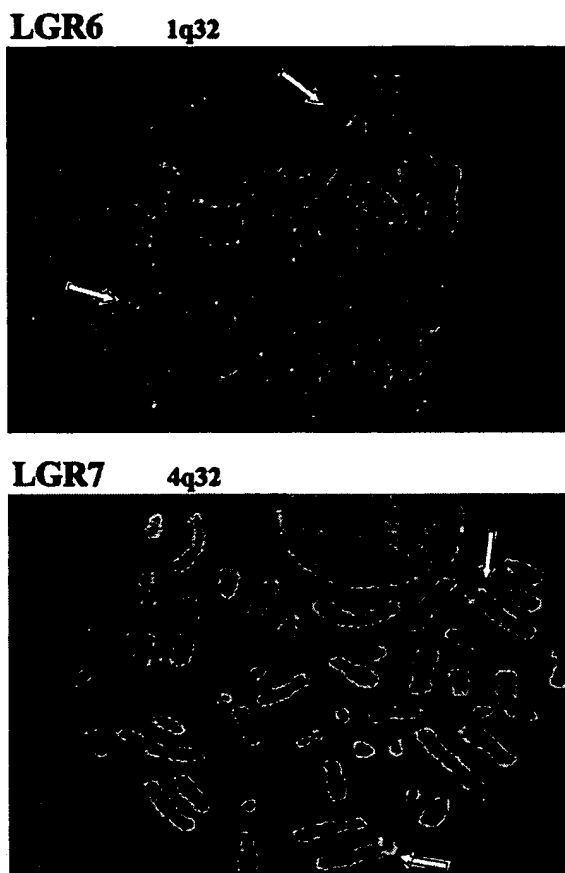


Fig. 5. Chromosomal Localization of LGR6 and LGR7 in Humans

Using DNA fragments of bacterial artificial chromosome containing human genomic fragments of LGR6 and LGR7 as probes, LGR6 (upper panel) and LGR7 (lower panel) genes were localized to chromosome 1q32 and 4q32 regions, respectively, by the fluorescence *in situ* hybridization method. Denatured chromosomes from synchronous cultures of human lymphocytes were hybridized with biotinylated probes for localization. Assignment of the mapping data was achieved by superimposing fluorescence signals with the 4,6-diamidino-2-phenylindole-banded chromosome. Specific signals on the banded chromosome are indicated by arrows.

abundant signaling molecules that allows the cell to communicate with its environment (31, 32), and the GPCR family proteins could account for more than 1% of human genes. Among the known mammalian GPCRs, the glycoprotein hormone receptors represent a unique group of family 1 GPCRs with a large ectodomain for interaction with their ligands. Based on modeling with a prototypic leucine-rich repeat-containing polypeptide, ribonuclease inhibitor (8, 9), it was envisioned that the multiple leucine-rich repeats in the ectodomain of mammalian glycoprotein hormone receptors are arranged in a horseshoe-shaped binding motif and the inwardly β -sheet structures interact with the specific ligand (7–9, 33). Unlike the glycoprotein hormone receptors with nine leucine-rich

repeats, newly isolated mammalian LGRs contain varying numbers of repeats, indicating that the binding domain in these receptors could have the same configuration, but with distinct curvature and size. The glycoprotein hormones have been widely used in the treatment of diverse diseases; the current finding of new LGRs and the possibility of finding additional hormones as ligands for these orphan LGRs could reveal novel endocrine regulatory mechanisms.

The physiological and pathophysiological actions of glycoprotein hormone receptors are mediated mainly through interaction with the Gs protein. Recent characterization of constitutively activated LH and TSH receptors, based on patients with specific etiology (18–20, 25), has allowed analyses of structural requirements for signaling by these receptors. Taking advantage of these observations, mutant LGR7 constructs were made to explore the putative signaling pathways of LGR7. Similar to LH and TSH receptors, mutation of a single structure-determining amino acid in the transmembrane VI region of LGR7 caused constitutive signaling, as reflected by increases in basal cAMP levels in transfected cells. It has been proposed that mutations causing constitutive activation alter the receptor conformation from an inactive to an active state, mimicking the ligand stimulation of these receptors (34–36). Thus, the increase of basal cAMP production by mutant LGR7 receptors could be the result of conformational changes as found for constitutively active LH and TSH receptors. The present findings suggest that wild-type LGR7 may signal through the cAMP-protein kinase A pathway, a mechanism similar to the related glycoprotein hormone receptors. Although the Gs activating mutants LGR7(1) D637Y and LGR7(2) D603Y do not stimulate IP turnover by transfected 293T cells, it is important to note that the coupling of LGR7 to other G proteins cannot be excluded. Other examples of signaling by orphan GPCRs include a wild-type orphan ACCA (adenylate cyclase constitutive activator) receptor found to constitutively activate adenylate cyclase in transfected cells (37).

Recently, endogenous ligands for several orphan receptors have been isolated by monitoring the stimulation of downstream signaling transduction (38–44). With no knowledge of the G protein signaling mechanism, several of these studies were made possible by coexpressing the orphan receptor with chimeric G proteins or G proteins that are promiscuous in receptor coupling. The present study demonstrates that mutagenesis of key residues in the transmembrane domain of GPCR is a novel approach to characterize signaling pathways for orphan GPCRs. While the present study demonstrated that mutagenesis of conserved residues is a useful approach for the characterization of signaling by the orphan LGR7, previous studies indicated that an FSH receptor mutant equivalent to D578Y in the LH receptor does not lead to receptor activation (27), suggesting this approach is only applicable to selective orphan GPCRs.

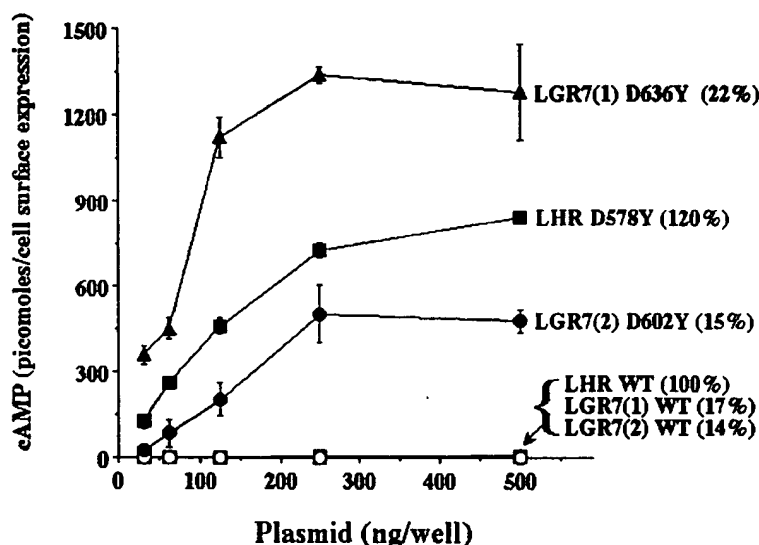


Fig. 6. Gain-of-Function Mutants of LGR7(1) and LGR7(2) Leads to Constitutive Increases of Basal cAMP Production by Transfected 293T Cells

Based on the gain-of-function point mutation (LHR D578Y) found in the LH receptor gene of patients with familial male-limited precocious puberty, LGR7(1) and LGR7(2) with homologous point mutation [LGR7(1) D637Y and LGR7(2) D603Y] were generated. The mutated residues in the TM VI of these two forms of LGR7 were identical, but the numbering of this mutation differs in these two LGR7 variants [D637 in LGR7(1) vs. D603 in LGR7(2)] due to dissimilar length in their N-termini. After transfection of expression constructs encoding wild-type or mutant receptors into 293T cells, basal cAMP levels were monitored using an RIA. Transfection of 293T cells with increasing concentrations (0–500 ng/well) of expression vectors encoding LGR7(1) D637Y, LGR7(2) D603Y, or LHR D578Y led to increases in basal cAMP levels in transfected cells. In contrast, cAMP levels in cells transfected with wild-type (WT) receptors were negligible. Production of cAMP by different receptors was normalized based on cell surface expression of FLAG epitope tagged at the N terminus of all receptor cDNAs determined by immunodetection. Numbers in parentheses denote percentage of receptor protein expression by individual constructs as compared with expression in cells transfected with the wild-type LH receptor construct (LHR WT), which was arbitrarily set as 100% ($n = 3$; mean \pm SE).

TABLE 1. PI Turnover in 293T Cells Expressing Wild-Type or Mutant LGR7 and LH Receptors

	Vector	LHR WT	LHR D578Y	LGR7 (1)WT	LGR7 (1)D637Y	LGR7 (2)WT	LGR7 (2)D603Y
Control	1311 \pm 46	1083 \pm 29	1004 \pm 50	1237 \pm 13	1065 \pm 63	1290 \pm 25	1279 \pm 56
hCG (100 ng/ml)	1161 \pm 25	3447 \pm 29*	2313 \pm 36*	1321 \pm 19	1095 \pm 22	1288 \pm 73	1220 \pm 17

For IP measurement, transfected cells were labeled for 24 h with myo-[3 H]inositol (4 μ Ci/ml) in inositol-free media. After washing, cells were treated with or without hCG at 37 C for 1 h. Data were the mean \pm SE (cpm/tube) of three independent measurements.

*Significantly different from controls without hormone treatment.

Because chimeric receptors with the ectodomain and transmembrane region from different glycoprotein hormone receptors have been shown to be functional (5, 27), we have attempted to characterize the potential coupling of LGR6 to Gs or Gq pathways by fusing the transmembrane region of LGR6 with the ectodomain of the LH receptor in a chimeric construct. Although the chimeric receptor could be expressed on the cell surface, no activation of the chimeric receptor by the LH receptor ligand was observed. Previous studies on similar chimeric receptors containing the ectodomain domain of the LH receptor and the transmembrane domain of LGR4 or LGR5 also suggest that such chimeric receptors do not react to ligand stimulation (15). Thus, either the ectodomain of the LH receptor and the transmembrane region of these orphan

receptors are incompatible, or they could signal through other unknown mechanisms. Indeed, a similar construct of the LH receptor ectodomain plus the LGR7 transmembrane domain failed to allow expression of the chimeric receptor on the cell surface of transfected cells.

The newly identified LGR7 shows close sequence homology with the only known snail LGR (13). Interestingly, the putative ligand-binding domains of these two receptors appear to have diverged. The most obvious difference is the number of LDL receptor cysteine-rich motifs in the N terminus of these two receptors. In the ectodomain of snail receptor, there are 12 LDL receptor cysteine-rich motifs, each encoding three conserved cysteine residues (13, 45) important for disulfide bond formation and ligand binding (46).

Unlike snail LGR, LGR7 contains only one typical LDL receptor cysteine-rich motif in its N terminus. Assuming the motifs in these two related receptors comprise part of their ligand-binding domain, the respective ligands for these two receptors could have diverged during evolution. Future studies on the LGR7 gene could reveal additional LGR7 variants that are closer to snail LGR, and uncover the evolutionary relationship of these two receptors.

Analysis of LGR6 sequences showed that LGR6 belongs to a subgroup of LGRs which includes LGR4 and LGR5, suggesting that these receptors may share similar ligand binding and signal transduction characteristics. However, the ectodomain of LGR6 is unique and contains only 13 leucine-rich repeats instead of the 17 repeats found in LGR4 and LGR5. It is unclear whether the cloned LGR6 cDNA is the only transcript encoded by the LGR6 gene. Observed differences in the number of leucine-rich repeats in the ectodomain of these receptors may be the result of alternative splicing. Recent studies on GPCRs have shown that within a given subfamily functional diversity is most often conferred by the existence of multiple receptor subtypes, each encoded by a distinct gene. Additional diversity results from alternative splicing of a given gene to form receptor variants (47). Indeed, our unpublished results showed that the LGR4 gene encodes multiple splicing variants, including one with only 14 leucine-rich repeats. Likewise, glycoprotein hormone receptor genes also encode multiple splicing variants with distinct functional characteristics (48), and two splicing variants of LGR7 were isolated here. Alternative splicing of these receptors, especially in the ectodomain, could result in alternative binding characteristics or specificity.

Sequence alignment showed that the three subgroups of LGRs could be distinguished merely by the amino acid sequences in their hinge regions between leucine-rich repeats and the transmembrane domain. In the glycoprotein hormone receptors, this region is flanked by the conserved YPSHCC and DXFNPCED motifs whereas LGR4, LGR5, and LGR6 contain YAYQCC and GXFKPCEX sequences in the corresponding regions, respectively. In contrast, these two motifs are absent in LGR7. Interestingly, recent studies on the TSH receptor have shown that point mutation of the serine residue in the conserved YPSHCC motif resulted in constitutive activation of the TSH receptor, leading to severe congenital hyperthyroidism in patients (49–51). Because LGR4, LGR5, and LGR6 share similar structural determinants in the hinge region, investigations on this region of the orphan receptors could provide insights toward the activation mechanisms of different LGRs.

Analysis using 11 known LGRs from diverse organisms indicated that LGRs from sea anemone, nematode, and *Drosophila* grouped under a single branch with mammalian glycoprotein hormone receptors while the newly isolated LGR4, LGR5, LGR6, and LGR7 diverged early during evolution. Assuming the

evolutionary pressures on these receptors are constant, the sequence divergence in mammalian LGRs suggests that the ancestral gene giving rise to modern LGRs could have evolved before the emergence of cnidarians for cell-cell communication. Also of interest, analysis of the completely sequenced *C. elegans* genome showed that this nematode contains only one GPCR with LGR characteristics (12), suggesting a possible gene loss during the evolution of modern nematodes and that different LGRs in present day organisms evolved to serve adaptive functions in different phylogenies.

Findings of multiple LGRs allow a better comparison of the relatedness of the LGR subfamily with other GPCRs in the superfamily. Previous studies have shown that known GPCRs can be divided into six major families with distinct evolutionary origins, and the majority of GPCRs with a peptide or neurotransmitter ligand belong to family 1 (21). Phylogenetic analysis of LGRs with other GPCRs in family 1 indicated that LGRs belong to a distinct branch and share the closest relatedness with a subgroup of GPCRs including receptors for bombesin, gastrin, thrombin, neuropeptide Y, angiotensin, PAF, and FMLP. This classification would allow a better understanding of the ligand signaling mechanisms for these receptors through comparison of their structure-function relationship.

In conclusion, we have cloned two novel mammalian LGRs (LGR6 and LGR7) and identified the putative signal transduction pathway for LGR7. The constitutive activation of cAMP production by the mutant LGR7 suggests that this orphan receptor could signal through the cAMP-dependent pathway. This study represents the first demonstration of the elucidation of the signaling mechanism for an orphan GPCR based on single-point mutations to allow constitutive activation of the protein. The present study also defines the existence of three subclasses of leucine-rich repeat-containing GPCRs in the human genome and possibly other metazoans. Identification and functional characterization of these novel LGRs allow elucidation of the evolutionary relationship of this subfamily of GPCRs with leucine-rich repeats. It also facilitates future studies on the physiology of this expanding subgroup of GPCRs and the identification of their cognate ligands.

MATERIALS AND METHODS

Hormones and Reagents

Purified hCG (CR-129) was supplied by the National Hormone and Pituitary Program (NIDDK, NIH, Bethesda, MD). FLAG M1 antibody and FLAG peptide were purchased from Sigma (St. Louis, MO). 125 I-Na and myo-[3 H] inositol were purchased from Amersham Pharmacia Biotech (Arlington Heights, IL). Dowex AG1-X8 was from Bio-Rad Laboratories, Inc. (Hercules, CA).

Computational Analysis

cDNA sequences related to invertebrate LGRs and mammalian glycoprotein hormone receptors were identified from the EST and genomic survey sequences (GSS) database at the National Center for Biotechnology Information and an Incyte EST database using the BLAST and Gapped BLAST server with the BLOSUM62 comparison matrix (52). Initially, four independent human DNA entries (three ESTs and one GSS AQ053279) were found to encode sequences homologous, but not identical, to the known mammalian LGRs. Based on these sequences, RACE experiments were used to clone the full-length cDNA sequences. After RACE, the four original DNA entries were found to encode different portions of two novel LGRs. The alignment of primary sequences for genes in the LGR family was carried out by the Blocks WWW server (<http://blocks.fhcrc.org/blocks/blockmkr>). The Block Maker program also calculated the branching order and phylogenetic relatedness of aligned sequences by the Cobble and Gibbs algorithms. To compare the phylogenetic relationship of LGRs with diverse peptide and neurotransmitter GPCRs, neighbor-joining (<http://www.bio-phys.kyoto-u.ac.jp/maketree2.html>) and parsimony methods (Phylogeny Inference Package) were used. In all studies, the full-length amino acid sequences of different GPCRs were used for phylogenetic analyses to provide the maximum possible information within families and subfamilies.

Additionally, the analyses of primary and secondary structures of these novel LGRs were conducted using the BCM search launcher (<http://gc.bcm.tmc.edu:8088/search-launcher/launcher.html>), Biology Workbench (<http://gc.bcm.tmc.edu:8088/search-launcher/launcher.html>), Blocks WWW server (<http://www.blocks.fhcrc.org/blocks/>), the eMotif maker server (<http://dna.stanford.edu/emotif/>), or the ExPASy Molecular Biology Server (<http://expasy.hcuge.ch/>).

Identification and Isolation of the Full-Length cDNAs for LGR6 and LGR7

For the isolation of full-length cDNA fragments, specific primers with a design based on EST sequences were used to prepare cDNA pools enriched with the candidate cDNAs derived from human ovary and testis mRNA. Two micrograms of mRNA were reverse transcribed by using 25 U of avian myoblastosis virus reverse transcriptase with oligo(dT) primer, 0.5 mM deoxynucleoside triphosphate (dNTP), and 20 U of RNase inhibitor. After second strand synthesis with T4 DNA polymerase, the cDNA pool was tailed at both ends with adaptor sequences to allow PCR amplification using specific primers. The tailed cDNA products were then employed as a template for 5'- and 3'-RACE with adaptor- and gene-specific primers. All PCR amplifications were performed under highly stringent conditions (annealing temperature >67°C) using Advantage DNA polymerase (CLONTECH Laboratories, Inc., Palo Alto, CA) or Pfu DNA polymerase (Stratagene, La Jolla, CA) to minimize mismatching and infidelity during PCR amplification. PCR products were fractionated using agarose electrophoresis, and specific bands showing hybridization with radiolabeled cDNA probes were subcloned into the pUC18 vector (Invitrogen, San Diego, CA) to further identify candidate clones. The PCR products were phenol/chloroform-extracted, precipitated with ethanol, phosphorylated with T4 polynucleotide kinase, and blunt-ended with the Klenow enzyme. The PCR products were then subcloned into the *Sma*I site in the pUC18 vector. At least two independent PCR clones were sequenced to verify the authenticity of the coding sequences of each cDNA. The resulting sequences were assembled into contigs using the Blast2 sequences server (<http://www.ncbi.nlm.nih.gov/gorf/bl2.html>) and ClustalW 1.7 at the BCM Search Launcher (<http://dot.imgen.bcm.tmc.edu:9331/multi-align>). After the initial round of RACE, it was determined that the multiple homologous sequences belong to two independent LGR genes, LGR6 and LGR7. The

full-length sequences were obtained and confirmed after three rounds of RACE.

Northern Blot Analysis

For mRNA analysis, membranes containing poly(A)⁺ RNA from various rat tissues were hybridized with specific cRNA probes. The rat mRNAs were extracted from 27-day-old rats using Trizol solution (Life Technologies, Inc., Gaithersburg, MD) followed by the Oligotex mRNA purification columns (QIAGEN Inc., Chatsworth, CA) to select for poly(A)⁺ RNA. The cRNA probes were synthesized using a Riboprobe Combination System (Promega Corp., Madison, WI). For hybridization using cRNA probes, membranes were prehybridized for 1 h at 60°C in the ExpressHyb solution (CLONTECH Laboratories, Inc.). This was followed by hybridization under the same conditions for 2 h but with 1×10^5 cpm/ml of ³²P-labeled LGR6 or LGR7 cRNA probes. After hybridization, the membranes were washed twice in $0.2 \times$ sodium chloride/sodium citrate (SSC), 0.5% SDS at 60°C, followed by two washes under high stringency conditions ($0.1 \times$ SSC, 1% SDS at 75°C) before exposure to RX film (Eastman Kodak Co., Rochester, NY) with intensifying screens (Amersham Pharmacia Biotech, Buckinghamshire, UK). To monitor the loading of mRNA samples from different tissues, membranes were stripped and rehybridized with a ³²P-labeled β -actin cDNA probe. The cDNA probe was generated by random priming (Life Technologies, Inc.). For hybridization using cDNA probes, membranes were washed to a stringency of $0.1 \times$ SSC, 1% SDS at 60°C.

Expression of LGR6 and LGR7 in Mammalian Cells

Wild-type and mutant LGR6 and LGR7 cDNAs were constructed by sequential PCR amplification and standard restriction digest and ligation procedures. To allow efficient targeting of receptors to the cell surface and immunodetection *in vitro*, a lead cDNA sequence containing a PRL signal peptide for cell surface expression (MNIKGGSPWKGSLLLLVNLLLQSVAP) and a FLAG (DYKDDDDK) epitope were added to the N terminus of the mature region of LGRs in all expression constructs (53). To construct chimeric LH/LGR6 and LH/LGR7 receptors, junctional amino acid sequences were designed to be CAPEPPDAFN/PCEYLFESWGIRL and CAPEPPDAFN/SCEDLMSNHVLRVS, respectively. For expression in eukaryotic cells, the receptor cDNAs were subcloned into the eukaryotic cell expression vector pcDNA3.1-Zeo (Invitrogen, San Diego, CA), and the plasmids were purified using the Maxi plasmid preparation kit (QIAGEN, Inc.). Each construct was sequenced on both strands using vector-derived primers and gene-specific primers before use in transfection experiments for the analyses of signal transduction and/or receptor binding.

Mammalian 293T cells derived from human embryonic kidney fibroblast were maintained in DMEM/Ham's F-12 (Life Technologies, Inc.) supplemented with 10% FBS, 100 μ g/ml penicillin, 100 μ g/ml streptomycin, and 2 mM L-glutamine. The cells were transfected with expression plasmids using the calcium phosphate precipitation method (54). After 18–24 h of incubation with the calcium phosphate-DNA precipitates, media were replaced with DMEM/F12 containing 10% FBS. Forty-eight hours after transfection, cells were washed twice with Dulbecco's PBS (D-PBS), harvested from culture dishes, and centrifuged at $400 \times g$ for 5 min. Cell pellets were then resuspended in DMEM/F12 supplemented with 1 mg/ml of BSA. Cells (2×10^5 /ml) were placed on 12-well tissue culture plates (Corning, Inc. Corning, NY) and preincubated at 37°C for 30 min in the presence of 0.25 mM 3-isobutyl-1-methyl xanthine (IBMX; Sigma) to prevent hydrolysis of cAMP before hormonal treatment for 16 h. To study basal cAMP production mediated by increasing numbers of receptors, each well was transfected separately with different amounts

of the expression plasmid. To detect signaling by the wild-type and mutated LGRs, levels of cAMP production by transfected cells were measured by specific RIA using [125 I] cAMP (Amersham Pharmacia Biotech) (27). Cells transfected with the empty plasmid (mock) were routinely used as negative controls. At the end of incubation, cells and medium in each well were frozen and thawed once before heating at 95°C for 3 min to inactivate phosphodiesterase activity. Total cAMP in each well was measured in triplicate. For IP measurement, transfected cells were labeled for 24 h with myo-[3 H]-inositol at 4 μ Ci/ml in inositol-free DMEM supplemented with 5% FBS. After washing three times with D-PBS, 2×10^5 cells were preincubated for 30 min in D-PBS containing 20 mM LiCl, and treated with or without hormones at 37°C for 1 h. Total IPs were extracted and separated as previously described (29). All experiments were repeated three times using cells from independent transfections. To monitor transfection efficiency, 0.5 μ g of RSV- β -gal plasmid was routinely included in the transfection mixture, and the β -galactosidase activity in the cell lysate was measured as previously described (55). Statistical analysis was performed using Student's *t* test.

Radioligand Binding Assays

For ligand binding analysis of the wild-type and mutant receptors, human CG (CR-129) was iodinated by the lactoperoxidase method (56) and characterized by a radioligand receptor assay using human LH receptors stably expressed in 293T cells. Specific activity and maximal binding of the labeled hCG were 100,000–150,000 cpm/ng and 40–50%, respectively. To estimate ligand binding to the cell surface, transfected cells were washed twice with D-PBS and collected in D-PBS before centrifugation at $400 \times g$ for 5 min. Pellets were resuspended in D-PBS containing 1 mg/ml BSA (binding assay buffer). Resuspended cells (2×10^5 /tube) were incubated with increasing doses (or a saturating dose) of labeled hCG at room temperature for 22 h in the presence or absence of unlabeled hCG (Pregnyl, 100 IU/tube; Organon, West Orange, NJ). At the end of incubation, cells were centrifuged and washed twice with the binding assay buffer. Radioactivity in the pellets was determined with a γ -spectrometer (53).

Determination of FLAG Epitope-Tagged Receptors on the Cell Surface

Transfected cells were washed twice with D-PBS, and resuspended cells (2×10^6 /tube) were incubated with FLAG-M1 antibody (50 μ g/ml) in Tris-buffered saline (pH 7.4) containing 5 mg/ml BSA and 2 mM CaCl_2 (assay buffer) for 4 h at room temperature in siliconized centrifuge tubes. Cells were then washed twice with 1 ml of assay buffer after centrifugation at $14,000 \times g$ for 15 sec. The [125 I]-labeled second antibody (antimouse IgG from sheep: ~400,000 cpm/tube) was added to the resuspended cell pellet and incubated for 1 h at room temperature. Cells were again washed twice with 1 ml of assay buffer by repeated centrifugation before determination of radioactivity in cell pellets. Background binding was determined by adding excess amounts of the synthetic FLAG peptide at a concentration of 100 μ g/ml.

Genomic Analysis and Chromosomal Localization of LGR6 and LGR7

To isolate genomic clones for LGR6, a human bacterial artificial chromosome (BAC) genomic DNA library was screened using the transmembrane region of LGR6 cDNA as a probe. The LGR7 genomic clone was identified by a sequence search of the GSS database and obtained from Genome Systems. These genomic fragments were then confirmed by

Southern blot hybridization. For the identification of the chromosomal localization of LGR6 and LGR7 genes, genomic fragments (>50 kb) were used as probes for FISH of human metaphase chromosomes. Denatured chromosomes from synchronous cultures of human lymphocytes were hybridized with biotinylated probes for signal localization.

Acknowledgments

We are thankful to R. Slater (Department of Cytogenetics, Erasmus University, Rotterdam, The Netherlands) for the chromosomal localization of LGRs. We also thank Caren Spencer for editorial assistance. The GenBank accession numbers for LGR6 and LGR7 are AF190501 and AF190500, respectively.

Received November 9, 1999. Revision received May 4, 2000. Accepted May 9, 2000.

Address requests for reprints to: Dr. Aaron J. W. Hsueh, Division of Reproductive Biology, Department of Gynecology and Obstetrics, Stanford University School of Medicine, Stanford, California 94305-5317. E-mail: aaron.hsueh@stanford.edu.

This study was supported by NIH Grant HD-31566. S.Y.H. was supported by NIH Training Grant T32 DK-07217. The GenBank accession numbers for LGR6 and LGR7 are AF190501 and AF190500, respectively.

* On sabbatical leave from the Department of Biochemistry and Cellular and Molecular Biology, The University of Tennessee, Knoxville, Tennessee 37996.

REFERENCES

- Pierce JG, Parsons TF 1981 Glycoprotein hormones: structure and function. *Annu Rev Biochem* 50:465–495
- Hsueh AJ, Eisenhauer K, Chun SY, Hsu SY, Billig H 1996 Gonadal cell apoptosis. *Recent Prog Horm Res* 51: 433–455
- Vassart G, Dumont JE 1992 The thyrotropin receptor and the regulation of thyrocyte function and growth. *Endocr Rev* 13:596–611
- Vassart G 1997 New pathophysiological mechanisms for hyperthyroidism. *Horm Res* 48:47–50
- Braun T, Schofield PR, Sprengel R 1991 Amino-terminal leucine-rich repeats in gonadotropin receptors determine hormone selectivity. *EMBO J* 10:1885–1890
- Ji TH, Ryu KS, Gilchrist R, Ji I 1997 Interaction, signal generation, signal divergence, and signal transduction of LH/CG and the receptor. *Recent Prog Horm Res* 52: 431–453
- Jiang X, Dreano M, Buckler DR, Cheng S, Ythier A, Wu H, Hendrickson WA, el Tayar N 1995 Structural predictions for the ligand-binding region of glycoprotein hormone receptors and the nature of hormone-receptor interactions. *Structure* 3:1341–1353
- Kajava AV, Vassart G, Wodak SJ 1995 Modeling of the three-dimensional structure of proteins with the typical leucine-rich repeats. *Structure* 3:867–877
- Kobe B, Deisenhofer J 1993 Crystal structure of porcine ribonuclease inhibitor, a protein with leucine-rich repeats. *Nature* 366:751–756
- Nothacker HP, Grimmlikhuizen CJ 1993 Molecular cloning of a novel, putative G protein-coupled receptor from sea anemones structurally related to members of the FSH, TSH, LH/CG receptor family from mammals. *Biochem Biophys Res Commun* 197: 1062–1069
- Vibede N, Hauser F, Williamson M, Grimmlikhuizen CJ 1998 Genomic organization of a receptor from sea ane-

- mones, structurally and evolutionarily related to glycoprotein hormone receptors from mammals. *Biochem Biophys Res Commun* 252:497-501
12. Kudo M, Chen T, Nakabayashi K, Hsu SY, Hsueh AJ 2000 The nematode leucine-rich repeat-containing, G protein-coupled receptor (LGR) protein homologous to vertebrate gonadotropin, thyrotropin receptors is constitutively activated in mammalian cells. *Mol Endocrinol* 14:272-284
13. Tensen CP, Van Kesteren ER, Planta RJ, Cox KJ, Burke JF, van Heerikhuizen H, Vreugdenhil E 1994 A G protein-coupled receptor with low density lipoprotein-binding motifs suggests a role for lipoproteins in G-linked signal transduction. *Proc Natl Acad Sci USA* 91:4816-4820
14. Hauser F, Nothacker HP, Grimmlikhuizen CJ 1997 Molecular cloning, genomic organization, and developmental regulation of a novel receptor from *Drosophila melanogaster* structurally related to members of the thyroid-stimulating hormone, follicle-stimulating hormone, luteinizing hormone/choriogonadotropin receptor family from mammals. *J Biol Chem* 272:1002-1010
15. Hsu SY, Liang SG, Hsueh AJ 1998 Characterization of two LGR genes homologous to gonadotropin and thyrotropin receptors with extracellular leucine-rich repeats and a G protein-coupled, seven-transmembrane region. *Mol Endocrinol* 12:1830-1845
16. McDonald T, Wang R, Bailey W, Xie G, Chen F, Caskey CT, Liu Q 1998 Identification and cloning of an orphan G protein-coupled receptor of the glycoprotein hormone receptor subfamily. *Biochem Biophys Res Commun* 247:266-270
17. Hermey G, Methner A, Schaller HC, Hermans-Borgmeyer I 1999 Identification of a novel seven-transmembrane receptor with homology to glycoprotein receptors and its expression in the adult and developing mouse. *Biochem Biophys Res Commun* 254:273-279
18. Shenker A, Laue L, Kosugi S, Merendino Jr JJ, Minegishi T, Cutler Jr GB 1993 A constitutively activating mutation of the luteinizing hormone receptor in familial male precocious puberty. *Nature* 365:652-654
19. Laue L, Chan WY, Hsueh AJ, Kudo M, Hsu SY, Wu SM, Blomberg L, Cutler Jr GB 1995 Genetic heterogeneity of constitutively activating mutations of the human luteinizing hormone receptor in familial male-limited precocious puberty. *Proc Natl Acad Sci USA* 92:1906-1910
20. Parma J, Duprez L, Van Sande J, Cochaux P, Gervy C, Mockel J, Dumont J, Vassart G 1993 Somatic mutations in the thyrotropin receptor gene cause hyperfunctioning thyroid adenomas. *Nature* 365:649-651
21. Bockaert J, Pin JP 1999 Molecular tinkering of G protein-coupled receptors: an evolutionary success. *EMBO J* 18:1723-1729
22. Kosugi S, Mori T, Shenker A 1996 The role of Asp578 in maintaining the inactive conformation of the human lutropin/choriogonadotropin receptor. *J Biol Chem* 271:31813-31817
23. Kosugi S, Mori T, Shenker A 1998 An anionic residue at position 564 is important for maintaining the inactive conformation of the human lutropin/choriogonadotropin receptor. *Mol Pharmacol* 53:894-901
24. Laue L, Wu SM, Kudo M, Hsueh AJW, Cutler Jr GB, Jelly DH, Diamond FB, Chan WY 1996 Heterogeneity of activating mutations of the human luteinizing hormone receptor in male-limited precocious puberty. *Biochem Mol Med* 58:192-198
25. Parma J, Duprez L, Van Sande J, Hermans J, Rocmans P, Van Vliet G, Costagliola S, Rodien P, Dumont JE, Vassart G 1997 Diversity and prevalence of somatic mutations in the thyrotropin receptor and $G_{s\alpha}$ genes as a cause of toxic thyroid adenomas. *J Clin Endocrinol Metab* 82:2695-2701
26. Russo D, Arturi F, Suarez HG, Schlumberger M, Du Villard JA, Crocetti U, Filetti S 1996 Thyrotropin receptor gene alterations in thyroid hyperfunctioning adenomas. *J Clin Endocrinol Metab* 81:1548-1551
27. Kudo M, Osuga Y, Kobilka BK, Hsueh AJW 1996 Transmembrane regions V and VI of the human luteinizing hormone receptor are required for constitutive activation by a mutation in the third intracellular loop. *J Biol Chem* 271:22470-22478
28. Gudermann T, Birnbaumer M, Birnbaumer L 1992 Evidence for dual coupling of the murine luteinizing hormone receptor to adenylyl cyclase and phosphoinositide breakdown and Ca^{2+} mobilization. Studies with the cloned murine luteinizing hormone receptor expressed in L cells. *J Biol Chem* 267:4479-4488
29. Hirsch B, Kudo M, Naro F, Conti M, Hsueh AJ 1996 The C-terminal third of the human luteinizing hormone (LH) receptor is important for inositol phosphate release: analysis using chimeric human LH/follicle-stimulating hormone receptors. *Mol Endocrinol* 10:1127-1137
30. Hsu SY, Hsueh AJ 2000 Discovering new hormones, receptors, and signaling mediators in the genomic era. *Mol Endocrinol* 14:594-604
31. Plasterk RH 1999 The year of the worm. *Bioessays* 21:105-109
32. Jansen G, Thijssen KL, Werner P, van der Horst M, Hazendonk E, Plasterk RH 1999 The complete family of genes encoding G proteins of *Caenorhabditis elegans*. *Nat Genet* 21:414-419
33. Lathorn AJ, Harris DC, Littlejohn A, Lustbader JW, Canfield RE, Machin KJ, Morgan FJ, Isaacs NW 1994 Crystal structure of human chorionic gonadotropin. *Nature* 369:455-461
34. Lefkowitz RJ 1993 G-protein-coupled receptors. Turned on to ill effect. *Nature* 365:603-604
35. Lin Z, Shenker A, Pearlstein R 1997 A model of the lutropin/choriogonadotropin receptor: insights into the structural and functional effects of constitutively activating mutations. *Protein Eng* 10:501-510
36. Abell AN, McCormick DJ, Segaloff DL 1998 Certain activating mutations within helix 6 of the human luteinizing hormone receptor may be explained by alterations that allow transmembrane regions to activate Gs. *Mol Endocrinol* 12:1857-1869
37. Eggerickx D, Deneff JF, Labbe O, Hayashi Y, Refetoff S, Vassart G, Parmentier M, Libert F 1995 Molecular cloning of an orphan G-protein-coupled receptor that constitutively activates adenylate cyclase. *Biochem J* 309:837-843
38. Chambers J, Ames RS, Bergsma D, Muir A, Fitzgerald LR, Hervieu G, Dytko GM, Foley JJ, Martin J, Liu WS, Park J, Ellis C, Ganguly S, Konchar S, Cluderay J, Leslie R, Wilson S, Sarau HM 1999 Melanin-concentrating hormone is the cognate ligand for the orphan G-protein-coupled receptor SLC-1. *Nature* 400:261-265
39. Sarau HM, Ames RS, Chambers J, Ellis C, Elshourbagy N, Foley JJ, Schmidt DB, Muccitelli RM, Jenkins O, Murdock PR, Herity NC, Halsey W, Sathe G, Muir AJ, Nuthallaganti P, Dytko GM, Buckley PT, Wilson S, Bergsma DJ, Hay DW 1999 Identification, molecular cloning, expression, and characterization of a cysineyl leukotriene receptor. *Mol Pharmacol* 56:657-663
40. Feighner SD, Tan CP, McKee KK, Palyha OC, Hreniuk DL, Pong SS, Austin CP, Figueroa D, MacNeil D, Cascieri MA, Nargund R, Bakshi R, Abramovitz M, Stocco R, Kargman S, O'Neill G, Van Der Ploeg LH, Evans J, Patchett AA, Smith RG, Howard AD 1999 Receptor for motilin identified in the human gastrointestinal system. *Science* 284:2184-2188
41. Hinuma S, Habata Y, Fujii R, Kawamata Y, Hosoya M, Fukusumi S, Kitada C, Masuo Y, Asano T, Matsumoto H, Sekiguchi M, Kurokawa T, Nishimura O, Onda H, Fujino

- M 1998 A prolactin-releasing peptide in the brain. *Nature* 393:272-276
42. Lynch KR, O'Neill GP, Liu Q, Im DS, Sawyer N, Metters KM, Coulombe N, Abramovitz M, Figueroa DJ, Zeng Z, Connolly BM, Bai C, Austin CP, Chateaufneuf A, Stocco R, Greig GM, Kargman S, Hooks SB, Hosfield E, Williams Jr DL, Ford-Hutchinson AW, Caskey CT, Evans JF 1999 Characterization of the human cysteinyl leukotriene CysLT1 receptor. *Nature* 399:789-793
43. Saito Y, Nothacker HP, Wang Z, Lin SH, Leslie F, Civelli O 1999 Molecular characterization of the melanin-concentrating-hormone receptor. *Nature* 400:265-269
44. Sakurai T, Amemiya A, Ishii M, Matsuzaki I, Chemelli RM, Tanaka H, Williams SC, Richardson JA, Kozlowski GP, Wilson S, Arch JR, Buckingham RE, Haynes AC, Carr SA, Annan RS, McNulty DE, Liu WS, Terrett JA, Elshourbagy NA, Bergsma DJ, Yanagisawa M 1998 Orexins and orexin receptors: a family of hypothalamic neuropeptides and G protein-coupled receptors that regulate feeding behavior. *Cell* 92:573-585
45. Russell DW, Schneider WJ, Yamamoto T, Luskey KL, Brown MS, Goldstein JL 1984 Domain map of the LDL receptor: sequence homology with the epidermal growth factor precursor. *Cell* 37:577-585
46. Esser V, Limbird LE, Brown MS, Goldstein JL, Russell DW 1988 Mutational analysis of the ligand binding domain of the low density lipoprotein receptor. *J Biol Chem* 263:13282-13290
47. Kilpatrick GJ, Dautzenberg FM, Martin GR, Eglen RM 1999 7TM receptors: the splicing on the cake. *Trends Pharmacol Sci* 20:294-301
48. Loosfelt H, Misrahi M, Atger M, Salesse R, Vu Hai-Luu Thi MT, Jolivet A, Guiochon-Mantel A, Sar S, Jallat B, Garnier J, Milgrom E 1989 Cloning and sequencing of porcine LH-hCG receptor cDNA: variants lacking transmembrane domain. *Science* 245:525-528
49. Gruters A, Schoneberg T, Biebermann H, Krude H, Krohn HP, Dralle H, Gudermand T 1998 Severe congenital hyperthyroidism caused by a germ-line neo mutation in the extracellular portion of the thyrotropin receptor. *J Clin Endocrinol Metab* 83:1431-1436
50. Duprez L, Parma J, Costagliola S, Hermans J, Van Sande J, Dumont JE, Vassart G 1997 Constitutive activation of the TSH receptor by spontaneous mutations affecting the N-terminal extracellular domain. *FEBS Lett* 409:469-474
51. Kopp P, Muirhead S, Jourdain N, Gu WX, Jameson JL, Rodd C 1997 Congenital hyperthyroidism caused by a solitary toxic adenoma harboring a novel somatic mutation (serine281→isoleucine) in the extracellular domain of the thyrotropin receptor. *J Clin Invest* 100:1634-1639
52. Altschul SF, Madden TL, Schaffer AA, Zhang J, Zhang Z, Miller W, Lipman DJ 1997 Gapped BLAST and PSI-BLAST: a new generation of protein database search programs. *Nucleic Acids Res* 25:3389-3402
53. Osuga Y, Kudo M, Kaipia A, Kobilka B, Hsueh AJ 1997 Derivation of functional antagonists using N-terminal extracellular domain of gonadotropin and thyrotropin receptors. *Mol Endocrinol* 11:1659-1668
54. Chen C, Okayama H 1987 High-efficiency transformation of mammalian cells by plasmid DNA. *Mol Cell Biol* 7:2745-2752
55. Su JG, Hsueh AJ 1992 Characterization of mouse inhibin alpha gene and its promoter. *Biochem Biophys Res Commun* 186:293-300
56. Miyachi Y, Vaitukaitis JL, Nieschlag E, Lipsett MB 1972 Enzymatic radioiodination of gonadotropins. *J Clin Endocrinol Metab* 34:23-28



REPORTS

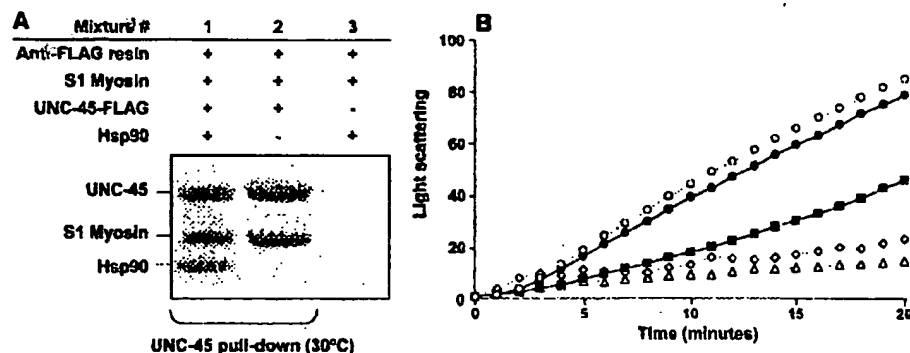


Fig. 3. UNC-45 prevented the thermal aggregation of S1 and formed stoichiometric complexes with Hsp90 and S1. (A) SDS-PAGE analysis of S1 (10 μ M) and/or Hsp90 (1 μ M) interacting with UNC-45 (1 μ M) at 30°C for 30 min. (B) The aggregation of S1 (1.0 μ M) at 43°C was measured by light scattering (320 nm) (11) with no additional protein (solid circles), 2.0 μ M bovine serum albumin (open circles), 0.5 μ M UNC-45 (squares), 1.0 μ M UNC-45 (diamonds), or 2.0 μ M UNC-45 (triangles).

myosin rod fragments and associated light chains (26, 27), and might require interaction with chaperones. We studied the binding of UNC-45 to myosin heads using myosin subfragment 1 (S1) that had been enzymatically cleaved from intact myosin. Full-length UNC-45, immobilized via its FLAG tag, was used to pull down scallop muscle S1 with or without Hsp90 at 30°C (11). UNC-45 formed stoichiometric complexes with S1 and Hsp90 (Fig. 3A). Thus, UNC-45 directly binds the myosin head in addition to Hsp90, which is consistent with the formation of a ternary complex. S1, like citrate synthase, aggregated when incubated at 43°C, but the addition of increasing amounts of UNC-45 reduced S1 aggregation in a concentration-dependent manner (Fig. 3B) (11), whereas bovine serum albumin had no effect. Thus, the myosin head is a substrate for the UNC-45 chaperone activity. The biological specificity of this UNC-45 activity toward myosin suggested by the genetic and cell biological experiments may be determined by parts of the molecule that make additional contacts with myosin, as well as by the actual localization of UNC-45 in vivo.

We have shown that UNC-45 binds myosin through its COOH-terminal regions and binds Hsp90 through its TPR domain. Both interactions appeared to be stoichiometric, similar to those of the progesterone receptor with Hsp90 and interacting co-chaperones (28). The interaction of UNC-45 with myosin required above-ambient temperatures consistent with a chaperone:substrate relationship. The hypothesis that UNC-45 is a myosin chaperone is supported by the fact that UNC-45 interacted and showed molecular chaperone activity in vitro with the myosin head. Thus, in conjunction with previous genetic studies that implicated UNC-45 in myosin assembly in vivo, our results suggest that the UCS proteins may function as myosin-directed chaperones analogously to Cdc37, which targets Hsp90 to protein kinases and exhibits chaperone activity in vitro (21). Previous studies show that the UNC-54 myosin heavy

chain in *unc-45* mutant backgrounds acts as a poison for thick filament assembly (7), accumulates at 50% lower levels than in the wild type (2), localizes abnormally (2, 15), and produces structurally altered thick filaments (2). These results may be explained by defects in the chaperone or co-chaperone activity of UNC-45 that lead to altered folding and assembly of myosin.

References and Notes

1. J. M. Barral, H. F. Epstein, *Bioessays* 21, 813 (1999).
2. J. M. Barral, C. C. Bauer, L. Ortiz, H. F. Epstein, *J. Cell Biol.* 143, 1215 (1998).
3. V. Berteaux-Lecellier et al., *EMBO J.* 17, 1248 (1998).
4. R. Jansen, C. Dowzer, C. Michaelis, M. Galova, K. Nasmyth, *Cell* 84, 687 (1995).
5. B. Wendland, J. M. McCaffery, Q. Xiao, S. D. Emr, *J. Cell Biol.* 135, 1485 (1996).
6. K. C. Y. Wong, N. I. Naqvi, Y. Iino, M. Yamamoto, M. K. Balasubramanian, *J. Cell Sci.* 113, 163 (2000).
7. L. Venolia, R. Waterston, *Genetics* 126, 345 (1990).
8. M. G. Price, J. M. Barral, H. F. Epstein, unpublished observations.

9. G. L. Blatch, M. Lässle, *Bioessays* 21, 932 (1999).
10. L. Venolia, W. Ao, S. Kim, C. Kim, D. Pilgrim, *Cell Motil. Cytoskeleton* 42, 163 (1999).
11. For supplementary figures and descriptions of materials and methods, see Science Online at www.sciencemag.org/cgi/content/full/295/5555/669/DC1.
12. L. C. Russell, S. R. Whitt, M.-S. Chen, M. Chinkers, *J. Biol. Chem.* 274, 20060 (1999).
13. C. Scheutler et al., *Cell* 101, 199 (2000).
14. Single-letter abbreviations for the amino acid residues are as follows: A, Ala; C, Cys; D, Asp; E, Glu; F, Phe; G, Gly; H, His; I, Ile; K, Lys; L, Leu; M, Met; N, Asn; P, Pro; Q, Gln; R, Arg; S, Ser; T, Thr; V, Val; W, Trp; and Y, Tyr.
15. H. F. Epstein, J. N. Thomson, *Nature* 250, 579 (1974).
16. W. Ao, D. Pilgrim, *J. Cell Biol.* 148, 375 (2000).
17. D. F. Smith, D. B. Schowalter, S. L. Kost, D. O. Toft, *Mol. Endocrinol.* 4, 1704 (1990).
18. K. D. Dittmar, K. A. Hutchison, J. K. Owens-Grillo, W. B. Pratt, *J. Biol. Chem.* 271, 12833 (1996).
19. S. Bose, T. Weikl, H. Böggl, J. Buchner, *Science* 274, 1715 (1996).
20. B. C. Freeman, D. O. Toft, R. Morimoto, *Science* 274, 1718 (1996).
21. Y. Kimura et al., *Genes Dev.* 11, 1775 (1997).
22. F. U. Hartl, *Nature* 381, 571 (1996).
23. J. Buchner, H. Grallert, U. Jakob, *Methods Enzymol.* 290, 323 (1998).
24. R. Srikulam, D. A. Winkelmann, *J. Biol. Chem.* 274, 27265 (1999).
25. E. M. McNally, E. B. Goodwin, J. A. Spudis, L. A. Leinwand, *Proc. Natl. Acad. Sci. U.S.A.* 85, 7270 (1988).
26. A. Delozanne, C. H. Bertol, L. A. Leinwand, J. A. Spudis, *J. Cell Biol.* 105, 2999 (1987).
27. V. L. Wolff-Long, L. D. Saraswat, S. Lowey, *J. Biol. Chem.* 268, 23162 (1993).
28. H. Kosano, B. Sterisgard, M. C. Charlesworth, N. McMahon, D. Toft, *J. Biol. Chem.* 273, 32973 (1998).
29. We thank H. F. Gilbert for his invaluable help with the chaperone assays and F. Liu and M. G. Price for advice and discussions. Scallop muscle myosin S1 was provided by A. G. Szent-Györgyi. Supported by grants from the Muscular Dystrophy Association and the National Institute of General Medical Sciences (H.F.E.) and a fellowship from the Boehringer Ingelheim Foundation (A.B.).

28 September 2001; accepted 5 December 2001

Activation of Orphan Receptors by the Hormone Relaxin

Sheau Yu Hsu,¹ Koji Nakabayashi,¹ Shinya Nishi,¹ Jin Kumagai,¹ Masataka Kudo,¹ O. David Sherwood,² Aaron J. W. Hsueh^{1*}

Relaxin is a hormone important for the growth and remodeling of reproductive and other tissues during pregnancy. Although binding sites for relaxin are widely distributed, the nature of its receptor has been elusive. Here, we demonstrate that two orphan heterotrimeric guanine nucleotide binding protein (G protein)-coupled receptors, LGR7 and LGR8, are capable of mediating the action of relaxin through an adenosine 3',5'-monophosphate (cAMP)-dependent pathway distinct from that of the structurally related insulin and insulin-like growth factor family ligand. Treatment of antepartum mice with the soluble ligand-binding region of LGR7 caused parturition delay. The wide and divergent distribution of the two relaxin receptors implicates their roles in reproductive, brain, renal, cardiovascular, and other functions.

Relaxin has diverse actions in the reproductive tract and other tissues during pregnancy (1). These actions include promotion of growth and dilation of the cervix, growth and quies-

cence of the uterus, growth and development of the mammary gland and nipple, and regulation of cardiovascular function. Although binding sites for relaxin have been found in reproduc-

REPORTS

tive tissues (2), brain (3), and heart (4), the nature of the relaxin receptor has not been determined. Prorelaxin, the precursor form of relaxin, has a domain arrangement similar to that of insulin and insulin-like growth factor (IGF) precursors, and several relaxin and insulin-related genes have been identified, including those encoding INSL3 (or Leydig cell relaxin), INSL4, INSL5, INSL6, and relaxin 3 (5-7). The abnormal testis descent phenotype of INSL3-null mice (5, 8) is similar to that of mice with a disruption of a G protein-coupled receptor (GPCR) encoded by the *GREAT* gene (9); this finding suggests that relaxin-related proteins may be ligands for GPCRs. Indeed, relaxin stimulates cAMP production in endometrial, anterior pituitary, and other cells (1), an event mediated by GPCRs.

The orphan leucine-rich repeat-containing GPCRs (LGRs) designated as LGR4 through LGR7 are structurally similar to the LGRs for gonadotropins and thyrotropin (10, 11). LGR7 can be distinguished from the other three orphan LGRs on the basis of structural motifs and phylogenetic analysis. Moreover, LGR7 likely couples to G_s proteins, because constitutively active LGR7 mutants show ligand-independent cAMP production (11). We screened the human genome with LGR7 in search of novel paralogs, and isolated LGR8 (12, 13). LGR8 proved to be the human ortholog of the mouse *GREAT* GPCR and shares about 60% sequence identity with LGR7 (13). Phylogenetic analysis also showed that LGR8 is closely related to an orthologous *Drosophila* receptor, DmLGR3, and to the snail LGR (13). Similar to the gain-of-function mutants identified for LGR7 (Asp⁶³⁷ → Tyr) (11) and the luteinizing hormone (LH) receptor (Asp⁵⁷⁸ → Tyr), an LGR8 mutant with the same amino acid substitution in transmembrane helix VI conferred a ligand-independent increase in basal cAMP production in transfected human fetal kidney 293T cells (13). Thus, LGR7 and LGR8 likely signal through the adenylate cyclase pathway.

Treatment of transfected cells expressing either LGR7 or LGR8 with porcine relaxin resulted in a dose-dependent increase in cAMP production, with median effective concentrations of 1.5 and 5.0 nM, respectively (Fig. 1). In contrast, treatment with structural homologs (insulin, IGF-I, or IGF-II) or with an unrelated peptide (glucagon) was ineffective. These findings indicate that relaxin is a cognate ligand for these two orphan GPCRs and that it activates adenylate cyclases through G_s proteins.

To determine whether the expression of LGR7 and LGR8 is consistent with known relaxin binding sites, we determined their expression patterns (13). Reverse transcription polymerase chain reaction (RT-PCR) analysis of 22 different human cDNAs indicated that LGR7 transcript is expressed in the brain, kidney, testis, placenta, uterus, ovary, adrenal, prostate, skin, and heart. However, LGR8 transcript is mainly present in brain,

kidney, muscle, testis, thyroid, uterus, peripheral blood cells, and bone marrow. Specific antibodies were generated against the ectodomain of LGR7 (14). Immunohistochemical analysis showed that the expression of LGR7 is cell type-specific in different rodent tissues (Fig. 2). In the uterus, LGR7 was expressed mainly in the myometrium and in the epithelial layer of the endometrium. In the vagina and cervix, LGR7 was found in muscularis

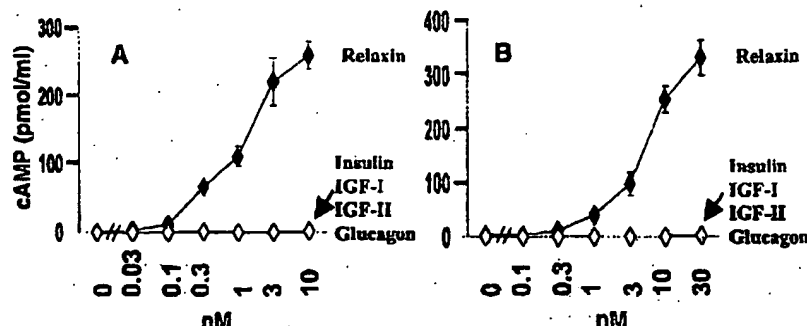


Fig. 1. LGR7 and LGR8 are relaxin receptors. Porcine relaxin stimulated dose-dependent cAMP production in transfected 293T cells (10^5 cells per culture) expressing LGR7 (A) or LGR8 (B) using the pcDNA3.1-Zeo expression vector (11). In contrast, treatment with insulin, IGF-1, IGF-II, or glucagon (a known G_s -coupled receptor activator) had no effect on cAMP production. Treatment with relaxin did not increase cAMP production by nontransfected cells or 293T cells overexpressing related receptors, LH receptor, LGR4, LGR5, or a short splicing variant of LGR7 (11). Total cAMP production was measured in triplicate by a specific radioimmunoassay (10, 28).

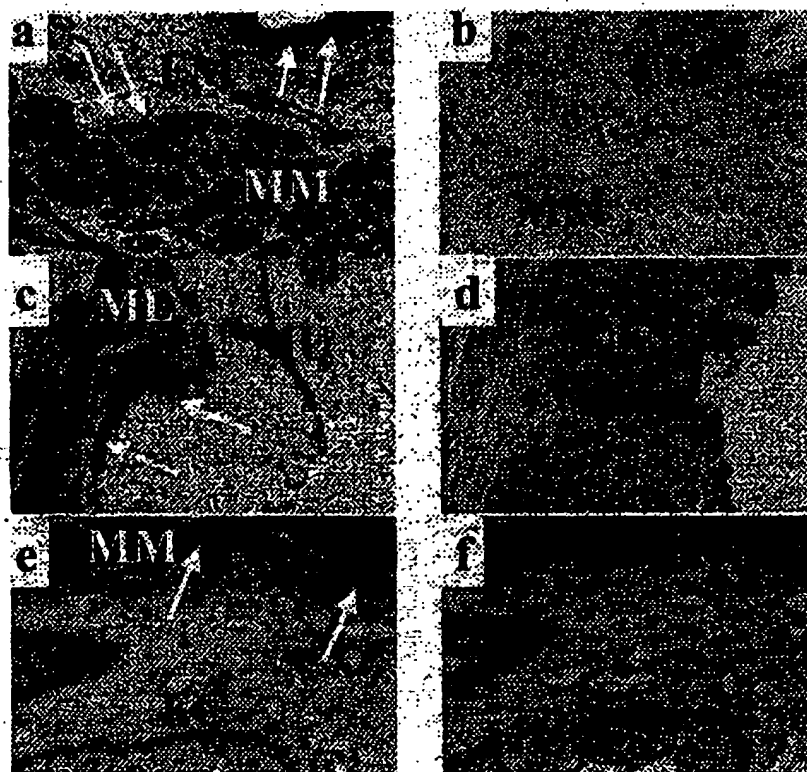


Fig. 2. Tissue distribution of LGR7, as assessed by immunohistochemical analysis in rodent tissues. Uterine tissues were obtained from postpartum rats; vagina and cervix were from rats at 19 days of pregnancy. Specific staining with antibody to LGR7 (14) in uterus (a), vagina (c), and cervix (e) is indicated by arrows. Nonimmune serum showed negligible staining in uterus (b), vagina (d), and cervix (f). Abbreviations: EM, endometrium; MM, myometrium; ML, muscularis layer; MU, mucosal layer; EC, endocervix. Immunohistochemical analysis was performed as described (6). Magnifications, $\times 100$.

¹Division of Reproductive Biology, Department of Gynecology and Obstetrics, Stanford University School of Medicine, Stanford, CA 94305, USA. ²Department of Molecular and Integrative Physiology, University of Illinois, Urbana-Champaign, IL 61801, USA.

*To whom correspondence should be addressed. E-mail: aaron.hsueh@stanford.edu

REPORTS

layers and the myometrium, respectively.

Following an anchored receptor approach previously used to generate soluble ectodomains of the gonadotropin and thyrotropin receptors for use as functional antagonists (15), we established stable cell lines expressing a fusion protein that comprised the ectodomain of LGR7 and the transmembrane region of a T cell surface antigen CD8. Upon treatment of cells with thrombin, a thrombin cleavage site located at the LGR7-CD8 junction allowed the release of the soluble ectodomain of LGR7, designated as 7BP. Western blot analysis indicated a single 7BP band of ~60 kD (Fig. 3A). Cross-linking analysis demonstrated the formation of high molecular weight complexes between relaxin and 7BP (Fig. 3B). In contrast, the soluble

ectodomain from rat LGR4 (4BP) showed negligible interaction with relaxin.

To determine whether soluble 7BP could serve as a functional antagonist by sequestering relaxin, we simultaneously treated transfected 293T cells expressing LGR7 with relaxin and 7BP (Fig. 4A). Both 7BP and antibodies to porcine relaxin effectively blocked the effects of relaxin. However, cotreatment of relaxin with boiled 7BP or purified 4BP had minimal effect. In addition, the stimulatory effect of relaxin on rat myometrial cells (16) was also antagonized by cotreatment with 7BP (Fig. 4B).

The antagonistic action of 7BP was further tested in vivo. Subcutaneous administration of 7BP (500 µg/day) for 4 days (days 17

to 20 after conception) in pregnant mice led to parturition delay by 27 hours (17). Most living pups had minimal milk in their stomachs. In antepartum mice, treatment with 7BP also led to the underdevelopment of nipples, as demonstrated by a 29% decrease in nipple size at about 12 hours after parturition (17). This finding is consistent with the deficiency of nipple development found in relaxin-null mice (18). An earlier study (19) also found a disruption of normal delivery in pregnant rats treated with antibodies to relaxin.

The signaling of relaxin through GPCRs is different from that of insulin and IGFs, which involves tyrosine kinase receptors (20). The existence of divergent receptor types for relaxin and insulin is consistent with the crystal structures of these ligands (21). However, the participation of downstream tyrosine kinases in relaxin signaling could not be ruled out (22). The common phenotypes of INSL3-null and GREAT-null mice indicate that INSL3 may be another ligand for LGR8, and possibly for LGR7.

Preterm labor and delivery remain major obstetrical problems. Studies on relaxin receptors could allow the design of agonistic or antagonistic relaxin analogs for the treatment of disorders of labor onset. Relaxin also has a role in regulating pituitary hormone release (1, 23), renal vasculature (24), and lung and skin remodeling (25) as well as in heart failure, angiogenesis, and tumor formation (26, 27). The identification of two relaxin receptors with overlapping tissue expression patterns could facilitate our understanding of relaxin actions in diverse physiological and pathological conditions.

References and Notes

- O. D. Sherwood, in *The Physiology of Reproduction*, E. Knobil, J. D. Neill, Eds. (Raven, New York, 1994), vol. 1, pp. 861-1009.
- G. Min, O. D. Sherwood, *Biol. Reprod.* 53, 1243 (1995).
- P. L. Osheroff, H. S. Phillips, *Proc. Natl. Acad. Sci. U.S.A.* 88, 6413 (1991).
- P. L. Osheroff, M. J. Cronin, J. A. Loftgren, *Proc. Natl. Acad. Sci. U.S.A.* 89, 2394 (1992).
- S. Zimmermann et al., *Mol. Endocrinol.* 13, 681 (1999).
- S. Y. Hsu, *Mol. Endocrinol.* 13, 2163 (1999).
- R. A. Bathgate et al., *J. Biol. Chem.* 276, 31 (2001).
- S. Neif, J. F. Parada, *Nature Genet.* 22, 295 (1999).
- P. A. Overbeek et al., *Genesis* 30, 26 (2001).
- S. Y. Hsu, S. G. Liang, A. J. Hsueh, *Mol. Endocrinol.* 12, 1830 (1998).
- S. Y. Hsu et al., *Mol. Endocrinol.* 14, 1257 (2000).
- The LGR8 open reading frame was deduced from genomic sequences by means of the gene prediction program GENES-M. cDNAs corresponding to human LGR8 were obtained by RT-PCR using mRNA from human testis and uterus as templates (17). The human LGR8 accession number (GenBank) is AF403384.
- Supplementary material is available at Science Online (www.sciencemag.org/cgi/content/full/295/5555/671/DC1).
- cDNA for the ectodomain of human LGR7, named as 7BP, was fused in frame with a prolactin signal peptide and the FLAG epitope at the 5' end and the transmembrane region of T cell surface antigen CD8 followed by a 6-His epitope at the 3' end. Stable 293T cell lines expressing 7BP in the pcDNA3.1-Zeo

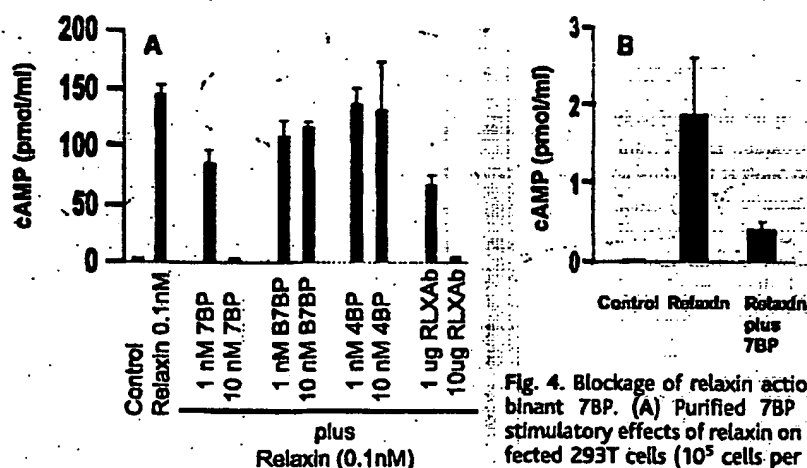
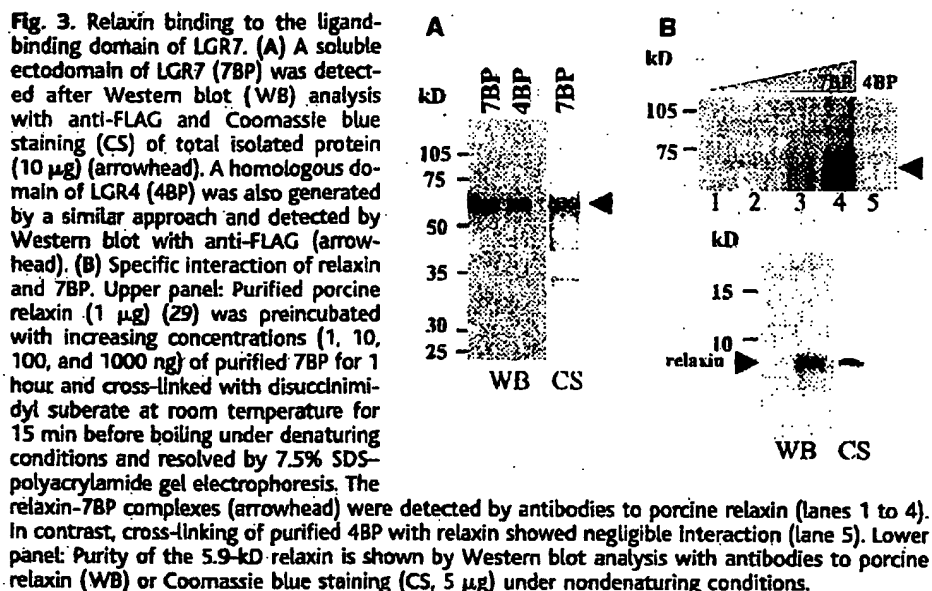


Fig. 4. Blockage of relaxin action by recombinant 7BP. (A) Purified 7BP blocked the stimulatory effects of relaxin on LGR7. Transfected 293T cells (10^5 cells per culture) stably expressing LGR7 from the pcDNA3.1-Zeo

expression vector were isolated (14) and treated (10^5 cells per culture) with 0.1 nM porcine relaxin in combination with different doses of 7BP, boiled 7BP (B7BP), or 4BP for 24 hours under serum-free conditions. In some cultures, antibodies to porcine relaxin (RLXAb) was also included with relaxin. (B) Treatment of cultured rat myometrial cells with 7BP blocked the relaxin stimulation of cAMP production. Uterine tissues were obtained from 25-day-old female rats implanted with diethylstilbestrol for 3 days. Myometrial cells were prepared by digestions with trypsin and collagenase as described (16). Cells (10^5 per culture) were treated with 1 nM porcine relaxin with or without 7BP for 24 hours.

REPORTS

- expression vector (Invitrogen) were selected using Zeocin (0.5 mg/ml). To release soluble 7BP anchored on the cell surface, we treated cells with thrombin (10 IU/ml) for 3 days under serum-free conditions. The cleaved 6-His- and FLAG epitope-tagged recombinant 7BP in serum-free conditioned media was purified by sequential nickel and anti-FLAG affinity chromatography. For antibody production, 5 mg of purified 7BP emulsified in Freund's adjuvant were injected into rabbits (Strategic BioSolutions Inc., Ramona, CA). Western blot analysis indicated that the antibody to 7BP does not recognize recombinant LGR8 proteins.
15. Y. Osuga, M. Kudo, A. Kaipia, B. Kobilka, A. J. Hsueh, *Mol. Endocrinol.* 11, 1659 (1997).
 16. C. J. Hsu, S. M. McCormack, B. M. Sanborn, *Endocrinology* 116, 2029 (1985).
 17. Eight-week-old female mice (strain C57/B6) were treated with equine chorionic gonadotropin (CG) (10 IU, National Hormone and Peptide Program) for 48 hours before ovulation induction with human chorionic gonadotropin (hCG, 10 IU). Mice were mated overnight after ovulation, and pregnant mothers were treated with purified 7BP (500 µg, once per day) for 4 days starting from postcoitus day 17. Parturition was monitored at 4- to 6-hour intervals. Five animals per treatment group were used. The pregnancy durations for control and 7BP-treated animals were 508.8 ± 9.0 hours and 536.0 ± 9.1 hours, respectively. The nipple sizes (length \times width, mm²) for control and 7BP-treated mice were 1.50 ± 0.05 and 1.07 ± 0.04 , respectively.
 18. L. Zhao et al., *Endocrinology* 140, 445 (1999).
 19. J. J. Hwang, R. D. Shanks, O. D. Sherwood, *Endocrinology* 125, 260 (1989).
 20. M. P. Czech, *Cell* 59, 235 (1989).
 21. C. Eigenbrot et al., *J. Mol. Biol.* 221, 15 (1991).

22. O. Bartsch, B. Bartlick, R. Iwell, *Mol. Hum. Reprod.* 7, 799 (2001).
23. B. J. Geddes, A. J. Summerville, *J. Neuroendocrinol.* 7, 411 (1995).
24. J. Novak et al., *J. Clin. Invest.* 107, 1469 (2001).
25. E. N. Unemori et al., *J. Clin. Invest.* 98, 2739 (1996).
26. D. Bani, *Gen. Pharmacol.* 28, 13 (1997).
27. T. Oschietz et al., *FASEB J.* 15, 2187 (2001).
28. J. B. Davoren, A. J. Hsueh, *Biol. Reprod.* 33, 37 (1985).
29. C. D. Sherwood, E. M. O'Byrne, *Arch. Biochem. Biophys.* 160, 185 (1974).
30. Partially supported by NIH grants HD23273 and DK58534. We thank C. Klein and A. Bhalla for technical help, C. Spencer for editorial assistance, and the National Hormone and Peptide Program for equine CG, hCG, and cAMP antiserum.

23 August 2001; accepted 7 December 2001

Plant Biotechnology in China

Jikun Huang,¹ Scott Rozelle,^{2*} Carl Pray,³ Qinfang Wang⁴

A survey of China's plant biotechnologists shows that China is developing the largest plant biotechnology capacity outside of North America. The list of genetically modified plant technologies in trials, including rice, wheat, potatoes, and peanuts, is impressive and differs from those being worked on in other countries. Poor farmers in China are cultivating more area of genetically modified plants than are small farmers in any other developing country. A survey of agricultural producers in China demonstrates that *Bacillus thuringiensis* cotton adoption increases production efficiency and improves farmer health.

Private life-science companies in the industrialized world perform most of the world's agricultural biotechnology research (1). Concerns have arisen in developing countries that their scientists and producers can only obtain genes and seeds from foreign companies and that biotechnology research does not focus on the crops that are important to the world's poor farmers. Recently, because of consumer resistance and governmental regulations affecting international trade in genetically modified (GM) products and the rising cost of commercializing new products, private research and development on plant biotechnology is declining, further jeopardizing the little private research that is done on developing country problems (2). In contrast, China is accelerating its investments in agricultural biotechnology research and is focusing on commodities that have been mostly ignored in the laboratories of industrialized countries. Small farmers in China

have begun to aggressively adopt GM crops when permitted to do so.

The overall goal of this paper is to answer the questions: What is China doing in agricultural biotechnology research? Is China's public-sector-dominated investment strategy efficient? Can China be a source of plant biotechnology for its own farmers and for farmers in the rest of the world?

The first two sections of the paper document China's scientific achievements and research investments. In order to understand the input and output trends of China's plant biotechnology research, in 2000, a two-stage survey elicited information covering approximately 80% of the nation's plant biotechnology research laboratories in nine provinces and two municipalities. In the first stage, based on funding information from the Ministry of Science and Technology (MOST), a list of laboratories that potentially could have been involved in plant biotechnology research was created. Interviews with the research directors identified 35 institutes that conducted research (more than US\$30,000) in tissue culture, genetic engineering, marker-assisted selection (MAS), diagnostic technology, microbiology, or other related areas. Twenty-nine institutes provided detailed information on their inputs and outputs for 1999, and 22 institutes provided historic data from 1986. The survey instrument, administered by Chinese Academy of Sciences and Chinese Academy of Agricultural Sciences

research staff, contained sections on each institute's total revenues and expenditures, its personnel, investments in biotechnology facilities, and the status of its current and past experiments in the regulatory process. Details of the survey process and a copy of the survey instrument can be found on the *Science* Web site (3). The third and fourth sections analyze the economic, environmental, and health impacts of plant biotechnology research using data from a survey of 282 GM cotton farmers in North China.

Although China has spent the last 50 years building the most successful agricultural research system in the developing world—employing more than 70,000 scientists—research in modern plant biotechnology did not begin until the mid-1980s (4). Scientists now apply advanced biotechnology tools to the field of plant science, regularly working on the synthesis, isolation, and cloning of new genes and the transformations of plants with these genes. With the initiation of a research program on rice functional genomics in 1997, China's researchers began using AC/DS transposons and T-DNA insertion methods to create rice mutagenesis pools (5). Biotechnologists also have initiated functional genomics research for *Arabidopsis*. Our survey of China's laboratories identified over 50 plant species and more than 120 functional genes that scientists are using in plant genetic engineering, making China a global leader in the field.

China's scientists have generated an impressive array of new technologies. From 353 applications between 1996 and 2000, China's Office of Genetic Engineering Safety Administration approved 251 cases of GM plants, animals, and recombinant microorganisms for field trials, environmental releases, or commercialization (Table 1, rows 1 and 2). Regulators approved 45 GM plant applications for field trials, 65 for environmental release, and 31 for commercialization (Table 1, rows 3 to 5).

Breakthroughs on food crops that have received little attention elsewhere (>40% of

¹Center for Chinese Agricultural Policy, Institute of Geographical Sciences and Natural Resource Research, Chinese Academy of Sciences (CAS), Building 917, Datun Road, Beijing 100101, China. ²Department of Agricultural and Resource Economics, University of California, 1 Shields Ave., Davis, CA 95616, USA. ³Department of Agricultural, Food, and Resource Economics, Rutgers University, 55 Dudley Road, New Brunswick, NJ 08901-8520, USA. ⁴Associate Professor, Biotechnology Research Institute, Chinese Academy of Agricultural Sciences (CAAS), 12 Zhongguancun Nandajie, Beijing 100081, China.

*To whom correspondence should be addressed. E-mail: rozelle@primal.ucdavis.edu

The Receptor-binding Site of Human Relaxin II

A DUAL PRONG-BINDING MECHANISM*

Erika E. Büllesbach, Su Yang, and Christian Schwabe

From the Department of Biochemistry and Molecular Biology, Medical University of South Carolina,
Charleston, South Carolina 29425

(Received for publication, July 13, 1992)

Recent structure/function studies on human relaxin II have led to the conclusion that the arginines B13 and/or B17 are important for biological activity. These studies have been confirmed and extended with the help of chemically synthesized derivatives, i.e. dicitrulline (B13, B17), two monocitrulline (B13 and B17), a dilysine (B13, 17), and alanine (B17) relaxins. The CD spectra of synthetic human relaxin and of the derivatives are indistinguishable. Yet, only the native human relaxin II is biologically active and binds strongly to relaxin receptor preparations *in vitro*. The inactivation is strictly due to side chain functions, in particular the replacement of either or both arginines in the positions B13 or B17. Binding is mediated by a two-prong electrostatic and hydrogen-binding interaction via arginines B13 and B17. Neither B13 nor B17 alone are sufficient and a positive charge equidistant from the B chain helix is equally insufficient. This binding mechanism appears to be unique, as concerns hormone receptor interaction.

Relaxins isolated from a variety of sources show a high degree of sequence heterology (1-5). With the exception of the relaxins of sea mammals (4, 6) and pigs (7, 8), the relaxins of purportedly closely related species vary by about 55% (1). The same differences exist also between mammalian and elasmobranch relaxins. Yet all relaxins share a few structural features such as the general size (6000 daltons), the insulin type cross-linking pattern and chain structure, 3 glycines in A12, B11, B23, and the arginine residues B13 and B17. Based on an insulin-like three-dimensional structure (9) and a recently published x-ray structure of human relaxin II (10), these arginines, positioned on the major B chain helix, protrude into the surrounding water, and although arginines are not considered typical active site residues, the prominence of this position on the molecular surface as well as the consistent appearance of these residues in all known relaxins suggest a specific role for the two B chain arginines. Previous experiments (11, 12) have provided supportive evidence for a biologically important role for the B chain arginines. In this paper we report a refinement of the active site structure as to its extent and special requirements.

* This work was supported by National Institutes of Health Grants DK 38348 and HD 23877 and the Medical University of South Carolina Institutional Research funds of 1991-1992. The costs of publication of this article were defrayed in part by the payment of page charges. This article must therefore be hereby marked "advertisement" in accordance with 18 U.S.C. Section 1734 solely to indicate this fact.

EXPERIMENTAL PROCEDURES

Materials

Amino acid derivatives were purchased from Bachem Bioscience, Inc. (Philadelphia, PA) or from Bachem, Inc. (Torrance, CA). Boc¹-[(S-(3-nitro-2-pyridinesulfonyl)cysteine)] was synthesized according to published procedures (13). Chloro-(N-tosyl-L-phenylalanine) methane-treated trypsin, L-citrulline, and Sephadex products were purchased from Sigma. The highest quality solvents for chromatography and peptide synthesis were purchased from Burdick and Jackson (Muskegon, MI).

Methods

Boc-citrulline was synthesized according to Moroder *et al.* (14) using L-citrulline (Sigma) (10 mmol), di-*tert*-butyl dicarbonate (Fluka, Ronkonkoma, NY) (9 mmol) and NaOH in isopropanol/water, 1:1, v/v, at pH 8.5. The reaction was performed for 1 h at room temperature, the organic solvent removed *in vacuo*, and cations (Na⁺, citrulline) bound to a strong acidic cation exchanger (Dowex 50WX, H⁺ form) suspended in water. The eluate was lyophilized, and Boc-Cit-OH was obtained as a white hygroscopic powder.

Peptide Synthesis—The methods of synthesis and chain combination have been reported previously (12). All derivatives reported here were synthesized with equal efficiency, although some variability in solubility was observed.

High Performance Liquid Chromatography (HPLC)—The solvent system used for all HPLC systems described was 0.1% trifluoroacetic acid in water (solvent A) and 0.1% trifluoroacetic acid in 80% acetonitrile (solvent B).

For preparative HPLC separations a SynChropak RP-P column (C₁₈, 10 × 250 mm) (SynChrom Inc., Linden, IN), equipped with a precolumn of Whatman Co: Pell ODS (30-38 μm), was attached to a Waters chromatography system (pump module 6000 A and a solvent programmer model 680). Flow rates were usually 3 ml/min, and eluents were detected by a Uvicord S monitor (226-nm filter) (LKB Products, Bromma, Sweden).

For analytical HPLC an Aquapore 300 (C₈, 2.1 × 30 mm) column (Applied Biosystems) was used in combination with an Applied Biosystems (Forster City, CA) HPLC model 130A. Flow rates of 100 μl/min were used in combination with linear gradients as follows: intact relaxin, 25-45% solvent B, 90 min (detection at 230 nm); tryptic digests, 0-45% solvent B, 40 min (detection at 230 nm); and for chain separation after reduction, 10-65% solvent B, 60 min (detection at 215 nm).

Amino Acid Analysis—Peptides were routinely hydrolyzed in 6 M HCl vapor containing 1% phenol under vacuum at 105 °C for 24 h. The dried amino acids were derivatized with phenyl isothiocyanate and analyzed on a Waters Pico/Tag system. Tryptophan was determined by UV spectroscopy. For the complete hydrolysis of Val-Ile bonds, the time of hydrolysis was extended to 72 h.

Enzymatic Digests and Peptide Maps—Relaxin or relaxin derivative (approximately 10 μg) were dissolved in 10 μl of water. A trypsin stock solution was prepared in 1 mM HCl, containing 1 μg/μl of trypsin and 1 μg/μl of calcium chloride. The stock solution was diluted 10-fold with 0.5 M NH₄HCO₃, and 2 μl of the enzyme solution was added to the relaxin solution (enzyme/substrate, 1:50). The digest was allowed to proceed for 2 h at 37 °C, acidified with 38 μl of 0.1%

¹ The abbreviations used are: Boc, *tert*-butoxycarbonyl; Cit, citrulline; HPLC, high performance liquid chromatography.

trifluoroacetic acid in water, and immediately transferred to the analytical HPLC system.

Reduction and Analytical Separation of the Relaxin Chains—About 5 μ g of the relaxin or relaxin derivative in 50 μ l of water was reacted with 50 μ l of a 50 mM dithiothreitol solution in a solvent containing 8 M guanidinium chloride and 0.5 M *N*-ethylmorpholine adjusted to pH 8.5 with acetic acid. The reduction was performed for 1.5 h at 37 °C, and 50 μ l of the reaction mixture was separated by analytical HPLC.

Spectroscopy—Absorbance was measured on a Cary 15 UV-visible spectrophotometer (Cary Instruments, Atlanta, GA), and circular dichroism measurements were made on a Cary spectropolarimeter 60 CD (Cary Instruments), using a quartz cell of 1-mm path length and a scale expansion of 0.1 or 0.2 degree (full scale). Peptide concentrations of 0.1–0.3 mg/ml in 50 mM phosphate buffer at pH 7.0 were used. The data points were converted to mean residual ellipticity as a function of wavelength (15).

Determinations of protein concentration were carried out either by UV spectroscopy, using a specific absorbance of 2.13 cm² mg⁻¹ at 282 nm for all derivatives, or by amino acid analysis.

Bioassays—The interpubic ligament assay was performed according to Steinetz *et al.* (16) using five ovariectomized virgin female ICR mice for each data point. The mice were primed with 5 μ g of estradiol 17 β -cypionate (Upjohn, Kalamazoo, MI) 5 days prior to the subcutaneous administration of relaxin or relaxin derivatives in 100 μ l of 0.1% benzopurpurin 4B. Sixteen hours later the mice were killed in an atmosphere of CO₂, the symphysis pubis dissected free, and the distance between the pubic bones measured by transillumination under a dissecting microscope.

Receptor Assay—For receptor assays crude membrane preparations were used as described (17). The brain tissue from either male or female mice (two per experiment) was homogenized in 10 ml 0.25 M sucrose in 25 mM Hepes buffer (pH 7.5), containing 0.14 M NaCl, 5.7 mM KCl, 0.2 mM phenylmethylsulfonyl fluoride, and 80 mg/liter of soybean trypsin inhibitor. Homogenization was performed three times for 10 s with a Polytron homogenizer (Brinkmann, Westbury, NY). The homogenate was centrifuged at 700 \times *g* for 5 min and the supernatant recovered. The pellet was suspended in 10 ml of buffer and recentrifuged. The combined supernatants were recentrifuged at 700 \times *g* for 5 min and the pellets discarded. The supernatant was spun at 10,000 \times *g* for 40 min, the pellet suspended in 5 ml of Hepes buffer, and centrifuged again at 10,000 \times *g* for 40 min. The final pellet was stored at -80 °C. For receptor binding experiments the frozen pellet was resuspended in buffer supplemented with bovine serum albumin (1%), glucose (2.8 mM), CaCl₂ (1.6 mM), MgCl₂ (25 μ M), and MnCl₂ (1.5 mM). The wash buffer was 150 mM NaCl in 5 mM Tris-HCl at pH 7.4. The tracer (A1-[¹²⁵I]3-5-diiododesaminotyrosyl porcine relaxin) was prepared as described (17).

The relaxin receptor binding assay was performed in 1-ml polypropylene bullet tubes. The sequence of addition was as follows: tracer followed by cold relaxin or derivative, buffer, and membrane preparation. The total volume was 100 μ l. The contents were mixed briefly on a Vortex mixer, and the tubes were left standing at room temperature for 1 h. Thereafter the membranes were washed twice with 1 ml of the wash buffer, followed by centrifugation for 5 min in an Eppendorf centrifuge. The tube tips, containing the pellets, were cut off and counted for 1 min in a γ counter (Minigamma, LKB). Specific binding was about 50% of the total counts.

RESULTS

The chemical synthesis of relaxin derivatives (Fig. 1) was performed as described previously (12). Homogeneity was verified in two different reversed-phase HPLC systems. Comparing the relative retention times, it was noted that [Lys^{B13}, Lys^{B17}]relaxin is the most hydrophilic derivative followed by human relaxin II > [Cit^{B13}]relaxin = [Cit^{B17}]relaxin > [Ala^{B17}]relaxin \approx [Cit^{B13}, Cit^{B17}]relaxin. Separation of the reduced

chains by reversed-phase HPLC revealed identical retention times for all A chains but different retention times for each B chain. Tryptic digests of the intact molecules and peptide mapping by reversed-phase HPLC resulted in identical elution profiles for [Lys^{B13}, Lys^{B17}]relaxin and unmodified human relaxin II, whereas all other derivatives showed different profiles due to the lack of one or two enzymatic cleaving sites.

The amino acid compositions showed, as expected, reduced values for arginine and increased values for alanine and lysine in [Ala^{B17}]relaxin and [Lys^{B13}, Lys^{B17}]relaxin, respectively. Chromatograms of citrulline-containing derivatives showed nonstandard peaks for citrulline and its hydrolysis product ornithine. The sum of both components gave the correct amino acid composition for citrulline-containing derivatives (Table I). All derivatives showed the correct amino acid sequence for the B chains (the A chains are blocked by pyroglutamic acid). Phenylthiohydantoin-citrulline eluted in the position of phenylthiohydantoin-threonine.

The CD spectra of all derivatives and human relaxin II were identical in the far-UV region (12), including the cross-over at 202 nm, the location of the minimum at 208 nm, the intensity of the absolute minimum and the ratio of the ellipticity of 1.22 at 208/222 nm (Fig. 2).

In the mouse symphysis pubis assay the synthetic human relaxin II was as potent as native porcine relaxin, whereas all derivatives had no significant activity at doses up to 40-fold higher than the effective human relaxin standard (Fig. 3). In fact, [Lys^{B13}, Lys^{B17}]relaxin, [Ala^{B17}]relaxin, and as previously reported, [Cit^{B13}, Cit^{B17}]relaxin (12), were absolutely inactive. The replacement of either arginine by citrulline yielded derivatives with trace activities at 40-fold higher doses.

All derivatives retained some affinity for relaxin receptors as demonstrated by binding assays on the crude membrane of mouse brain (17). The amount in nanograms of human relaxin and derivatives required to displace 50% of the A1-[¹²⁵I]3-5-diiododesaminotyrosyl porcine relaxin tracer (17) is given in Table II. The shapes of the dose-response curves of all the derivatives are very similar to that of human relaxin II, which indicates that ligand and tracer are indeed competing for the same receptor (Fig. 4).

DISCUSSION

Previous chemical modification experiments with arginine-specific reagents left no doubt about the importance of arginine side chains for the biological activity of relaxin (11). Furthermore, by comparison of the sequences of relaxins of different species, it could be concluded that the 2 arginines located in the central helix of the B chain might be important for the receptor binding. This hypothesis was verified when both B chain arginines in positions 13 and 17 in human relaxin were replaced by citrullines during the chemical synthesis of this hormone (12). From the experiments reported in this paper, it is clear that both arginines B13 and B17 are required for bioactivity and that replacement of either or both amino acids by different carriers of a positive charge (Lys) or by the isosteric, but uncharged, citrulline residues cause dramatic losses in bioactivity as well as receptor affinity.

The insulin-like relaxin model (9, 18, 19), as well as the

FIG. 1. Primary structure of human relaxin II (21, 25). The various derivatives discussed in this paper are shown to indicate the positions substituted by citrulline, alanine, and lysine.

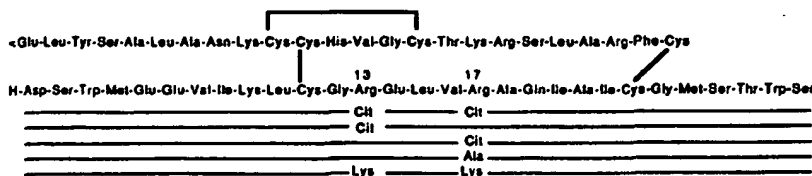


TABLE I
Amino acid compositions of native and modified human relaxin II (hRlx)

	hRlx	[Ala ^{B17}]	[Lys ^{B13} , Lys ^{B17}]	[Cit ^{B13}]	[Cit ^{B17}]	[Cit ^{B13} , Cit ^{B17}]
Asp	2.04 (2)	2.13	2.00	2.00	2.13	2.00
Thr	1.93 (2)	1.94	1.93	1.90	1.88	1.91
Ser	4.56 (5)	4.84	4.88	4.82	4.89	4.57
Glu	4.67 (5)	4.83	4.94	4.92	4.99	4.54
Gly	3.01 (3)	3.32	3.32	3.12	3.17	3.39
Ala	4.80 (5)	5.98	5.08	5.04	5.03	4.93
Val ^a	2.40 (3)	2.97	2.60	2.45	2.56	2.50
Met	1.86 (2)	1.98	1.87	2.00	1.95	1.83
Ile ^a	2.30 (3)	2.97	2.67	2.44	2.48	2.38
Leu	5.20 (5)	5.32	5.32	4.89	5.22	5.33
Tyr	1.10 (1)	1.05	1.03	1.04	1.07	1.09
Phe	0.98 (1)	1.07	1.10	1.07	1.11	1.06
His	0.90 (1)	1.00	0.97	0.92	0.93	0.87
Lys	3.03 (3)	3.00	4.98	3.08	3.08	2.87
Arg	4.00 (4)	3.00	2.00	3.03	3.18	2.18
Cit				0.72	0.62	1.45 (2)
Orn ^b				0.24	0.23	0.29 (0)

^a Low values are due to the incomplete hydrolysis of the Val-Ile bond.

^b Ornithine is a hydrolysis product of citrulline; estimate based on lysine as standard.

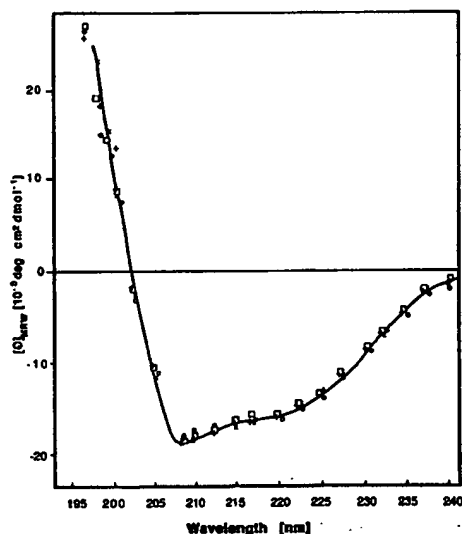


FIG. 2. CD of human relaxin (x), [Cit^{B13}]relaxin (O), [Cit^{B17}]relaxin (+), and [Cit^{B13}, Cit^{B17}]relaxin. The relaxins were dissolved in 3.3 mM HCl and diluted with 0.2 M phosphate buffer (pH 7.0) (3:1, v/v). All derivatives show the features of human relaxin such as a crossover at 202 nm, a minimum at 208 nm, and a shoulder at 222 nm and the same ratio of 1.22 for the molar ellipticities at 208/222 nm.

recently published x-ray structure of human relaxin (10), shows the 2 arginines protruding from the B chain helix into the water essentially parallel to each other. The side chains are fully extended and positioned at the edge of the dimerization surface so that the arginines would be exposed even in the dimer. Since the dimer dissociation constant is in the range of 10^5 M^{-1} , it is most likely that relaxin acts as a monomer (20).

The parallel projection of the 2 arginines would require that parallel "receptacles" exist on the receptor surface. The binding pockets probably carry a negative charge, which would explain why the isosteric citrulline cannot replace arginine. The ϵ -amino group of lysine cannot give rise to the hydrogen bonding pattern as compared with the guanidino group and may therefore be inactive. From these experiments we are

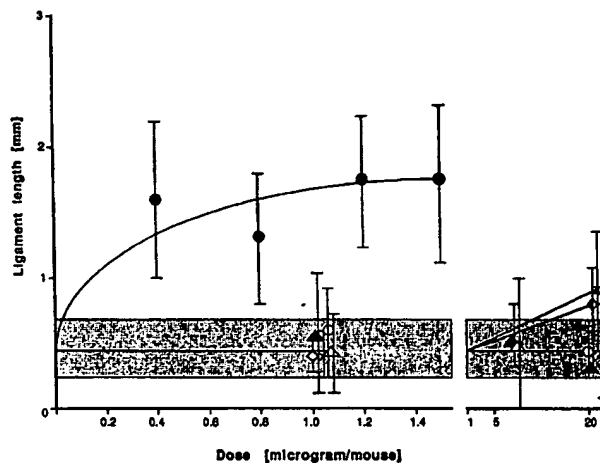


FIG. 3. Bioassay of synthetic human relaxin (●) and the [Cit^{B13}, Cit^{B17}]relaxin (Δ), [Cit^{B13}]relaxin (x), [Cit^{B17}]relaxin (O), [Ala^{B17}]relaxin (O), and [Lys^{B13}, Lys^{B17}]relaxin (Δ). Ovariectomized mice (18–20 g) were given 5 μg of depot estrogen 5 days prior to relaxin injection. Relaxin and relaxin derivatives were injected subcutaneously in 100 μl of 0.1% benzopurpurin 4B. The length of the symphyseal ligament was measured 16 h later. Benzopurpurin-injected mice served as controls.

TABLE II
Receptor binding of various relaxin derivatives

Relaxin	50% binding ng/ml
Ala ^{B17}	4,500
Cit ^{B13, B17}	3,800
Cit ^{B13}	6,500
Cit ^{B17}	3,500
Lys ^{B13, B17}	4,500
Human II	2
Insulin	>120,000

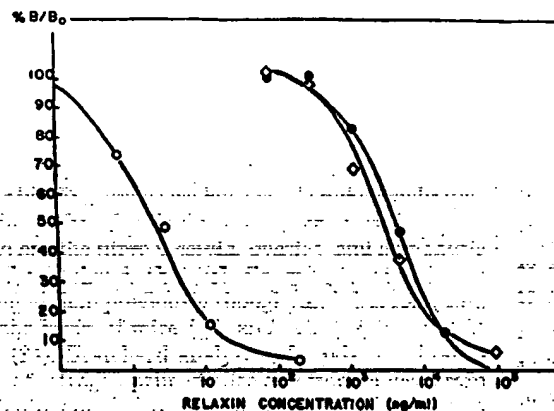


FIG. 4. Representative receptor binding curves of human relaxin (O), B17 citrulline relaxin (O), and B13;17 citrulline relaxin (●). Insulin did not displace 50% of the tracer at a concentration of 120 $\mu\text{g}/\text{ml}$.

concluding that the positive charge, even if positioned equidistant from the helix, is not sufficient to cause strong receptor binding.

Although all modifications of the arginines B13 and B17 in the B chain cause about a 1700–3200-fold reduction of receptor affinity the relaxin derivatives are still bound specifically as compared with insulin, which did not displace the porcine relaxin tracer by 50% even at concentrations as high as 120 $\mu\text{g}/\text{ml}$ (Table II). Thus there is a contribution of receptor

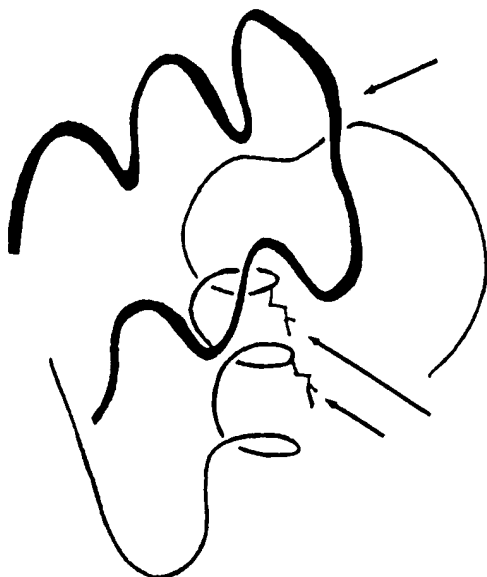


FIG. 5. The schematic representation of relaxin (Ref. 9) shows the topographical relationship of the A chain loop (top arrow) and the critical arginine residues in the B chain helix (bottom arrows show binding site arginines (B9,13)).

binding by features of the relaxin molecule other than the 2 arginines. This proposal finds support in our previous study concerning the influence of the A chain loop on biological activity and binding of relaxin to its receptor.² From the relaxin structure (Fig. 5) it is clear that the A chain loop is on the surface opposite to the surface formed by the central portion of the B chain helix which carries the 2 active arginine residues. As reported previously replacement of the glycine A14 in human relaxin by isoleucine induces a steric shift which is measurable by CD spectroscopy and which significantly reduces the activity of the molecule. It is highly unlikely that this shift would disturb the geometry of a fairly tight helix on the opposite side of the molecule or, by extension, the relative position of the arginines B13 and B17. It seems, therefore, necessary to conclude that there are ancillary receptor interaction sites which are subject to perturbation by a shifting A chain loop.

For receptor binding assays we have used crude membranes of mouse brain. Although relaxin is a reproductive hormone and its targets are the uterus, cervix, ovaries, and symphysis pubis, it has been shown that relaxin receptors are more widely distributed than previously thought and that receptors are found in the brain of mice (17) and rats (22, 23) and in the rat heart (24). Scatchard analyses of crude membranes from the uteri of estrogen-primed mice and from mouse brain showed no significant differences in binding affinities and receptor concentrations per unit of protein. In addition, relaxin receptors in the brain are independent of sex or estrogen priming (23). At the state of our knowledge of relaxin receptors, both sources can be used interchangeably for receptor binding assays.

In light of the receptor-binding data, it is difficult to explain

that the replacement of only arginine B13 with citrulline appears to cause greater disturbance than the exchange of both B13 and B17 positions. The slightly better binding of the citrulline B17 derivative (as compared with B13) suggests that B13 is the more important arginine residue (Table II). This trend is also noted in the bioassay (Fig. 3), although more experiments are needed to verify this observation.

The CD spectra (Fig. 2) of all derivatives and that of unmodified human relaxin are indistinguishable. Such perfect superimposition of spectra, combined with the high sensitivity of optical ellipticity measurements to the largely helical relaxin-like conformations (see CD changes after A chain loop modification),² gives us confidence that the B chain derivatives have a "native" backbone and that all changes in receptor affinity and biological activity reported in this paper are strictly due to side chain effects.

As it stands we can conclude from our studies that the 2 arginines B13 and B17 interact with the receptor like a prong and that binding is mediated by both a positive charge and by the hydrogen-bonding network which can be induced by the guanidino groups. The arginines appear to be a necessary but not sufficient condition for receptor interaction and biological activity, and we predict that additional interacting regions may be found in the relaxin B chains.

Acknowledgments—We thank Robert Bracey for the syntheses of the relaxin chains and amino acid analyses and Barbara Rembisa for excellent technical assistance.

REFERENCES

- Schwabe, C., and Büllesbach, E. E. (1990) *Comp. Biochem. Physiol.* 96B, 15-21.
- Crawford, R. J., Hammond, V. E., Roche, P. J., Johnston, P. D., and Tregear, G. W. (1989) *J. Mol. Endocrinol.* 3, 169-174.
- Stewart, D. R., Nevis, B., Hadas, E., and Vandlen, R. (1991) *Endocrinology* 129, 375-383.
- Woods, A. S., Cotter, R. J., Yoshioka, M., Büllesbach, E. E., and Schwabe, C. (1991) *Int. J. Mass Spectrom. Ion Processes* 111, 77-88.
- Lee, Y. A., Bryant-Greenwood, G. D., Mandel, M., and Greenwood, F. C. (1992) *Endocrinology* 130, 1165-1172.
- Schwabe, C., Büllesbach, E. E., Heyn, H., and Yoshioka, M. (1989) *J. Biol. Chem.* 264, 940-943.
- Schwabe, C., McDonald, J. K., and Steinetz, B. G. (1976) *Biochem. Biophys. Res. Commun.* 70, 397-405.
- Schwabe, C., McDonald, J. K., and Steinetz, B. G. (1977) *Biochem. Biophys. Res. Commun.* 75, 503-510.
- Bedarkar, S., Turnell, W. G., Blundell, T. L., and Schwabe, C. (1977) *Nature* 270, 449-451.
- Eigenbrodt, C., Randal, M., Quan, C., Burnier, J., O'Connell, L., Rinderknecht, E., and Kossiakoff, A. A. (1991) *J. Mol. Biol.* 221, 15-21.
- Büllesbach, E. E., and Schwabe, C. (1988) *Int. J. Pept. Protein Res.* 32, 361-367.
- Büllesbach, E. E., and Schwabe, C. (1991) *J. Biol. Chem.* 266, 10764-10761.
- Bernatowicz, M. S., Matsueda, R., and Matsueda, G. R. (1986) *Int. J. Pept. Protein Res.* 28, 107-112.
- Moroder, L., Hallett, A., Wünsch, E., Ketter, O., and Wersin, G. (1976) *Hoppe Seyler's Z. Physiol. Chem.* 357, 1651-1653.
- Adler, A. J., Greenfield, N. J., and Fasman, G. D. (1973) *Methods Enzymol.* 27, 675-735.
- Steinetz, B. G., Beach, V. L., Kroc, R. L., Staall, N. R., Nussbaum, R. E., Nemeth, P. J., and Dun, R. K. (1960) *Endocrinology* 67, 102-115.
- Yang, S., Rembisa, B., Büllesbach, E. E., and Schwabe, C. (1992) *Endocrinology* 130, 179-185.
- Isasca, N., James, R., Niall, H., Bryant-Greenwood, G., Dodson, G. G., Evans, A., and North, A. C. T. (1978) *Nature* 271, 278-281.
- Dodson, G. G., Eliopoulos, E. E., Isasca, N. W., McCall, M. J., Niall, H. D., and North, A. C. T. (1982) *Int. J. Biol. Macromol.* 4, 399-405.
- Shire, S. J., Holladay, L. A., and Rinderknecht, E. (1991) *Biochemistry* 30, 7703-7711.
- Stults, J. T., Bourell, J. H., Canova-Davis, E., Ling, V. T., Laramee, G. R., Winslow, J. W., Griffin, P. R., Rinderknecht, E., and Vandlen, R. L. (1990) *Biomed. Environ. Mass Spectrom.* 19, 655-664.
- Osheroff, P. L., Ling, V. T., Vandlen, R. L., Cronin, M. J., and Lofgren, J. A. (1990) *J. Biol. Chem.* 265, 9396-9401.
- Osheroff, P. L., and Phillips, H. S. (1991) *Proc. Natl. Acad. Sci. U.S.A.* 88, 6413-6417.
- Osheroff, P. L., Cronin, M. J., and Lofgren, J. A. (1992) *Proc. Natl. Acad. Sci. U.S.A.* 89, 2384-2388.
- Hudson, P., John, M., Crawford, R., Haralambidis, J., Scanlon, D., Gorman, J., Tregear, G., Shine, J., and Niall, H. (1984) *EMBO J.* 3, 2333-2339.

² E. E. Büllesbach, S. Yang, and C. Schwabe, submitted for publication.

The Relaxin Receptor-binding Site Geometry Suggests a Novel Gripping Mode of Interaction*

Received for publication, June 29, 2000

Published, JBC Papers in Press, August 23, 2000, DOI 10.1074/jbc.M005728200

Erika E. Büllesbach and Christian Schwabe†

From the Department of Biochemistry and Molecular Biology, Medical University of South Carolina, Charleston, South Carolina 29425

Relaxin has a unique, clearly identifiable, mixed function receptor-binding region comprising amino acid residues that evolve sequentially from the central portion of the B chain α -helix. Two arginine residues in positions B13 and B17 that project like forefinger and middle finger from the helix provide the electrostatic element opposed by the hydrophobic (thumb) element isoleucine (B20), offset from the arginines by about 40°. The binding intensity of relaxin to its receptor decreases by 3 orders of magnitude if alanine is substituted for the newly discovered binding component isoleucine in position B20. The arginine residues cannot be replaced by other positive charges, nor can the guanidinium group be presented on a longer or shorter hydrocarbon chain. In contrast, the hydrophobic interaction is incremental in nature, and the contribution to the total binding energy is roughly proportional to the number of hydrocarbon units in the side chain. It appears that a hydrophobic surface exists on the receptor that offers optimal van der Waals' interaction with β -branched hydrophobic amino acids. The binding energy increases roughly 10-fold with each methylene group whereby β -branching is more effective per surface unit than chain elongation. Aromatic side chains appear to demarcate the extent of the binding region in so far as residues larger than phenylalanine decrease receptor binding. The exceptional clarity of binding site geometry in relaxin makes for an excellent opportunity to design peptido-mimetics.

Relaxin, a small, two-chain protein, the physiological mediator of parturition in most mammals (1), has recently been shown to influence significantly the symptoms of scleroderma (2, 3). Since its discovery (4) relaxin has provided a share of unusual features including an insulin-like structure (5–9) and a receptor-binding site composed of two charged residues, i.e. arginine in position B13 and B17 (10, 11). The binding residues are positioned one turn apart on the major B chain helix and are projecting parallel into the surrounding water (12). This observation led to the suggestion that relaxin would bind to the receptor by a dual prong mechanism involving the interaction of the guanidinium groups with two negative charges at the bottom of a binding pocket in the receptor (11). Although both

arginines are indispensable, the fact that arginine-containing peptides would not interfere with binding suggested that other binding site members might exist. In this paper, we are reporting that the receptor-binding site of relaxin includes isoleucine in position B20, which is located three-quarter of one turn further toward the C-terminal end of the same helix so that the hydrophobic side chain opposes the two arginines forming a quasi-prehensile unit that points to a novel binding mechanism. Evidence presented in this paper supports the conclusion that Ile-B20 is as important for receptor-binding as either of the critical arginines and that the relaxin/receptor interaction is trivalent.

EXPERIMENTAL PROCEDURES

Materials

Amino acid derivatives were purchased from either Advanced ChemTech (Louisville, KY), Bachem Bioscience (Torrance CA), or Nova Biochem (San Diego, CA). Solvents for peptide synthesis and HPLC¹ were Burdick and Jackson high quality grade. Reagents for peptide synthesis were purchased from PerkinElmer Life Sciences. Other chemicals and reagents were of analytical grade.

Methods

Peptide Syntheses

Human relaxin B29 and B33, Gln-B14, Asp-B14, and GRER-dpp insulin were synthesized as described (13, 14). All other human relaxin derivatives and GRER-dpp-insulin B chain were synthesized by Fmoc (N-(9-fluorenyl)methoxycarbonyl) chemistry using trifluoroacetic acid labile protecting groups (15, 16) for all side chains except unprotected tryptophan, methionine sulfoxides, and S-acetamidomethyl cysteine (B11). The synthesis was performed on an ABI model 433A protein synthesizer starting with 0.25 mmol of peptide on the resin up to residue B21. Thereafter the resin was split into three equal portions, each of which was used to produce one B chain analog using the standard 0.1-mmol chemistry protocol. The peptidyl resin was deprotected with trifluoroacetic acid/ethanedithiol/thioanisole/phenol/water (10:0.25:0.5:0.75:0.5 v/v/v/v/v) (17) for 2 h at room temperature, the resin was filtered off, and the peptide was collected by ether precipitation and dried and purified by preparative HPLC (yield, 15–25 mg). The B chain was dissolved in 5 ml of 1 M acetic acid, and 20 mg of 2,2'-dipyridyldisulfide in 2 ml of methanol added, and the solution was stirred for 30 min at room temperature. The mixture was separated by gel filtration on Sephadex G25sf in 1 M acetic acid and lyophilized (yield, 90–100%). The partially protected B chain carried an acetamidomethyl group in cysteine B11, a 2-pyridinesulfonyl group in cysteine B23, and sulfoxides in the methionine side chains.

The A chain with the intact intra-chain disulfide bond, an acetamidomethyl group in position A11, and a sulfhydryl group in position A24 was prepared according to the literature (13, 14). The A chain was dissolved in 0.1 M acetic acid, pH 4.5, in 8 M guanidinium chloride (5 mg/ml) and added to the dry B chain (1:1 molar ratio), which dissolved instantaneously. The reaction was stirred for 24 h at 37 °C, and the products were separated on Sephadex G50sf in 1 M acetic acid, followed

* This work was supported by National Institutes of Health Grant GM 48893. The costs of publication of this article were defrayed in part by the payment of page charges. This article must therefore be hereby marked "advertisement" in accordance with 18 U.S.C. Section 1734 solely to indicate this fact.

† To whom correspondence should be addressed: Dept. of Biochemistry and Molecular Biology, Medical University of South Carolina, 173 Ashley Ave., P.O. Box 250509, Charleston, SC 29425. Tel.: 843-792-9929; Fax: 843-792-4322; E-mail: schwabec@musc.edu.

¹ The abbreviations used are: HPLC, high pressure liquid chromatography; GRER-dpp, Gly (A10), Arg(B9), Glu(B10), Arg(B13) desptapeptide(B26–30)insulin amide.

by HPLC on Synchropak RP-P C18 (10 × 250 mm) (yield, 50% based on the chains). To remove the acetamidomethyl groups partially protected relaxin (9 mg) was dissolved in 0.9 ml of 0.1 M HCl, diluted with 6.1 ml of glacial acetic acid and 2 ml of 50 mM iodine in glacial acetic acid were added. After 15 min at room temperature excess iodine was reduced by pouring the reaction mixture slowly into a stirred solution of 40 ml of 0.1 M ascorbic acid. The relaxin was desalted on Sephadex G25sf in 1 M acetic acid, lyophilized, and further purified by reversed phase HPLC (yield, 1.55 mg; 17.2% for relaxin and 39.4% for GRER1-dpp insulin). The methionine sulfoxides were reduced with ammonium iodide in 90% trifluoroacetic acid (13), and the relaxin analog was HPLC purified (yield, 60–80%).

High Performance Liquid Chromatography

Semipreparative HPLC was performed on Synchropak RP-P (C₁₈, 10 × 250 mm). The solvent system consisted of 0.1% trifluoroacetic acid in water (solvent A) and 0.1% trifluoroacetic acid in 83% acetonitrile (solvent B). These solvents were used unless stated otherwise. The flow rate was 3 ml/min, and a 30-min linear gradient from 30 to 50% B was employed for all separations. Peptides were detected by UV absorbance at 226 nm.

Chemical Analyses of the Relaxin Analogs

Analytical HPLC—Two different HPLC systems were used. System 1: a Bakerbond widebore C₁₈ column (4.1 × 250 mm) was used in combination with a Waters HPLC system. About 10–20 µg of the peptide was injected and separated using a 30-min linear gradient from 20 to 60% B at a flow rate of 1 ml/min. The effluent was monitored by UV absorbance at 220 nm.

System 2 consisted of an ABI model 130A chromatograph equipped with an Aquapore 300 (2.1 mm × 30 mm) C8 column. About 1–2 µg of the corresponding relaxin was applied via an automatic sample injector. Separation was achieved at a flow of 100 µl/min, and the eluate was detected by UV absorbance at 230 nm. Intact relaxins were separated using a 60-min linear gradient from 25–45% B.

For reduction 2 µg of the protein was dissolved in 30 µl water and 30 µl of 50 mM DTT in 0.2 M Tris/HCl at pH 8.6 in 6 M guanidinium chloride was added. After 60 min at 37 °C the solution was acidified with 10 µl of glacial acetic acid and the product separated by reversed phase HPLC (system 2) using a 60-min linear gradient from 25–60% B.

For tryptic digestion and peptide mapping 2 µg of the relaxin was dissolved in 20 µl of 25 mM Tris/HCl at pH 7.5. Tosylphenylalanyl chloromethyl ketone-treated trypsin (EC 3.4.21.4) (100 ng in 2 µl of 50 mM NH₄HCO₃, E:S 1:20) was added, and the digest was maintained at 37 °C for 1 h. Hydrolysis was stopped by the addition of 38 µl of 0.1% trifluoroacetic acid, and 50 µl were used for analysis in HPLC (system 2). Tryptic fragments were separated using a 40-min linear gradient from 0 to 40% B.

Amino Acid Composition—Peptides were hydrolyzed in vapor phase 6 M HCl containing 0.1% phenol for 1 h at 150 °C. The amino acids were modified with phenylisothiocyanate and separated by HPLC (Pico-Tag system, Waters).

Sequence Analysis—Phe-B20 or Ala-B20 relaxin was sequenced using a Procise protein sequencer (PerkinElmer Life Sciences) connected to an inline phenylthiohydantoin analyzer.

Protein Determination—Protein concentrations were measured by UV spectroscopy using an Olis Cary-15 spectrophotometer conversion (On-Line Instrument Systems, Inc.). Relaxin analogs (0.2–0.5 mg/ml) were dissolved in water. The specific absorption coefficient was calculated with 1.95 cm⁻² mg⁻¹ for B33 relaxin and relaxin analogs and 2.19 cm⁻² mg⁻¹ for B29 relaxin analogs.

CD Spectroscopy—CD spectra were measured on a Jasco J710 spectropolarimeter at a resolution of 0.2 nm, with a bandwidth of 2 nm. Ten spectra were averaged for each derivative. For far UV spectroscopy (250–190 nm), the relaxin analogs were dissolved in 25 mM Tris/HCl, pH 7.5, at a concentration of 0.0833 mg/ml using a cell of 0.1 cm pathlength. Mean residue ellipticity was calculated according to the literature (18). Protein concentrations were derived from UV spectroscopy and confirmed by amino acid analysis after total acid hydrolysis.

Matrix-assisted Laser Desorption/Ionization Mass Spectrometry—Relaxin analogs (1 µg/µl) were dissolved in 0.1% trifluoroacetic acid and mixed with 50 mM α-cyano-4-hydroxycinnamic acid in 80% acetonitrile (1:3 v/v). 1 µl was placed on a sample probe and air dried. Mass spectra were acquired with a Voyager-DE Biospectrometry Workstation (Perceptive Biosystems). Analyses were performed at the MUSC Mass Spectrometry Facility.

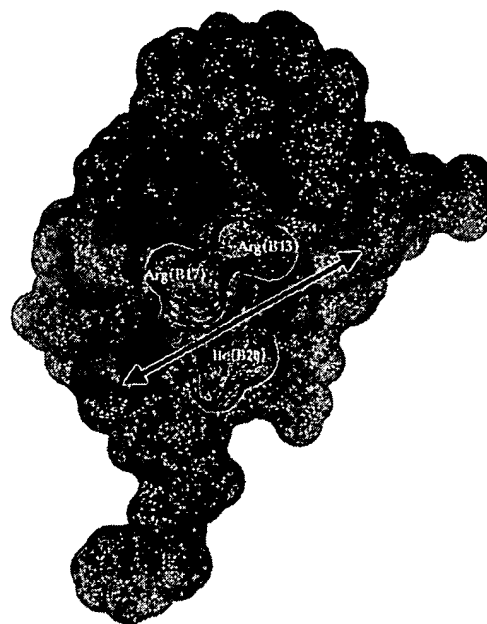


FIG. 1. Three-dimensional structure of human relaxin with view on the B chain helix emphasizing Arg-B13, Arg-B17, and Ile-B20 in blue. The arrow marks the purported path of the binding ridge on the receptor.

Biochemical Characterization

Tracer Preparation—Phe-A3,Tyr-B30 human relaxin protected at the tryptophan (formyl) and methionine side chains (sulfoxides) was synthesized as described for the human relaxin synthesis (13). Radioactive labeling of Tyr-B30 with ¹²⁵I⁻ was performed by the chloramine T method, followed by the removal of the indole protecting groups (19). Phe-A3-¹²⁵I-Tyr-B30 relaxin di-sulfoxide was isolated by HPLC on an Aquapore 300 column using a 60-min linear gradient from 25 to 40% B. The eluate was collected into 100 µl of a 1% bovine serum albumin solution in water. For receptor-binding assays this tracer was remade every 2 weeks.

Receptor-binding Assays—were performed on crude membrane preparations of mouse brain (20). Two freshly dissected mouse brains were dropped into 15 ml of chilled homogenizing buffer (25 mM Hepes, 0.14 M NaCl, 5.7 mM KCl, 8 mg/liter soybean trypsin inhibitor, supplemented with 0.25 M sucrose and 0.4 mM phenylmethylsulfonyl fluoride, pH 7.5) and homogenized using a Polytron homogenizer at position 7 for 10 s. After centrifugation for 10 min at 4 °C and 700 × g, the supernatant was collected. The pellet was again homogenized in 10 ml, the process was repeated, and the supernatants were pooled. The crude membranes were collected by centrifugation at 20,000 × g for 60 min at 4 °C, the supernatant was discarded, and the pellet was suspended in 25 ml of 25 mM Hepes buffer without sucrose. After a second centrifugation at 20,000 × g for 60 min at 4 °C, the supernatant was discarded, and the pellet of each vial was suspended in 1.5 ml of ice-cold binding buffer (25 mM Hepes, 0.14 M NaCl, 5.7 mM KCl, 2.8 mM glucose, 1.6 mM CaCl₂, 25 µM MgCl₂, and 1.5 mM MnCl₂, supplemented with 1% bovine serum albumin and 0.2 mM phenylmethylsulfonyl fluoride). The pellets of six brains were pooled into a 6 ml polypropylene vial, chilled on ice, and homogenized with a hand-held Polytron for 20–30 s at maximum speed. Thereafter aliquots of 1.4 ml of the suspension were distributed into 1.5-ml Eppendorf vials and kept on ice. One vial was used for one dose-response curve. In general, six mouse brains were sufficient to generate four dose-response curves, each consisting of nine duplicate points.

Assays were performed in 1.5-ml Eppendorf vials: 40 µl of various concentrations of relaxin or analogs, 20 µl of tracer (60,000–80,000 cpm; final concentration, 125–165 pM), and 60 µl of crude membranes were added, gently mixed and incubated for 1 h at room temperature. Thereafter 1 ml of ice-cold wash buffer (25 mM Hepes, 0.14 M NaCl, 5.7 mM KCl, and 0.2% bovine serum albumin) was added, and the membranes were collected by centrifugation at 14,000 rpm for 10 min in an Eppendorf centrifuge. The supernatant was discarded, and the tip of the vial was cut and counted in a γ-counter. Nonspecific binding was determined in the presence of 2600 nM B33 human relaxin. In a typical

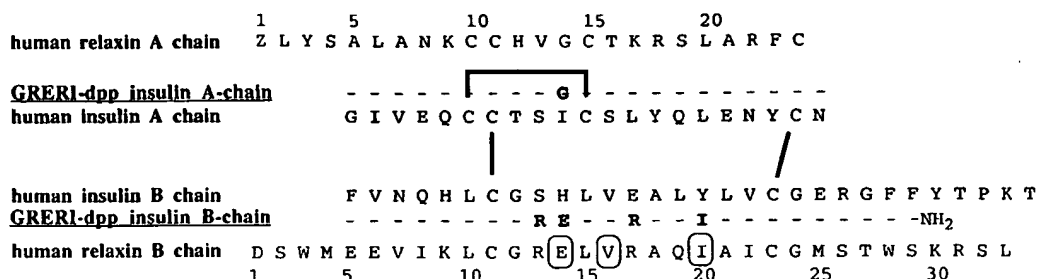


FIG. 2. Sequence of human relaxin II, human insulin and a insulin-relaxin hybrid (GRERI-dpp insulin) in which relaxin residues are substituted for the corresponding insulin residues. Circles indicate relaxin residues that were investigated during this study. Z, pyroglutamine).

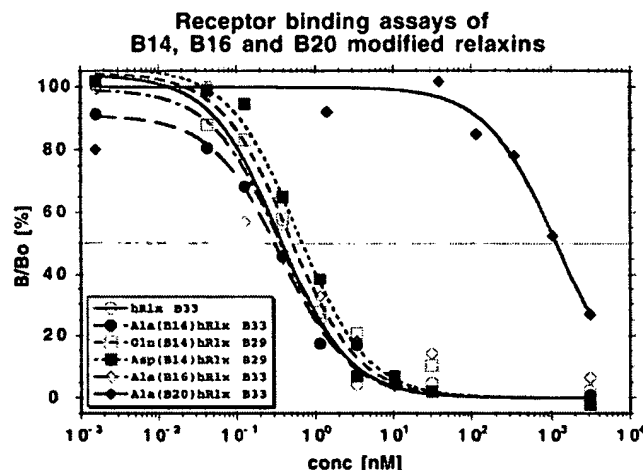


FIG. 3. Receptor binding assays of B14, B16, and B20 modified relaxins using crude membrane preparations of mouse brain and 125 I-Phe-A3-Tyr-B30 human relaxin for tracer. Three independent dose-response curves of each analog were averaged.

experiment total binding was 7–10% of the total radioactivity added, and specific binding was 35–50% of the total binding. Each point was measured in duplicate, and each analog was determined in at least three independent experiments. As a control each set of experiments contained a dose-response curve of human relaxin. Data were averaged and fitted as described by De Lean *et al.* (21).

Mouse Symphysis Pubis Assay—Mouse interpubic ligament assays were carried out as described by Steinetz *et al.* (22), using virgin female mice. Mice were primed with 5 μ g of estrogen cypionate in 100 μ l of sesame oil and 5 days later were injected subcutaneously with relaxin or relaxin analogs in 100 μ l of 1% benzopurpurin 4B or with 1% benzopurpurin 4B alone as control. After 16 h the mice were killed in an atmosphere of CO_2 ; the symphysis pubis were dissected free of adhering tissue, and the distance between the interpubic bones was measured with a dissecting microscope fitted with transilluminating fiber optics.

RESULTS AND DISCUSSION

The evidence that two arginine residues (B13 and B17) on the surface of the B chain helix are in the relaxin-receptor interaction site (11, 13) pointed to a novel binding mechanism. The x-ray structure of human relaxin shows that these arginines are located on the edge of the dimerization surface (12), which suggests that relaxin acts as a monomer and that the two side chains would project away from the molecular surface. Although it is clear that these two B chain arginines are indispensable, both in terms of charge and geometry, they are not sufficient for binding. For example, helical peptides with two arginines in positions *i* and *i*+4 do not compete for the relaxin receptor-binding site regardless of concentration. Conversely, relaxins from different species that show more than 50% sequence differences still bind the test (mouse) receptor quite well. The display of the Connolly surface (23) derived from the

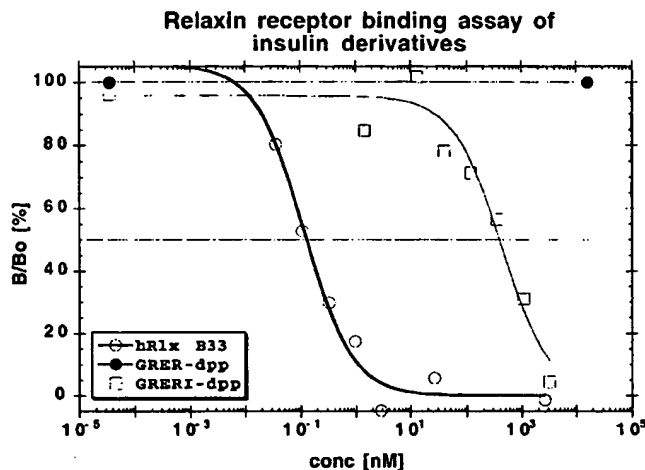


FIG. 4. Receptor binding assays of GRERI-dpp insulin on crude membrane preparations of mouse brain using 125 I-Phe-A3-Tyr-B30 human relaxin for tracer. The effect was compared with human relaxin and GRER-dpp insulin, which were run in parallel. Three independent dose-response curves were acquired. GRER-dpp insulin lacks the critical Ile-B20.

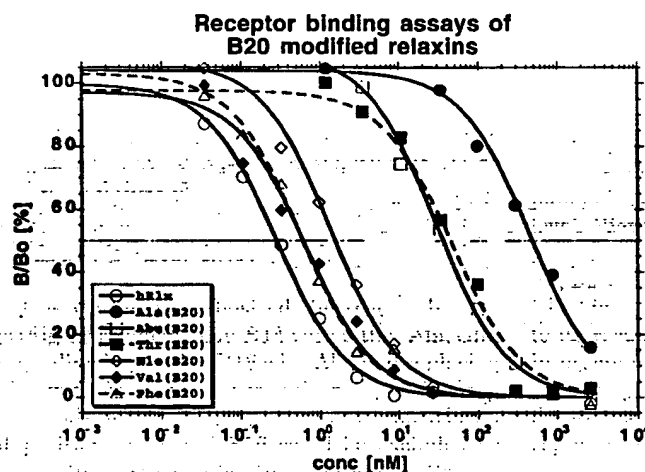


FIG. 5. Receptor binding assays of B20 modified relaxins using crude membrane preparations of mouse brain and 125 I-Phe-A3-Tyr-B30 human relaxin for tracer. Three independent dose-response curves of each analog were averaged.

x-ray structure gives the impression that the two arginines form a contiguous surface feature in the binding region of relaxin together with Glu-B14, Val-B16, and Ile-B20 (Fig. 1). Ile-B20 was not an absolutely constant feature, but replacement was rare and only with large hydrophobic residues such as Leu in hamster (24) and Val in porcine relaxin (6). Positions B14 and B16 would show a glycine and alanine, respectively, in

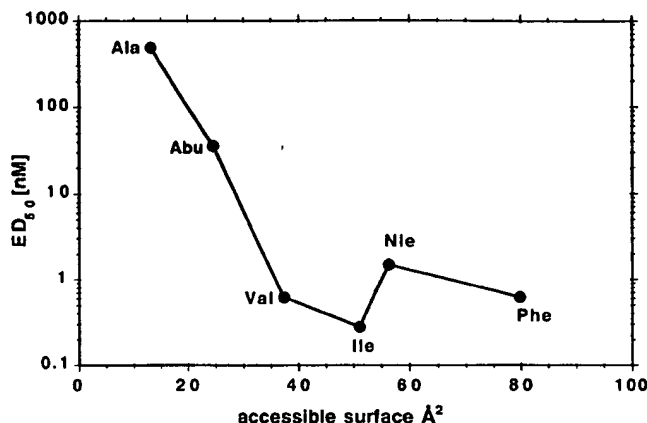


FIG. 6. Affinity of relaxin analogs for the relaxin-receptor *versus* the accessible area of hydrophobic amino acid residues in position B20. For each amino acid the Connolly surface was calculated using the Sybyl software (Tripos). The differences of the accessible surface areas of alkylamino acids and glycine are displayed. The binding affinity corresponds to the ED₅₀ values measured in receptor binding assays.

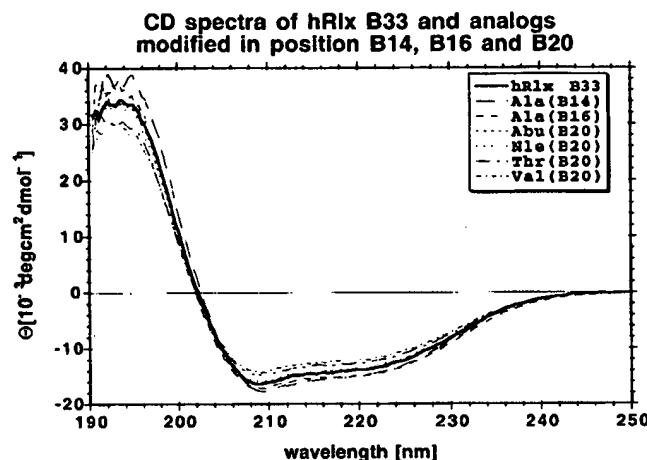


FIG. 7. CD of relaxin and relaxin analogs with modification in positions B14, B16, and B20. Relaxins were dissolved in 25 mM Tris/HCl buffer at pH 7.5 at a concentration of 13 μ M. Data were collected at a resolution of 0.2 nm and a bandwidth of 2 nm, and 10 spectra were averaged. Substitutions in positions B14, B16, and B20 do not induce major structural changes.

a few natural relaxins so that these positions seemed less critical (25).

To test our ideas we have synthesized the several human relaxin analogs (Fig. 2) replacing Glu-B14 with either Ala, Gln, or Asp, replacing valine in position B16 with Ala, and replacing Ile in position B20 with Ala. The results of the receptor binding assays (Fig. 3) on crude membrane preparations of mouse brain suggested that positions B14 and B16 could be excluded as active site residues. In contrast, substitution of Ala for Ile-B20 reduced receptor binding by three orders of magnitude indicating that Ile-B20 is as important for receptor interaction as the arginines B13 and B17. This conjecture found impressive confirmation when we redesigned and synthesized our insulin-relaxin Zwitterhormon (GRER-dpp) (14) with Ile instead of Tyr in the position corresponding to B20 and found significant receptor-binding in the mouse brain receptor assay. In fact the binding curve for (GRER-dpp) runs parallel to that of relaxin (Fig. 4), whereas the Zwitterhormon without Ile-B20 recognized only the rat relaxin receptor as previously reported (14).

Probing for fine structural binding requirements as concerns position B20, we extended alanine by one methylene group

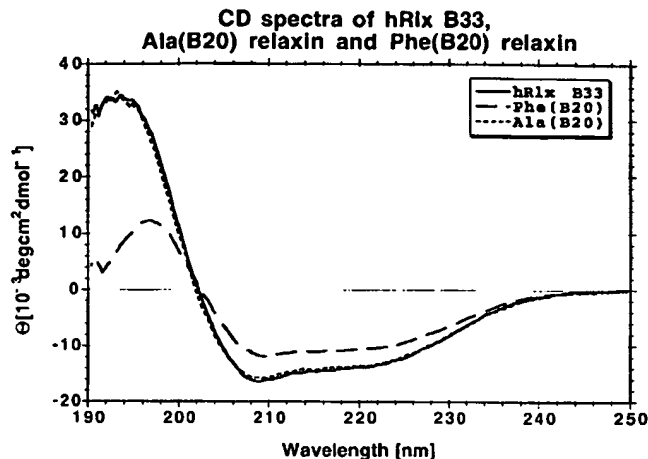


FIG. 8. CD of human relaxin in comparison with Ala-B20 relaxin and Phe-B20 relaxin. Relaxins were dissolved in 25 mM Tris/HCl buffer at pH 7.5 at a concentration of 13 μ M. Data were collected at a resolution of 0.2 nm and a bandwidth of 2 nm, and 10 spectra were averaged. The spectrum of Phe-B20 relaxin is severely perturbed when compared with other derivatives (Fig. 7).

(α -aminobutyric acid) and by three methylene groups (norleucine) (Fig. 5). Remarkably, each CH₂ group gives a 10-fold increase in binding energy. Reducing the chain length from norleucine and adding a β -branch (valine) resulted in a further 2.5-fold increase in binding intensity, suggesting that bulk at the base of the side chain is favorable. In line with this argument we noted that threonine, which is isosteric with valine, produced a significant improvement over alanine despite its polar character at the β -carbon. On the other hand, the larger surface of phenylalanine does not compensate for the missing β -branch (Fig. 5). Plotting the log of the binding affinity (nM) against the surface area shows a nearly linear relationship from alanine to isoleucine with norleucine and phenylalanine lying outside possibly because of size limitations (Fig. 6). We have synthesized a B20 *p*-benzoylphenylalanine relaxin derivative that, despite its hydrophobic character, does not bind, possibly because it exceeds the dimensions of the surface on the receptor and thus prohibits the proper alignment of Arg-B13 and Arg-B17 with the binding site.

These considerations invoke the rather unique but certainly plausible mode of prehensile binding action at the molecular level: Viewed normal to the axis of the B chain α -helix, comparison with portions of a human hand suggests itself, with arginine fingers on one side opposed by a thumb that, if diminished in surface, will cause reduced holding power of the ligand to its receptor. The idea also invites the proposal that relaxin interacts with a ridge on the receptor as opposed to the more commonly found pocket. One is hard pressed to explain the drastic destabilization of the di-arginine-mediated relaxin/receptor interaction by removal of one member of the binding triad (Ile) if relaxin slides into a deep binding pocket on the receptor surface.

To confirm that our studies are based upon relaxin derivatives with the proper structure, the homogeneity of each analog was verified in two reversed phase HPLC systems. Upon reduction each analog yielded two chains; the A chain showed identical retention times for all analogs, whereas the retention times of B chains differed. Tryptic digest and peptide mapping by HPLC of the B (20) relaxin analogs showed the expected difference for the C-terminal cystinyl peptide A (23–24)/B (18–30), and all other fragments were identical. Mass spectrometry indicated the correct molecular mass of each analog. Amino acid analysis of the total acid hydrolysate resulted in the ex-

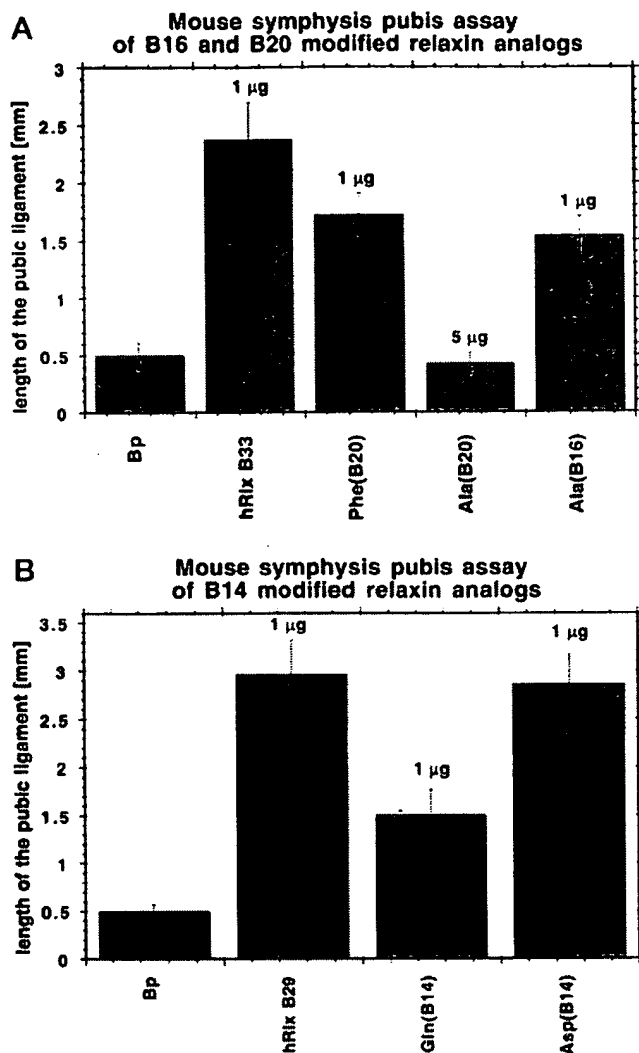


FIG. 9. Mouse symphysis pubis assay. Estrogen-primed mice were injected subcutaneously with relaxin or relaxin analog in 100 μ l of 1% aqueous benzopurpurin 4B. The mice were killed, the symphyses pubis were freed of adherent tissue, and the distances between the pubic bones were measured. A, benzopurpurin (Bp) (seven mice), 1 μ g of human relaxin B33 (eight mice), 1 μ g of Phe-B20 B33 (eight mice), 5 μ g of Ala-B20 B33 (seven mice), and 1 μ g of Ala-B16 B33 (seven mice). B, benzopurpurin (Bp) (15 mice), 1 μ g of human relaxin B29 (15 mice), 1 μ g of Gln-B14 B29 (14 mice), and 1 μ g of Asp-B14 B29 (14 mice).

pected amino acid composition, and sequence analysis of Ala-B20 and Phe-B20 relaxin confirmed the structure.

The results of CD spectroscopy shown in Fig. 7 support the idea that the reduced affinity is not due to a conformational change. In contrast, the dichroic intensity of Phe-B20 relaxin is reduced (Fig. 8), and a red shift of the maximum to 197 nm is observed as well as a reduced maximum to minimum ratio ($\Theta_{197\text{ nm}}/\Theta_{209\text{ nm}} = 0.93$) when compared with human relaxin ($\Theta_{197\text{ nm}}/\Theta_{209\text{ nm}} = 1.71$). The changes seem, however, mostly

quantitative and of such nature that this analog retained a relatively high potency.

To assure that binding would be an indicator of bioactivity, a selected number of analogs were tested in the mouse symphysis pubis assay. Relaxin derivatives with modification in positions B14 (Gln and Asp), B16 (Ala), and Phe(B20) were active at a dose of 1 μ g/mouse, whereas Ala-B20 relaxin was inactive at a dose of 5 μ g/mouse (Fig. 9). These results are in full agreement with the receptor binding assays and suggest that binding may be synonymous with bioactivity.

We conclude that the relaxin receptor-binding site comprises three crucial binding residues, Arg-B13, Arg-B17, and Ile-B20, which form a triangular contact region on the relaxin surface (Fig. 1). Remarkably, the components of this binding site are strongly hydrophilic on one side, opposed by a strongly hydrophobic component on the other, and all held in proper relation to each other by the geometry of the same α -helix.

Acknowledgments—We thank Robert Bracey and George Fullbright for technical assistance and Dr. Kevin Schey and the mass spectrometry facility at the Medical University of South Carolina for help. Computergraphics were made possible by the Biomolecular Computing Resource at the Medical University of South Carolina.

REFERENCES

- Sherwood, O. D. (1994) in *Physiology of Reproduction* (Knobil, E., and Neill, J. D., eds) Vol. 1, 2nd Ed., pp. 861–1010, Raven Press, New York
- Seibold, J. R., Clements, P. J., Furst, D. E., Mayes, M. D., McCloskey, D. A., Moreland, L. W., White, B., Wigley, F. M., Rocco, S., Erikson, M., Hannigan, J. F., Sanders, M. E., and Amento, E. P. (1998) *J. Rheumatol.* **25**, 302–307
- Seibold, J. R., Korn, J. H., Simms, R., Clements, P. J., Moreland, L. W., Mayes, M. D., Furst, D. E., Rothfield, N., Steen, V., Weisman, M., Collier, D., Wigley, F. M., Merkel, P. A., Csuka, M. E., Hsu, V., Rocco, S., Erikson, M., Hannigan, J. F., Harkonen, W. S., and Sanders, M. E. (2000) *Ann. Intern. Med.* **132**, 871–879
- Hisaw, F. L. (1926) *Proc. Soc. Exp. Biol. Med.* **23**, 661–663
- Schwabe, C., McDonald, J. K., and Steinetz, B. G. (1976) *Biochem. Cell Biol.* **70**, 397–405
- Schwabe, C., McDonald, J. K., and Steinetz, B. G. (1977) *Biochem. Cell Biol.* **75**, 503–510
- Schwabe, C., and McDonald, J. K. (1977) *Science* **197**, 914–915
- Bedarkar, S., Turnell, W. G., Blundell, T. L., and Schwabe, C. (1977) *Nature* **270**, 449–451
- James, R., Niall, H., Kwok, S., and Bryant-Greenwood, G. (1977) *Nature* **267**, 544–546
- Büllesbach, E. E., and Schwabe, C. (1988) *Int. J. Peptide Protein Res.* **32**, 361–367
- Büllesbach, E. E., Yang, S., and Schwabe, C. (1992) *J. Biol. Chem.* **267**, 22957–22960
- Eigenbrot, C., Randal, M., Quan, C., Burnier, J., O'Connell, L., Rinderknecht, E., and Kossiakoff, A. A. (1991) *J. Mol. Biol.* **221**, 15–21
- Büllesbach, E. E., and Schwabe, C. (1991) *J. Biol. Chem.* **266**, 10754–10761
- Büllesbach, E. E., Steinetz, B. G., and Schwabe, C. (1996) *Biochemistry* **35**, 9754–9760
- Atherton, E., Holder, J. L., Meldal, M., Sheppard, R. C., and Valerio, R. M. (1988) *J. Chem. Soc. Perkin Trans. 1*, 2887–2894
- Fields, G. B., and Noble, R. L. (1990) *Int. J. Peptide Protein Res.* **35**, 161–214
- King, D. S., Fields, C. G., and Fields, G. B. (1990) *Int. J. Peptide Protein Res.* **36**, 255–266
- Adler, A. J., Greenfield, N. J., and Fasman, G. D. (1973) *Methods Enzymol.* **27**, 675–735
- Büllesbach, E. E., and Schwabe, C. (1999) *J. Biol. Chem.* **274**, 22354–22358
- Yang, S., Rembisesa, B., Büllesbach, E. E., and Schwabe, C. (1992) *Endocrinology* **130**, 179–185
- De Lean, A., Munson, P. J., and Rodbard, D. (1978) *Am. J. Physiol.* **235**, E97–E102
- Steinetz, B. G., Beach, V. L., Kroc, R. L., Stasilli, N. R., Nussbaum, R. E., Nemeth, P. J., and Dun, R. K. (1960) *Endocrinology* **67**, 102–115
- Connolly, M. L. (1986) *J. Mol. Graphics* **4**, 3–6
- McCaslin, R. B., and Renegar, R. H. (1995) *Biol. Reprod.* **53**, 454–461
- Schwabe, C., and Büllesbach, E. E. (1994) *FASEB J.* **8**, 1152–1160

New Products

Insulin-like 3 protein (INSL3)

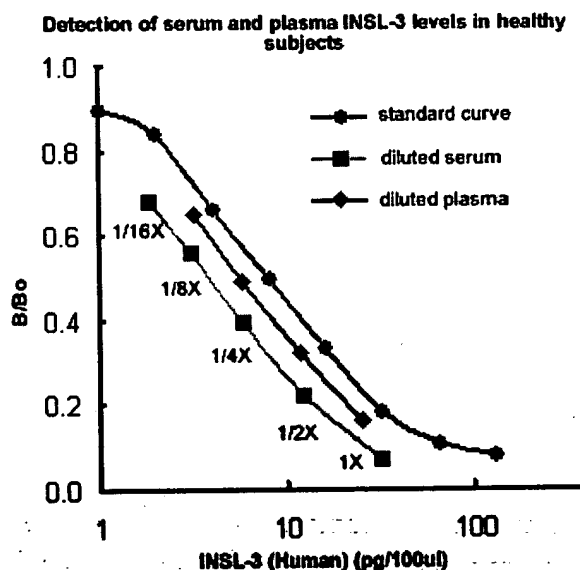
A New Circulating Hormone !!

Gender Specific Application for INSL3 circulating hormone

Insulin-like protein (INSL3, INSL4, INSL5, INSL6 & INSL7/H3 Relaxin) belongs to the insulin-like growth factor family, which encompasses insulin, relaxin, and insulin-like growth factors I (IGF1) and II (IGF2). Insulin-like growth factors I and II have specific functions. Members of this family are characterized by a common structure consisting of a connecting C chain, and an A chain. A preliminary in-house study performed at Phoenix Peptide, Inc. using INSL3 RIA Kit (RK-035-27) on male samples were approximately ten times greater than that found in female samples.

April 18, 2003 Phoenix Pharmaceuticals, Inc. Belmont, CA

Insulin-like 3 is a new insulin-like circulating hormone. Preliminary result from our lab indicated that the circulating levels of human Insulin-like 3 in male was 10~12 times greater than female.



Measurement of human Insulin-like 3-Immunoreactivity (non-extracted serum and plasma samples) in healthy subjects:

	Male (Mean \pm SD, n=8)	Female (Mean \pm SD, n=8)
Serum	758.42 \pm 83.21 pg/ml	59.42 \pm 25.76 pg/ml
Plasma	594.10 \pm 118.7 pg/ml	47.13 \pm 19.84 pg/ml

© April 18, 2003 Copyright Phoenix Pharmaceuticals, Inc. All Rights Reserved

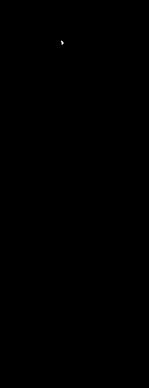
Physiological or pathological - a role for relaxin in the cardiovascular system?

The omnipresent 6kDa polypeptide relaxin (RLX) is emerging as a multi-functional endocrine hormone with a wide range of target tissues that includes the cardiovascular system. Humans and other high

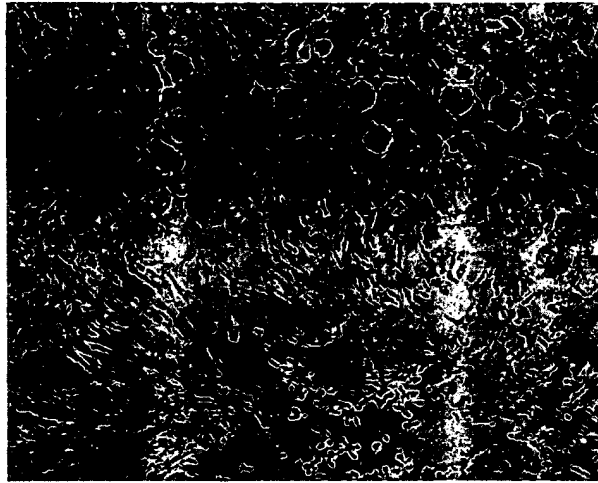
Samuel CS, Parry LJ, Summers RJ. *Curr Opin Pharmacol* 2003 Apr;3(2):152-8

The insulin-like hormone INSL-3, also named relaxin-like factor (RLF) or Leydig-derived in various reproductive tissues and is regarded a marker of differentiation in human test identified differential expression of human INSL-3 in neoplastic Leydig cells and mamma involvement of INSL-3 in tumor biology. Here we have investigated the expression of IN lines and in the human thyroid gland which has been shown to express transcripts for th LGR8. When we determined the expression of INSL-3 in eight human thyroid carcinoma containing a 95 bp out-of-frame insertion at the beginning of exon II of the INSL-3 gene anaplastic thyroid carcinoma cell line 8505C with diethylstilbestrol (DES) caused a signif down-regulation of INSL-3 and a marked up-regulation of LGR8. Employing in situ hybri specific rabbit antisera against the INSL-3 proteins, both INSL-3 isoforms were detected follicular carcinomas (FTC; n=12), papillary carcinomas (PTC; n=9) and undifferentiated contrast, thyrocytes of all 15 benign goiter tissues studied were devoid of both INSL-3 is indicate that INSL-3 hormone is up-regulated in hyperplastic and neoplastic human thyr isoforms may serve as additional markers for hyperplastic and neoplastic human thyr cell line 8505C, the regulation of both INSL-3 and LGR8 by estrogen may be the first inc auto-/paracrine INSL-3 LGR8 ligand receptor system active in human thyroid carcinoma

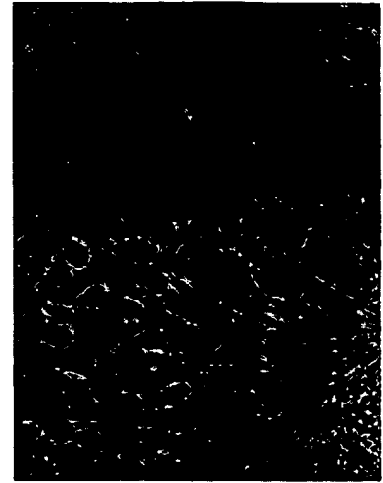
Anti-INSL-3 (Mouse) antiserum works in rat brain and testis



Rat brain tissue was stained by a
antiserum (Catalog No.: H-4



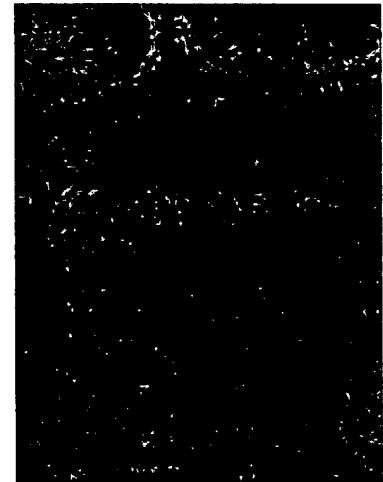
Rat testis tissue was stained by Pre-immune serum



Rat testis tissue was stained by anti-INSL3 antibody
(Catalog No.: H-035-43)



Rat testis tissue was stained by Pre-immune serum



Rat testis tissue was stained by anti-INSL3 antibody
(Catalog No.: H-035-43)



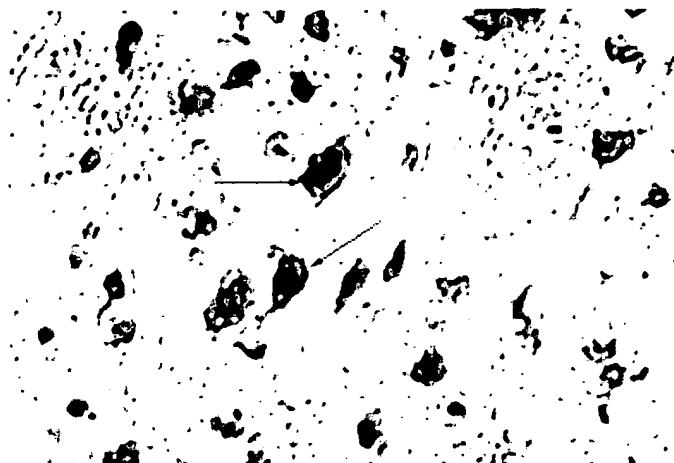
Rat testis tissue was stained by Pre-immune serum



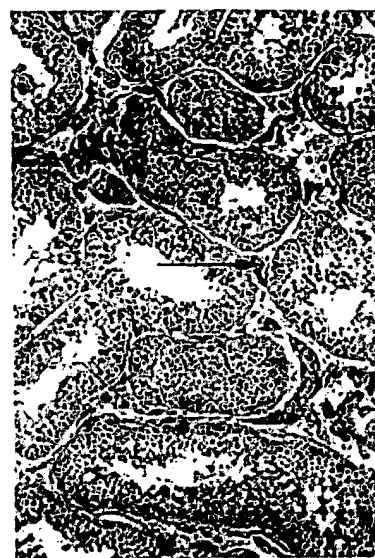
Rat testis tissue was stained by anti-INSL3 antibody
(Catalog No.: H-035-43)

INSL 3 (Mouse) Immunohistochemistry Protocol

INSL 3 (Mouse) Immunohistochemistry Protocol

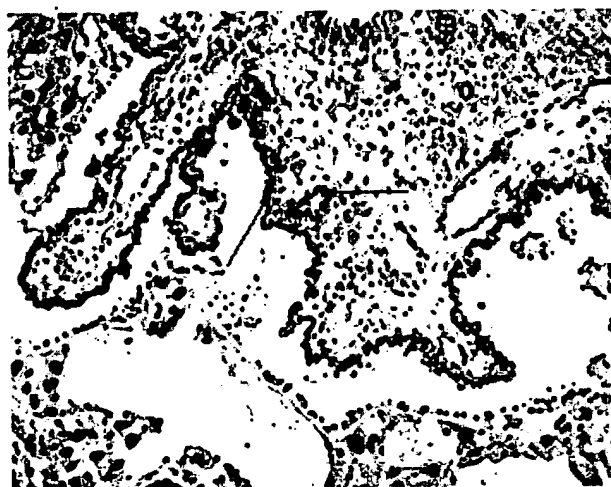


Rat cortex tissue was stained by Anti-INSL7/H3 relaxin (Human) Serum (Catalog No.: H-035-36)



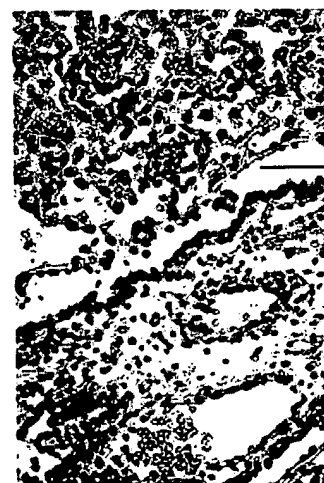
Human testis tissue was stained by Anti-INSL3 (Human) Serum (Catalog No.: H-035-33)

INSL 7/H3 relaxin Immunohistochemistry Protocol



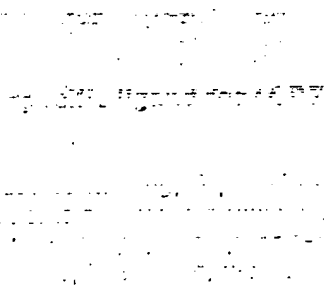
Rat placenta was stained by Anti-INSL 4 (Human) Serum (Catalog No.: H-035-33, Price: \$450/50 ul)

INSL 3 Immunohistochemistry Protocol

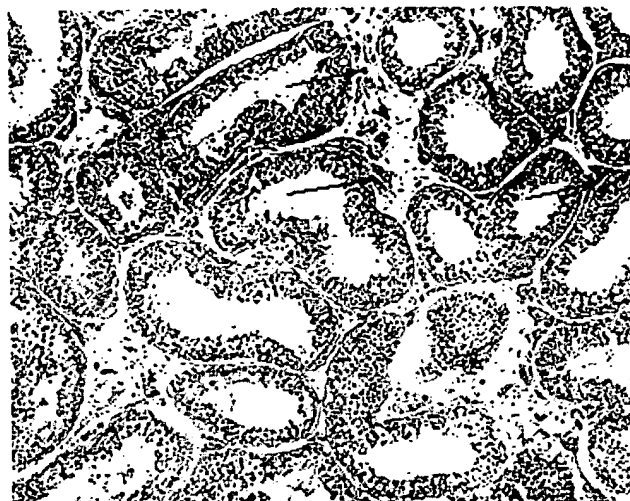


Rat placenta was stained by Anti-INSL 3 (Human) Serum (Catalog No.: H-035-33, Price: \$450/50 ul)

INSL 4 Immunohistochemistry Protocol



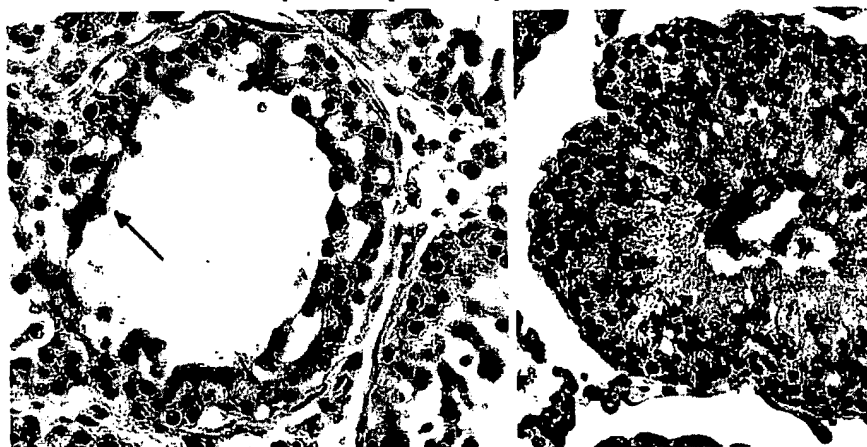
Rat placenta was stained by Anti-INSL 4 (Human) Serum (Catalog No.: H-035-33, Price: \$450/50 ul)



Human testis was stained by Anti-INSL 6 Serum (Catalog No.: H-035-30, Price: \$450/50 ul)

INSL 6 Immunohistochemistry Protocol

INSL-6/RIF-1 (Human) Immunohistochemistry



Human testis was stained by Anti-INSL-6, B Chain (Human) Serum (Catalog No. H-035-29)

Rat testis was stained by Anti-INSL-6, A C Serum (Catalog No. H-035-28)

INSL 6 B-Chain Immunohistochemistry Protocol

INSL 6 A-Chain Immunohistochemistry Protocol

H3 relaxin is a specific ligand for LGR7 and activates the receptor by interacting exoloop 2

Leucine-rich repeat-containing, G protein-coupled receptors (LGRs) represent a unique class of receptors with a large ectodomain. Recent studies demonstrated that relaxin activates two orphan GPCRs. Human relaxin 3 (H3) relaxin specifically activates LGR8. Human relaxin 3 (H3) relaxin specifically activates LGR8. Here, we demonstrated that H3 relaxin activates LGR7 but not LGR8. The overlapping specificity of these three ligands for the two related LGRs, chimeric receptor mechanism of ligand activation of LGR7. Chimeric receptor LGR7/8 with the ectodomain region from LGR8 maintains responsiveness to relaxin but was less responsive to H3 relaxin. The decreased ligand signaling was accompanied by decreases in the ability of H3 relaxin to bind to the chimeric receptor. However, replacement of the exoloop 2, but not exoloop 1, restored ligand binding and receptor-mediated cAMP production. These results suggest that the molecular basis of ligand signaling for this unique subgroup of G protein-coupled receptors involves specific binding of the ligand to both the ectodomain and the exoloop 2, thus providing a molecular basis for ligand signaling for this unique subgroup of G protein-coupled receptors.

Sudo S. et al. J. Biol. Chem, Feb 2003; 278: 7855 - 7862.

Restricted, but abundant, expression of the novel rat gene-3 (R3) relaxin in the

Relaxin is a peptide hormone with known actions associated with female reproductive physiology in the brain. Only one relaxin gene had been characterized in rodents until recently when rat R3 (R3) and its mouse equivalent (M3) were identified. The current study reports the identification of R3 relaxin that is highly expressed in a discrete region of the adult brain. The full R3 relaxin cDNA and 3' and 5' RACE protocols. The derived amino acid sequence of R3 relaxin retains all the amino acids of the peptide and has a high degree of homology with H3 and M3 relaxin. The distribution of R3 relaxin was determined and highly abundant expression was only detected in neurons of the ventral horn in the pons, whereas all other brain areas were unlabelled or contained much lower mRNA levels. mRNA immunoreactivity was also detected in the vmDTg. These together with earlier findings suggest that multiple relaxin peptides as neurotransmitters and/or modulators in the rat CNS.

Burazin TC, Bathgate RA, Macris M, Layfield S, Gundlach AL, Tregear GW. J Neurochem

Relaxin-like bioactivity of ovine Insulin 3 (INSL3) analogues

Relaxin is an insulin-like peptide consisting of two separate chains (A and B) joined by two disulfide bonds. Binding to its receptor requires an Arg-X-X-Arg-X-X-Ile motif in the B-chain. A superfamily, INSL3, has a tertiary structure that is predicted to be similar to relaxin. It is a member of the relaxin superfamily, although this is displaced by four amino acids towards the C-terminus of relaxin. We have previously shown that synthetic INSL3 itself does not display relaxin-like bioactivity. In order to identify further the structural features that impart relaxin function, we prepared three additional analogues for bioassay. Each of these contained point substitutions in the B-chain. Analogue D contained the full human relaxin binding cassette, Analogue G consisted of the full human relaxin binding cassette with an Arg to Ala substitution, and Analogue E was a further modification of Analogue A, with the full human relaxin binding cassette and a further modification of Analogue A, with the full human relaxin binding cassette. Detailed circular dichroism spectroscopy showed that Analogue D caused little alteration of secondary structure and, hence, overall conformation. However, Analogue E showed relaxin-like activity. These results indicate that while the arginine cassette is vital for relaxin binding, yet unidentified structural requirements for relaxin binding.

Claasz AA, Bond CP, Bathgate RA, Otvos L, Dawson NF, Summers RJ, Tregear GW, Wade JD (24):6287-93

INSL3/Leydig insulin-like peptide activates the LGR8 receptor important in testis

Several orphan G protein-coupled receptors homologous to gonadotropin and thyrotropin-releasing hormone and named as LGR4-8. INSL3, also known as Leydig insulin-like peptide or relaxin-like factor, is expressed in testis Leydig cells and ovarian theca and luteal cells. Male mice mutant for testis descent due to abnormal gubernaculum development whereas overexpression of INSL3 in females. Because transgenic mice missing the LGR8 gene are also cryptorchid, INSL3 was shown to show that treatment with INSL3 stimulated cAMP production in cells expressing recombinant LGR8. Interactions between INSL3 and LGR8 were demonstrated following ligand receptor cross-linking, showing that the LGR8 transcripts are expressed in gubernaculum whereas treatment of cultured gubernaculum with INSL3 stimulated cAMP production and thymidine incorporation. The present study identified the ligand for LGR8 based on common phenotypes of ligand and receptor null mice. Demonstration of INSL3 as the ligand for LGR8 allows understanding of the mechanism of testis descent and allows studies on the role of INSL3 in testis processes.

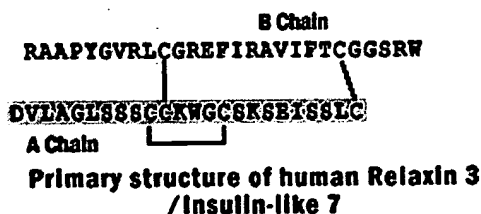
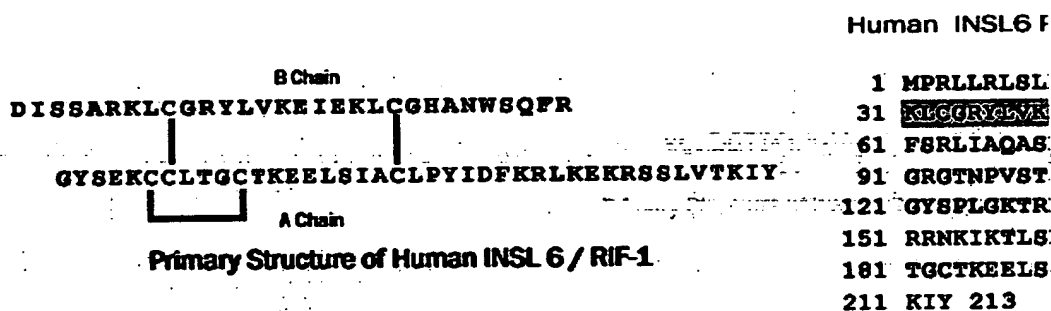
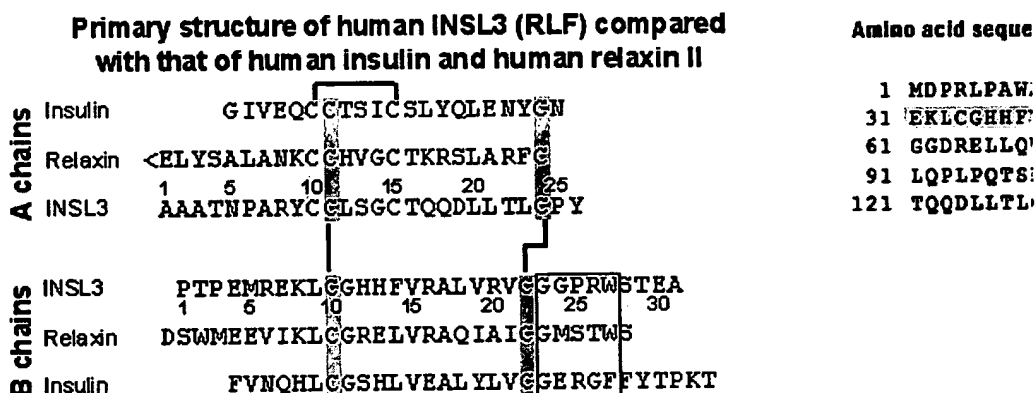
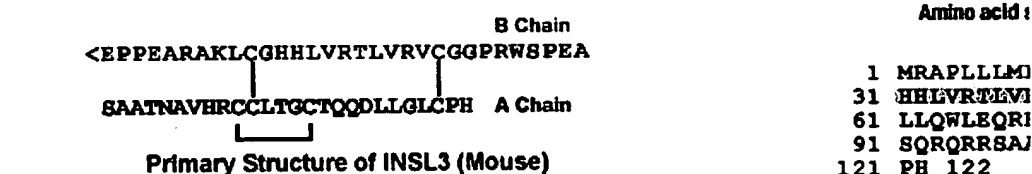
Kumagai J, Hsu SY, Matsumi H, Roh JS, Fu P, Wade JD, Bathgate RA, Hsueh AJ. J Biol Chem

Reproductive Biology of the Relaxin-Like Factor (RLF/INSL3)

The relaxin-like factor (RLF), which is the product of the insulin-like factor 3 (INSL3) gene, is a member of the relaxin-insulin family. In male mammals, it is a major secretory product of the testis, being expressed constitutively but in a differentiation-dependent manner. In the adult testis, it is fully differentiated adult-type Leydig cells, but it is only weakly expressed in prepubertal testis that have become hypertrophic or transformed. It is also an important product of the fetal

been demonstrated using knockout mice to be responsible for the second phase of testis. INSL3 knockout mice are cryptorchid, and in estrogen-induced cryptorchidism, RLF level RLF is also made in female tissues, particularly in the follicular theca cells of small antra cycle and pregnancy. The ruminant ovary has a very high level of RLF expression, and a theca-lutein cells indicated that, as in the testis, expression is probably constitutive but knockout mice have altered estrous cycles, where RLF may be involved in follicle selection. observations on bovine secondary follicles. Recently, a novel 7-transmembrane domain tentatively identified as the RLF receptor, and its deletion in mice leads also to cryptorchidism. 2002 Sep;67(3):699-705

INSL3 Gene Map, Structure, and Mapping Information Additional GPCR LGR7 and LGR8 Information



Amino acid sequence

1 MARYML

31 GYRLCG

61 EAMGDT

91 LALTKS

121 LAGLSS

A Chain Aligns

	1	5	10	15	20
Human 1	RPYVALFEKCLIGCTKRS LAKYC				
Human 2	QLYSALANKCCHVGCTKRS LARFC				
Cons 1,2,3	...+L...CC...GC+K...++...C				
Human 3	DVLAGLSSSCCKWGCSKSEISSLC				
Cons 3	DVLAGLSSSCC+WGCSKS+ISSLC				
Rat 3	DVLAGLSSSCCEWGCSKSQISSLC				
Mouse 3	DVLAGLSSSCCEWGCSKSQISSLC				
Cons Mouse	+...+S...CC...GCS+...I...L-C				
Mouse 1	ESGGLMSQQCCHVGCSRRSIAKLYC				

Alignment of A-Chain sequences from H3 and M3 relaxin with other human and mouse relaxin sequence

B Chain Aligns

Human 1	
Human 2	
Cons 1,2,3	
Human 3	
Cons 3	
Mouse 3	
Cons Mouse	
Mouse 1	RV

Alignment of B-Chain sequences from H3 and M3 relaxin with other human and mouse relaxin sequence

Primary Structure of human INSL4 (Insulin-like Peptide 4)

B Chain: QLLRESIAAEIRGCGPRFGKHLISYCPMDEKTFITTPGGWL

A Chain: SGRHREFDPFCCEVICDDGTSVKLCT

Amino acid sequence

1 MASLFRSYL

31 CGPRFGKHL

61 SGRPKEMVS

91 PELKKPLSE

121 DPFCCEVIC

Primary Structure of human INSL5 (Insulin-like Peptide 5)

B Chain: SKESVRLGGLYGGRTVLYLCASSRM

A Chain: RQDLQTLCCCTDGCSTDLALC

Amino acid sequence

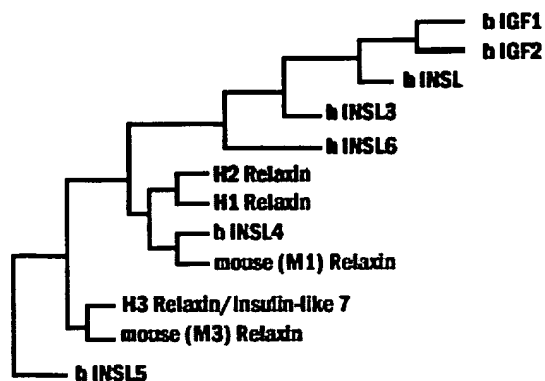
1 MKGSIFTL

31 GYRLCG

61 TGNPQLP

91 DRLWGGQMI

121 CCTDGCST



Phylogenetic tree of evolution of H3 and M3 relaxin full-length sequences with human sequences of the relaxin/insulin/IGF superfamily

INSL3-C Peptide of INSL3 [INSL3 , Prepro, (58-105) (Human)]	035-48	⁵⁸ PAAGGDRELLQWLERRHLLHGL'
INSL 3-C Peptide [INSL 3 , Prepro, (51-94) (Mouse)]	035-47	⁵¹ TQPVETRDRELLQWLEQRHLLH/

Code#	Product Name	Quai
H-035-36	INSL 7/H3 Relaxin (Human) Antiserum for Immunohistochemistry	50 µl
G-035-36	INSL 7/H3 Relaxin (Human) Purified IgG	200 µg
FG-G-035-36	INSL 7/H3 Relaxin (Human) Purified IgG, FAM labeled	100 µl
B-G-035-36	INSL 7/H3 Relaxin (Human) Purified IgG, Biotin labeled	100 µl
FC3-G-035-36	INSL 7/H3 Relaxin (Human) Purified IgG, Cy3 labeled	100 µl
FC5-G-035-36	INSL 7/H3 Relaxin (Human) Purified IgG, Cy5 labeled	100 µl
FRP-G-035-36	INSL 7/H3 Relaxin (Human) Purified IgG, R-PE labeled	100 µl
035-36	<u>INSL 7 - Insulin-like 7 / H3 Relaxin (Human)</u>	20 µg
T-035-36	<u>INSL 7 - Insulin-like 7 / H3 Relaxin (Human), Iodine 125 Labeled Tracer</u>	10 µCi
035-34	<u>INSL 7 - A Chain - Insulin-like 7 / H3 Relaxin (Human)</u>	100 µg
T-035-34	<u>INSL 7 - A Chain - Insulin-like 7 / H3 Relaxin (Human), Iodine 125 Labeled Tracer</u>	10 µCi
B-035-34	<u>INSL 7 - A Chain - Insulin-like 7 / H3 Relaxin (Human), Biotin labeled</u>	20 µg
035-35	<u>INSL 7 - B Chain - Insulin-like 7 / H3 Relaxin (Human)</u>	100 µg
T-035-35	<u>INSL 7 - B Chain - Insulin-like 7 / H3 Relaxin (Human), Iodine 125 Labeled Tracer</u>	10 µCi
B-035-35	<u>INSL 7 - B Chain - Insulin-like 7 / H3 Relaxin (Human), Biotin labeled</u>	20 µg

035-41	<u>INSL 3 - A Chain - Insulin-like 3 (Mouse)</u>	100 µg
035-42	<u>INSL 3 - B Chain - Insulin-like 3 (Mouse)</u>	100 µg
035-47	<u>INSL 3 - C Peptide - Insulin-like 3 Prepro (51-94)(Mouse)</u>	100 µg
FG-035-47	<u>INSL 3 - C Peptide - Insulin-like 3 Prepro (51-94)(Mouse), FAM labeled</u>	1 nmole
B-035-47	<u>INSL 3 - C Peptide - Insulin-like 3 Prepro (51-94)(Mouse), Biotin labeled</u>	20 µg
035-48	<u>INSL 3 - C Peptide - Insulin-like 3 Prepro (58-105)(Human)</u>	100 µg
FG-035-48	<u>INSL 3 - C Peptide - Insulin-like 3 Prepro (58-105) (Human), FAM labeled</u>	1 nmole
B-035-48	<u>INSL 3 - C Peptide - Insulin-like 3 Prepro (58-105) (Human), Biotin labeled</u>	20 µg
RAB-035-27	<u>INSL 3 - Insulin-like 3 (Human) - Antibody for RIA</u>	125 RIA tub
H-035-27	<u>INSL 3 - Insulin-like 3 (Human) - Antiserum for Immuno-histochemistry</u>	100 µl
EK-035-27	<u>INSL 3 - Insulin-like 3 (Human) - EIA Kit</u>	96 wells
FG-G-035-27	<u>INSL 3 - Insulin-like 3 (Human) - FAM Labeled Purified IgG</u>	100 µl
B-035-27	<u>INSL 3 - Insulin-like 3 (Human) - Monobiotinylated - Biotin Labeled</u>	20 µg
G-035-27	<u>INSL 3 - Insulin-like 3 (Human) - Purified IgG Antibody</u>	200 µg
B-G-035-27	<u>INSL 3 - Insulin-like 3 (Human) - Purified IgG - Biotin Labeled</u>	100 µl
FC5-G-035-27	<u>INSL 3 - Insulin-like 3 (Human) - Purified IgG - Cy5 Labeled</u>	100 µl
FRP-G-035-27	<u>INSL 3 - Insulin-like 3 (Human) - R-PE Labeled Purified IgG</u>	100 µl
FR-G-035-27	<u>INSL 3 - Insulin-like 3 (Human) - Rhodamine Labeled Purified IgG</u>	100 µl
RK-035-27	<u>INSL 3 - Insulin-like 3 (Human) - RIA Kit</u>	125 RIA tub
FC3-G-035-27	<u>INSL 3 - Insulin-like 3 (Human) - Purified IgG - Cy3 Labeled</u>	100 µl
035-43	<u>INSL 3 - Insulin-like 3 (Mouse)</u>	20 µg
T-035-43	<u>INSL 3 - Insulin-like 3 (Mouse) - Iodine 125 Labeled Tracer</u>	10 µCi
H-035-43	<u>INSL 3 - Insulin-like 3 (Mouse) Antiserum</u>	100 µl
G-035-43	<u>INSL 3 - Insulin-like 3 (Mouse) Antibody, Purified IgG</u>	200 µg
B-G-035-43	<u>INSL 3 - Insulin-like 3 (Mouse) Antibody, Purified IgG, Biotin labeled</u>	100 µl
FG-G-035-43	<u>INSL 3 - Insulin-like 3 (Mouse) Antibody, Purified IgG, FAM labeled</u>	100 µl

FRP-G-035-43	<u>INSL 3 - Insulin-like 3 (Mouse) Antibody, Purified IgG, R-PE labeled</u>	100 µl
035-27	<u>INSL 3 - Insulin-like 3 (RLF)(Human)</u>	100 µg
T-035-27	<u>INSL 3 - Insulin-like 3 (RLF)(Human) - Iodine 125 Labeled Tracer</u>	10 µCi
035-31	<u>INSL 4 - A Chain - Insulin-like 4 (Human)</u>	100 µg
035-32	<u>INSL 4 - B Chain - Insulin-like 4 (Human)</u>	100 µg
H-035-33	<u>INSL 4 - Insulin-like 4 (Human) - Antiserum for Immuno-histochemistry</u>	50 µl
T-035-33	<u>INSL 4 - Insulin-like 4 (Human) - Iodine 125 Labeled Tracer</u>	10 µCi
035-33	<u>INSL 4 - Insulin-like 4 (RLF)(Human)</u>	20 µg
035-37	<u>INSL 5 - A Chain - Insulin-like 5 (Human)</u>	100 µg
035-38	<u>INSL 5 - B Chain - Insulin-like 5 (Human)</u>	100 µg
035-39	<u>INSL 5 - Insulin-like 5 (Human)</u>	** Discontinue
035-40	<u>INSL 5 - Insulin-like 5 (Mouse)</u>	20 µg
035-45	<u>INSL 6 - A Chain - Insulin-like 6 (Mouse)</u>	100 µg
035-28	<u>INSL 6 - A Chain - Insulin-like 6 (RLF / RIF-1)(Human)</u>	100 µg
H-035-28	<u>INSL 6 - A Chain - Insulin-like 6 (RLF / RIF-1)(Human) - Antiserum for Immuno-histochemistry</u>	50 µl
FG-G-035-28	<u>INSL 6 - A Chain - Insulin-like 6 (RLF / RIF-1)(Human) - FAM Labeled Purified IgG</u>	200 µl
G-035-28	<u>INSL 6 - A Chain - Insulin-like 6 (RLF / RIF-1)(Human) - Purified IgG Antibody</u>	200 µg
B-G-035-28	<u>INSL 6 - A Chain - Insulin-like 6 (RLF / RIF-1)(Human) - Purified IgG - Biotin Labeled</u>	100 µl
PE-G-035-28	<u>INSL 6 - A Chain - Insulin-like 6 (RLF / RIF-1)(Human) - Purified IgG - R-PR Labeled</u>	100 µl
FR-G-035-28	<u>INSL 6 - A Chain - Insulin-like 6 (RLF / RIF-1)(Human) - Rhodamine Labeled Purified IgG</u>	100 µl
035-07	<u>Insulin B (21-26) Peptide Analog (DP-432)</u>	5 mg
035-08	<u>Insulin B (22-25) Peptide</u>	5 mg
035-06	<u>Insulin (Human)</u>	20 µg
T-035-06	<u>Insulin (Human) - Iodine 125 Labeled Tracer</u>	10 µCi
035-09	<u>Insulin-like Growth Factor 1 (D-Domain 62-70)</u>	1 mg
035-10	<u>Insulin-like Growth Factor I (24-41)</u>	1 mg

035-11	<u>Insulin-like Growth Factor I (30-41)</u>	1 mg
035-12	<u>Insulin-like Growth Factor I (71-105) Pro (Human)</u>	200 µg
035-19	<u>Insulin-like Growth Factor II (105-128) Pro (Human)</u>	200 µg
035-20	<u>Insulin-like Growth Factor II (131-154) Pro (Human)</u>	200 µg
035-14	<u>Insulin-like Growth Factor II (33-40)</u>	1 mg
035-16	<u>Insulin-like Growth Factor II (54-67)</u>	1 mg
035-18	<u>Insulin-like Growth Factor II (68-102) Pro (Human)</u>	200 µg
035-17	<u>Insulin-like Growth Factor II (69-84)</u>	500 µg
035-13	<u>Insulin-like Growth Factor II (D-Domain (62-67))</u>	1 mg
035-21	<u>Insulin-Like Growth Factor Plasma Binding Protein</u>	500 µg
035-25	<u>Preptin (16-34) (Human)</u>	200 µg
035-26	<u>Preptin (16-34) (Rat)</u>	200 µg
035-24	<u>Preptin (Human)</u>	100 µg
035-22	<u>Preptin (Mouse)</u>	100 µg
035-23	<u>Preptin (Rat)</u>	100 µg

● Insulin-like (INSL) Related Protein products

© 2003-2004 Copyright Phoenix Pharmaceuticals, Inc. All Rights Reserved.
530 Harbor Boulevard • Belmont, CA • 94002 USA
Tel: 650-610-8883 or 800-988-1205 • Fax: 650-610-8882 • E-mail: info@phos.com

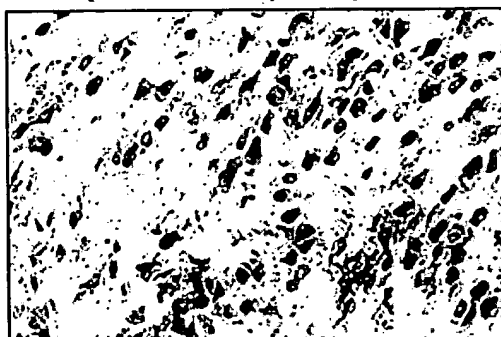
New Products

PI

LGR7 (Relaxin Receptor 1) and LGR8 (Relaxin Receptor 2)

Two Newly Identified orphan G Protein-Coupled Receptors

LGR7 (Relaxin Receptor 1) and LGR8 (Relaxin Receptor 2) Antibodies for Imm



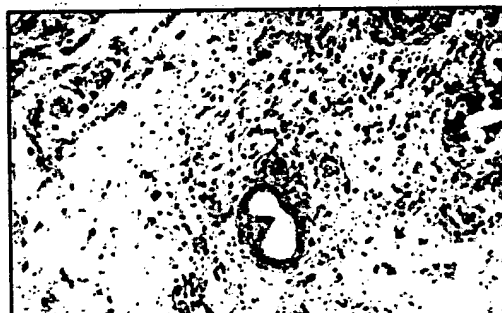
Rat uterus tissue was stained by Rabbit Anti-LGR7 (735-757) (Human) (Catalog No. H-001-53)



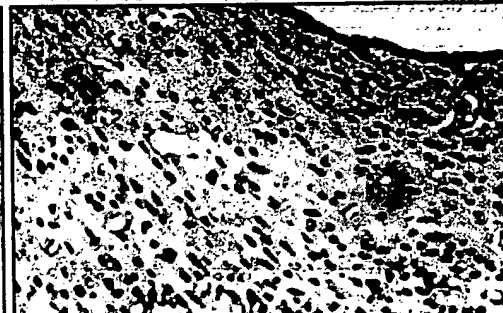
Rat uterus tissue was stained by Rabbit Anti-LGR7 (735-757) (Human) Serum (Catalog No. H-001-53)

LGR7 (735-757), (Human) Antibody for IHC

Tissue Sample	Rat uterus
Fixative	10% formalin
Embedding	paraffin
Negative Control	No primary antibody
Pretreatment	Intact
Blocking	2% Normal Goat Serum, 3%H2O2
Primary Antibody	LGR7 (735-757), (Human) Antiserum (Catalog No.: H-001-53)
Optimal Dilution	1:100 (1 hour at RT)
Secondary Antibody	Goat Anti-Rabbit IgG, Biotinylated (1:400)
Amplification	ABC (Vector)
Detection System	HRP
Substrate	DAB (Sigma)
Counterstained	Hematoxylin



Rat uterus tissue was stained by Rabbit Anti-LGR8 (737-754), Cys⁰, (Human) Serum (Catalog No. H-001-54)



Rat hypothalamus was stained by Anti-LGR8 (737-754), Cys⁰, (Human) Serum (Catalog No.: H-001-54)

LGR8(737-754), Cys⁰, (H) Antibody for IHC

Tissue Sample	Rat hypothalamus
---------------	------------------

HOME

NEW
PRODUCTS

SEARCH

ANTIBODIES

KITS

FLUORESCENT
PEPTIDESRADIOACTIVE
PEPTIDESCATALOG
PEPTIDESCUSTOM PEPTIDE
SYNTHESIS & GMPTECHNICAL
SUPPORT

Fixative	10% formalin
Embedding	paraffin
Negative Control	No primary antibody
Pretreatment	Pronase
Blocking	2% Normal Goat Serum, 3% H ₂ O ₂
Primary Antibody	LGR8 (737-754), Cys ⁰ , (Human) Antiserum (Catalog No.: H-001-54)
Optimal Dilution	1:100 (1 hour at RT)
Secondary Antibody	Goat Anti-Rabbit IgG, Biotinylated (1:400)
Amplification	ABC (Vector)
Detection System	HRP
Substrate	DAB (Sigma)
Counterstained	Hematoxylin

Code#	Product Name	Quantit
001-53	<u>LGR7 (735-757) (H)</u>	100μ
H-001-53	<u>LGR7 (735-757) (H) Antiserum for Immuno-histochemistry</u>	50l
B-G-001-53	<u>LGR7 (735-757) (H) Biotinylated Purified IgG</u>	100l
FG-G-001-53	<u>LGR7 (735-757) (H) FAM labeled Purified IgG Antibody</u>	100l
G-001-53	<u>LGR7 (735-757) (H) Purified IgG</u>	200μ
FR-G-001-53	<u>LGR7 (735-757) (H) Rhodamine labeled purified IgG Antibody</u>	100l
001-54	<u>LGR8 (737-754) Cys⁰ (H)</u>	100μ
H-001-54	<u>LGR8 (737-754) Cys⁰ (H) Antiserum for Immuno-histochemistry</u>	50l
B-G-001-54	<u>LGR8 (737-754) Cys⁰ (H) Biotinylated purified IgG</u>	100l
FG-G-001-54	<u>LGR8 (737-754) Cys⁰ (H) FAM labeled Purified IgG</u>	100l
G-001-54	<u>LGR8 (737-754) Cys⁰ (H) Purified IgG</u>	200μ
FR-G-001-54	<u>LGR8 (737-754) Cys⁰ (H) Rhodamine labeled purified IgG Antibody</u>	100l

Activation of orphan receptors by the hormone relaxin

Relaxin is a hormone important for the growth and remodeling of reproductive and other. Although binding sites for relaxin are widely distributed, the nature of its receptor has been demonstrated that two orphan heterotrimeric guanine nucleotide binding protein (G protein) and LGR8, are capable of mediating the action of relaxin through an adenosine 3',5'-cyclic monophosphate dependent pathway distinct from that of the structurally related insulin and insulin-like growth factor. Treatment of antepartum mice with the soluble ligand-binding region of LGR7 caused a divergent distribution of the two relaxin receptors implicates their roles in reproductive, and other functions.

Hsu S.Y., et al. Science 2002 Jan 15;295(5555):671-4

References:

1. Hsu, S. Y.; Nakabayashi, K.; Nishi, S.; Kumagai, J.; Kudo, M.; Sherwood, O. D.; I orphan receptors by the hormone relaxin. Science 295: 671-674, 2002.
2. Hsu, S. Y.; Kudo, M.; Chen, T.; Nakabayashi, K.; Bhalla, A.; van der Spek, P. J.; : The three subfamilies of leucine-rich repeat-containing G protein-coupled recept LGR6 and LGR7 and the signaling mechanism for LGR7. Molec. Endocr. 14: 1157-
3. Zhao, L.; Roche, P. J.; Gunnersen, J. M.; Hammond, V. E.; Tregear, G. W.; Wintc without a functional relaxin gene are unable to deliver milk to their pups. Endocri
4. Converse P. J. et al. OMIM #606654

LGR8 (Relaxin Receptor 2) (Human) Amino Acid Sequence

```

1  MIVFLVFKHL FSLRLITHFF LLHFIVLINV KDFALTQCSH 40
41  ITPSCQKGYF PCGNLTCLP RAFHEDGKDD CGNGADEENC 80
81  GDTSCWATIF GTVHCNANSV ALTQECFLKQ YPQCCDCKET 120
121 ELECVNGDLK SVPHISNNVT LLSLKKKKIH SLPDKVFIKY 160
161 TKLKKIFLQH NCIRHISRKA FFGLCNLQIL YLNHNCITTL 200
201 RPGIFKDLHQ LTWLILDDNP ITRISQRLFT GLNSLFFLSH 240
241 VNNYLEALPK QMCAQMPQLN WVDLEGNRIK YLTNSTFLSC 280
281 DSLTVLFLPR NQIGFVPEKT FSSLKNLGLL DLSSNTITEL 320
321 SPHLFKDKL LQKLNLSNP LMYLHKNQFE SLKQLQSLDL 360
361 ERRIEIPNINT RMFQPMKNLS HIYFKNFRYC SYAPHVRICH 400
401 PLTDGISSFE DLLANNI...FCNLFFVIGHR 440
441 SFIKAENTTH AMSIK...DCIMGVYLFV VGIPTIKYRC 480
481 QYQKYALLWH KSVQCRMHGF LAHLSTSVS...LLLTYLTER 520
521 FLVIVFPPSN IRPGKRO...SV ILICTUMAGF LIAVFPFUNK 560
561 DYFCNPFYGN CVCFPLYDQ TEDIGSKGYS LGIFLCVNL 600
601 AFLIIVFSYI...TH...CSIQRTA LQTEVRNCF GREVAVANR 640
641 FFIVFSDATC...VIVFVVKLI SLFRVEIPDT HTSWIVIFFL 680
681 PVNSALNPIL YLTITNFFKD KLKQLLHKHQ RKSIFKIKKK 720
721 SLSTSIWIR DSSSLK...GVL NKITLGDSIH KPVS 754

```

7 transmembrane region

Rabbit Anti-LGR8 (737-754), Cys⁰, (H)

Hsu, S.Y., et al. Science 295 (5555), 671-674 (2002)

LGR7 (Relaxin Receptor 1) Amino Acid Sequence

```

1  HTSGSVFFYI LIFCRYFSHC GGQDVKCSLG YFPCGNITKC 40
41  LPQLLHCNGV DDCGNQADED NCGDNNGQSH QFDRYFASY 80
81  KHTSQYPPFA ETPECLVGSV PVQCLCQGLE LDCDETNLRA 120
121 VPSVSSNVIA HSLQWNLIK LPPDCFRNYH DLQRLYLQNN 160
161 KITSISIIYAF RGLNSLTCLY LSHNRITFLK PGVFEDLHRL 200
201 EWLIIDNHL SRISPPTFYC LNSLILLVLH NNVLRLPDK 240
241 PLCQHMPRLH WLDLEGNHH NLNLTFISC SNLTVLVHRK 280
281 NKINHLNENT FAPLQKLDL DLGSNKIENL PPLIFKDLKE 320
321 LSQNLSTYNP IQKIQANQFD YLVKLKSLSL EGIRISNIQQ 360
361 RMFRPLHMLS HIYFRKFQYC GYAPHVRSCK PNTDGISSLE 400
401 ... 440

```

© 2003-2004 Copyright Phoenix Pharmaceuticals, Inc. All Rights Reserved.
530 Harbor Boulevard • Belmont, CA • 94002 USA
Tel: 650-610-8883 or 800-988-1205 • Fax: 650-610-8882 • E-mail: info@phoenixpept



SPECIFICATION SHEET

Important Note: Vial Contains Small Quantity. Centrifuge Product Before Opening!

Catalog #: E24520M **Lot #:** 4G18803

Description: MAb to Relaxin 1
Monoclonal Antibody to Human Relaxin 1

Specificity: Human Relaxin 1. Does not cross-react with human Relaxin 2.

Clone: 6F1willi

Host Animal: Mouse **Isotype:** IgG₁

Source: Cell culture supernatant

Immunogen: Human Relaxin 1

Format: Purified, Lyophilized.
Reconstitution in 10ul double distilled water.

Purification: Protein G

Concentration: 1mg/ml (prior to lyophilization)

Affinity Constant: Not determined.

Buffer: Lyophilized from PBS, pH 7.4

Preservative: 0.1% Sodium Azide

Applications: Suitable for use in ELISA and Flow cytometry. Each laboratory should determine an optimum working titer for use in its particular application. Suitability for use in IHC or Western blot has not been determined but use in such assays should not necessarily be excluded.

Storage: Store lyophilized product at 2-8°C. After reconstitution, store at -20°C. Avoid multiple freeze/thaw cycles.

Warning: This product contains sodium azide, which has been classified as Xn (Harmful), in European Directive 67/548/EEC in the concentration range of 0.1 – 1.0 %. When disposing of this reagent through lead or copper plumbing, flush with copious volumes of water to prevent azide build-up in drains.

FOR RESEARCH USE ONLY. NOT FOR USE IN DIAGNOSTIC PROCEDURES.

2/4/04



SPECIFICATION SHEET

Important Note: Vial Contains Small Quantity. Centrifuge Product Before Opening!

Catalog #: E24230M **Lot #:** 11H22403

Description: MAb to Pro-Relaxin 2
Monoclonal Antibody to Human Pro-Relaxin 2

Specificity: Human Pro-Relaxin 2. Does not cross-react with human Relaxin 1.

Clone: fred

Host Animal: Mouse **Isotype:** IgG₁

Source: Tissue culture supernatant

Immunogen: Human Pro-Relaxin 2

Format: Purified, Lyophilized.
Reconstitute in 10ul double distilled water.

Purification: Protein G

Concentration: Not applicable.

Affinity Constant: Not determined.

Buffer: PBS, pH 7.4

Preservative: 0.1% Sodium Azide

Applications: Suitable for use in ELISA. Suitability for use in IHC, Western blot or IFA has not been determined but use in such assays should not necessarily be excluded.

Storage: Store lyophilized product at 2-8°C. After reconstitution, store at -20°C. Avoid multiple freeze/thaw cycles.

Warning: This product contains sodium azide, which has been classified as Xn (Harmful), in European Directive 67/548/EEC in the concentration range of 0.1 – 1.0 %. When disposing of this reagent through lead or copper plumbing, flush with copious volumes of water to prevent azide build-up in drains.

FOR RESEARCH USE ONLY. NOT FOR USE IN DIAGNOSTIC PROCEDURES.

8/12/03